Thesis for the Master's degree in chemistry

Showan Jafar Nori

Study of particulate matter (PM_{10}) in air in Taiyuan, Shanxi, China

60 study points

DEPARTMENT OF CHEMISTRY
Faculty of mathematics and natural sciences
UNIVERSITY OF OSLO 10/2005

Acknowledgements

A master thesis is a big work. Therefore it is important to have helpful people round you that can absolutely sustain you. Fortunately there is a good environment in environmental group which gives good teaching, advice and care. So there are many persons that deserve thanks.

First of all, I thank my family for their support and care during the whole of my life.

I thank my superviser Hans Martin Seip and co-supervisers Ruikai Xie and Thorjørn Larssen for their supervision and creation of co-operative environment in the group.

I thank every member in the environmental group for their attempt to create a social atmosphere and find time for entertainment which minimizes our stress during preparing our thesis. Especially I thank Jose` for his activity in entertainment efforts.

I thank Hege Lynne from the analytical group for her technical help during my work in the analytical laboratories.

I thank also Hans Erik and Karl Espen Yttri from NILU for their help.

Contnets

Abstract

The work in this master thesis consists of two parts: The first part is related to analyses of organic and elemental carbon in particulate matter (PM_{10}) in samples collected on glass fiber filters in Taiyuan city, Shanxi province, China and the second part related to analyses of inorganic components in particulate matter (PM_{10}) in samples collected on Teflon filters in the same site.

Glass fiber filters were predried and preweighed in Norway and sent to the Technical University in Taiyuan for sampling. Sampling was conducted in March 2004 and the samples were brought to Oslo in April 2004. Eight Samples were collected.

The samples were analysed using instrumentation available at the Department of Chemistry by a titrimetric method and at the Norwegian Institute for Air Research (NILU) by thermal method.

Elemental analyses were conducted in the Department of Chemistry by using ICP-AES and ICP-MS methods.

The obtained data was analysed and discussed in the context of the air pollution situation in Taiyuan and other Chinese cities, particularly in relation to air pollution reduction measures. The results should make it easier to identify sources of particles.

The results gave very high concentration of carbonaceous species. This indicates very high consumption of coal in Taiyuan. The measured concentrations were different in the two methods. This may be due to the difference in operational definitions of the fractions.
The measured accuracy of modified Walkley-Black method was +18%, -35% and +2% for OC, EC and TC, respectively, the precision was ±3%, ±13% and ±8%.

The results of elemental analysis show strong relationship between some elements and coal combustion processes. The measured accuracy of ICP-AES and ICP-MS was < 10.7 and < 28.1 respectively.

1. Introduction

Airborne particulate matter, in particular particles with an aerodynamic diameter less than 10 μm (PM_{10}), is a major air pollution problem in many areas, especially in developing countries, including China. This problem is enhanced by the rapid economic growth in China (Cao et al., 2003).

Particulate elemental matter can be released from coal combustion, metallurgical industry, building material industry and soil dust. It has a diverse health effect because of their ultrafine size and some soluble transition metals such as Cu, Fe, V, Ni, Zn (Xie, 2002). Overall, it is believed to have a cooling effect on climate.

PM_{10} may consist of inorganic components (i.e. S- and N-oxides, NH_4^+ and metals), organic components (i.e. carbonaceous matter), or a mixture of both. The carbonaceous matter is commonly present in ambient air as solid particles or as aerosols. Carbonaceous matter is classified as elemental carbon (EC, often named black carbon or soot) and organic carbon (OC). These components are large contributors to the fine particle burden in the urban atmosphere and heavily industrialized locations. The contribution ranges from about 10 % in remote areas to about 40 % in some urban areas (Lee, 2002).

EC and OC particles of anthropogenic sources have fine or ultrafine aerodynamic diameter < (1-0.1) μm and they can be inhaled into and accumulate in the respiratory system and cause serious health problem. The "Asian Brown Cloud" mainly associated with carbonaceous aerosol over south Asia, may be causing the premature deaths of about half-million people in India each year (Cao et al., 2003).

EC and OC play an important role in various atmospheric processes. EC acts as a positive climate forcing and may be the second most important component of global warming after CO_2 (Cao et al., 2003). Both EC and OC contribute to visibility degradation by either absorption or scattering of light.

It has been estimated that EC emissions in China account for roughly one fourth of the global anthropogenic emissions (Lee, 2002). Several studies suggest that EC emission from China and India may be responsible for the increase in droughts in northeast China and flooding in southeast China in the summer observed during the last 20 years (Yu, et al., 2004).

This thesis deals with particle pollution in Taiyuan, Shanxi province in China, carbonaceous particles, SO_2, nitrogen oxides and other pollutants produced by coal combustion, have rendered Taiyuan to be the most polluted city among China's 42 major cities (U.S. embassy Beijing, 2001).

2. Site Description

2.1 Shanxi Province

Shanxi province lies in the central parts of North China and has an area of 156,300 km^2. The Yellow River borders the province from the west. Large parts of the province consist of mountains and the province has a continental monsoonal climate, which means that most of the precipitation falls in summer. The province contains 118 counties; Taiyuan city is the capital. The total population of Shanxi is 31.7 million. About 16.2 million live in urban areas. Shanxi has 21.3 million hectars of forest, which cover 13.8 % of the province's land surface area (Aunan et al., 2004).

Shanxi is one of China's major energy bases with rich coal and iron deposits. Coal and coal related industries are extremely important in the province accounting for about a third of the total output from industry and agriculture in 2000. The province produces 25 % of the country's coal, 40 % of its coke (a high-carbon residue obtained from distilling coal and used in making steel (Aunan et al., 2004).

The main sources of air pollution within carbonaceous particles in major Shanxi cities are coal burning, coking, power plants, where the province burns about 100 million tones of coal a year for power generation (U.S. embassy Beijing, 2001), and metallurgical industries. In addition there is widespread use of coal in small coal-fired commercial boilers for heating and steam generation as well as for heating and cooking in the household sector (Aunan, et al., 2004).

2.2 Taiyuan City

Taiyuan city has 2.93 million residents with an area of 6,988 km^2. It lies 800 m above sea level at 37° 27′N- 38° 25′N; 111° 30′E- 113° 09′E. It is situated in a mountain basin in central Shanxi, surrounded by hills and mountains on three sides (Xie, 2002). Meteorological conditions are typically continental and monsoonal. The average wind speed is 1.98 m/s. Northerly and north-westerly winds prevail in winter, while southerly and south-easterly winds prevail in summer. The annual average temperature is 10.8 °C, with the average of the coldest month (January) -5.6 °C, the warmest month (July) 24.4 °C. Annual precipitation is 293.2 mm. The relative humidity is 54 %. The topography leads to periods of inversion and stagnant air masses during the winter, thus enhancing the concentration of air pollutants. The thickness of the inversion layer in summer is averagely 247 mm and 490 mm in winter (Xie, 2002).

Besides the city's topography mentioned above, there are several reasons for Taiyuan's pollution problems (Mestl et al., 2005):

1- More than 75 % of industrial GDP is from polluting, heavy industries which are mainly two power plants, with installed capacities of 1000 and 600 MW, respectively, a large iron and steel company (Aunan et al., 2004), cement industries, and copper and aluminum industries.
2- The extent of state owned enterprises with old-fashioned technology and low productivity.
3- Industrialization of rural areas has led to increase coal consumption in town and village enterprises resulting in high emissions encircling the city (Mestl et al., 2005).

Other sources contributing to pollution problems in Taiyuan are emissions from gasoline and diesel fired motor vehicles, and crop residue combustion (Streets et al., 2001).

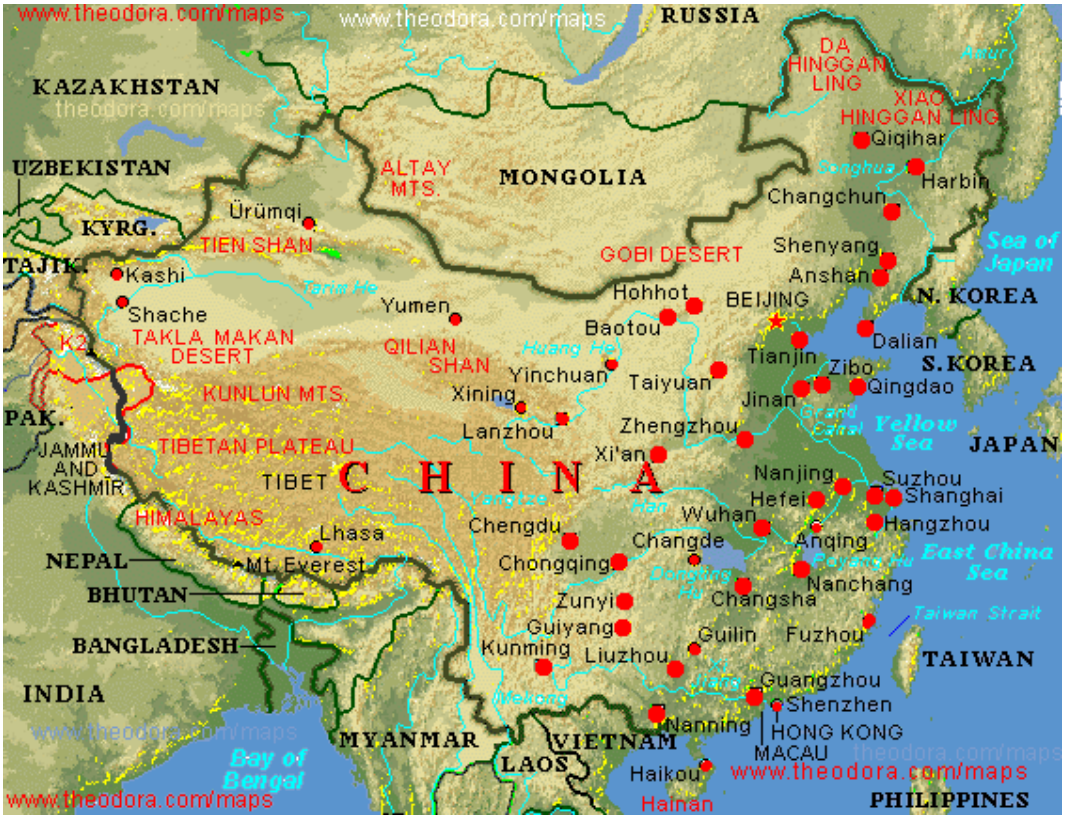

Fig 2.1 China map (Theodora.com)

3. Annual Consumption of Coal in China :

China has proven, recoverable coal reserves of about 126 billion short tons, and potential resereves of as much as 4 trillion short tons. Almost four-fifths of China's coal reserves is moderately low sulfur bituminous coal, with 15 % as lignite and 6 % as anthracite. Most of the reserves, including almost all of the highest-quality coal, is located in the northeastern part of the country (Cslforum, 2004).

China is the largest coal consumer in the world (Table 3.1), its coal consumption accounts for one fourth of that of the world total, and half increase of the coal consumption of the world is contributed by China (Cslforum, 2004).

Table 3.1 World coal consumption, 2001 to 2025 in millions of tons (Anderson, 2005)

Region	2001	2025	Percent change %
United States	1060	1567	47.8
Western Europe	574	463	- 19.3
Japan	166	202	21.7
Former Soviet Union	446	436	- 2.2
China	1383	2757	99.3
India	360	611	69.7
Rest of the world	1274	1538	20.7
Total World	5263	7574	43.9

In 2002, domestic coal use in China reached 1370 Mt (Youguo, 2003). It was distributed in different sectors (Fig 3.2)

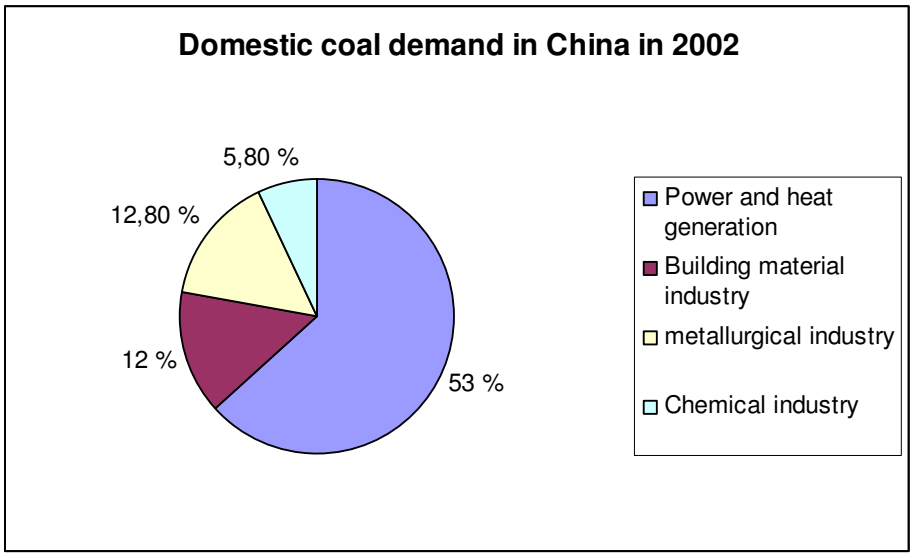

Fig 3.1 Domestic coal demand in China in 2002

Since 1980s and till 1996, coal consumption in China experienced a rapid continuous increase, where the annual average rate of coal consumption was increased by 5.08 %. Coal consumption decreased from 1997. The decline assumed that local governments had followed Beijing's instructions to close thousands of small, unsafe mines producing low-grade coal and many heavily polluting small power plants (Bradsher, 2003), in addition, China's economy suffered during the Asian economic crisis of 1997 to 1998, and many factories decreased production or shut down because of economic restructuring policies (Streets et al., 2001). In 1999 and 2000, the coal consumption recovered slowly, driven by the growth of power generation coal and coal export in 2001 and 2002 (Youguo, 2003). After 2002 the coal consumption increased sharply. Officals from Chinese coal industry have estimated that coal consumption may be rising more than 10 % a year (Bradsher, 2003).
Table 3.2, illustrates the coal production and consumption in China, 1990-2002 in millions of short tons (Cslforum, 2004).

Table 3.2 Coal production and consumption in China, 1990-2002 (in millions of short tons)

	1990	1991	1992	1993	1994	1995	1996	1997	1998	1999	2000	2001	2002
Production	1190	1199	1229	1304	1404	1537	1545	1507	1429	1365	1314	1459	1521
Anthracite	235	240	244	251	271	297	321	275	267	238	237	262	312
Bituminous	906	910	933	989	1066	1170	1163	1167	1103	1068	1025	1138	1140
Lignite	50	49	52	63	67	70	61	65	59	60	53	58	69
Consumption	1124	1165	1200	1276	1390	1498	1517	1450	1392	1343	1282	1357	1422

Table 3.3 shows the consumption of different types of fuel in China in 2003 and 2004 (BPs, 2004)

Table 3.3 Consumption by fuel in China

Fuel	Consumption (Million tones oil equivalent)		Consumption growth (%)
	2003	2004	
Oil	266.4	308.6	13.67
Natural gas	29.5	35.1	15.95
Coal	834.7	956.9	12.77
Nuclear energy	9.9	11.3	12.39
Hydroelectricity	63.7	74.2	14.15

Taiyuan produced 34 million tons of raw coal in 2003, which was 2.5 % of total raw coal production in China and consumed 28 million tons (Xie et al., 2005).

According to CIEPCP (2003) the total coal consumption by industrial sectors in Taiyuan in 2000 was about 21.5 Mt (Table 3.4) while another study by (Shanxi Environmental Bureau, 2004) found the total consumption to be 28 Mt. If these studies are accurate, the total coal consumption in Taiyuan increased between 2000-2003 by 23%.

Table 3.4 Coal Consumption in different industrial sectors in Taiyuan, 2000

Industrial sector	Coal consumption (10000 tones)	%
Coal mining industry	89.61	4.17
Oil processing and coking	731.21	34.02
Chemical raw materials and chemical products manufacturing	23.79	1.11
Non-metal mineral manufacturing	35.77	1.66
Ferrous metal metallurgy and forging	309.05	14.38
Non-ferrous metal metallurgy and forging	19.05	0.89
Machinery and electronic manufacturing	95.00	4.42
Power, steam and hot water production and supply	565.75	26.32
Others	208.33	13.03
Total	2149.56	100

4. Atmospheric Dispersion and Transport of Pollutants

There are many factors that affect the dispersion and transport of the pollutants:

Wind speed: The concentration of pollutants is inversely proportional to the wind speed. Wind speed at ground level tends to decrease overnight and increase again during the morning especially during cloud-free conditions. Emissions also tend to decrease overnight and increase rapidly during the morning, resulting in high pollution levels, before wind speed increases causing improved conditions (Harrison, 1999).

Wind direction: Areas located downwind of the pollution sources are most affected by pollutants. Knowing the prevailing wind direction is therefore important in predicting the likely impact of these sources.

Pollutant stability: The stability or persistence of a pollutant depends on the presence or absence of clouds, fog, or precipitation, the pollutant solubility in water, reactivity with other atmospheric constituents (which may be a function of temperature) and the presence of sunlight. The stability can be expressed by atmospheric residence time. The residence time for particles is dependent on the diameter, hygroscopicity and thermal diffusion (thermal difference between regions). Particles with large residence time can be transported over long distances.

Atmospheric stability: It is dependent on the time of day and the nature of the earth's surface. The roughness of the ground produces a certain amount of turbulence in the boundary layer which promotes the mixing and dispersion of pollutants.
The main factor influencing atmospheric stability and turbulence is thermal buoyancy. The pressure in the atmosphere decreases exponentially with height. Ascending air expands as the pressure decreases and as it expands it cools. The variation of temperature with height is called the lapse rate. The ideal lapse rate is called adiabatic lapse rate (a change of 1 °C/100 for every 100 m of dry air). The value is somewhat lower for moist air. In the real atmosphere the lapse rate can be greater than, smaller than, or close to the adiabatic lapse rate.

4.1 Temperature Inversion

During temperature inversion the air will be very stable with little mixing of material. The effect of temperature inversion can be stronger when there is low wind speed, low temperature, dew, frost, or fog (Harrison, 1999; Seinfeld and Pandis, 1998).

There are two types of temperature inversion, ground level inversion and subsidence inversion. The first type is caused by overnight radiative cooling of the ground which leads to low level temperature inversion on clear nights. It can occur also in areas covered with snow and towns situated in valleys. Ground level temperature inversion causes high level of pollution near the ground.

The other type of temperature inversion takes place during anticyclonic conditions. Inside an anticyclone, air is diverging from a high pressure region and at the centre subsides from a

high level to lower levels of the atmosphere. As it subsides it warms resulting in the development of an elevated inversion layer (Harrison, 1999). Subsidence temperature inversion can be formed in warm, dry weather and provides the ideal conditions for a long range transport of pollutants.

4.2 Dry and Wet Deposition

Particles may be removed from the atmosphere by dry and wet deposition. Dry deposition is the removal of gases and particles from atmosphere on the Earth's surface by direct transport processes.

The dry deposition process can be imagined by three separate steps:

1- Species are transported through the atmosphere to places near the surface. This can be carried out by turbulent atmospheric motions near the earth's surface.
2- Then they cross the surface itself (by diffusive or Brownian mechanisms).
3- The species are taken up by or deposited on the surface. Factors affecting the uptake of the gas or particle on the surface include shape and smoothness of the surface, the amount of moisture on it, the solubility of the depositing species and specific chemical or biological interactions.

Species that are moderately soluble are reversibly absorbed, while highly soluble species are absorbed rapidly and irreversibly (Wolff and Klimisch, 1982) .

Rates of dry deposition are expressed by a semi-empirical equation:

$$F = u_d * C$$

Where F is the flux of dry deposition of a species whose concentration is C at a certain height above the surface, u_d is the deposition velocity. It is assumed that F remains constant up to a certain reference height, actually F and u_d depend likely on height above the surface (Wayne, 2002).

Wet deposition includes incorporation into falling precipitation (washout), where the particles collide with existing droplets or ice crystals, and incorporation into cloud droplets (rainout), where the particles act as a nucleating agent in the formation of cloud droplets or ice crystals.

Washout is expressed by the following factor:

W = Concentration of a material in rain ($\mu g\ kg^{-1}$)/Concentration of a material in air ($\mu g\ kg^{-1}$)

Wet deposition is only significant for those carbonaceous species that are water-soluble or readily hydrolysed. (Wayne, 2002)

Wet deposition is thought to occur in several separate steps:

1- The atmospheric condensed water (hydrometeor) and the species to be removed must encounter one another.
2- The species must be taken up by the hydrometeor.
3- The hydrometeor must reach the Earth's surface.

5. Carbonaceous Matter in the Atmosphere

Elemental carbon (EC) is also called “black carbon”, “soot”, or “graphitic carbon”, has a chemical structure similar to impure graphite and is emitted directly into the atmosphere predominantly during combustion. Organic carbon (OC) is either emitted directly by sources (primary OC) or can be formed in *situ* by condensation of low volatility products by photo oxidation of hydrocarbons (secondary OC). Note that OC refers to only a fraction of the mass of the organic material (the rest is hydrogen, oxygen, nitrogen, etc), but because the carbon fraction is measured directly the term is used routinely. Additional amount of aerosol carbon, usually small, may exist either as carbonate (e.g., $CaCO_3$) or CO_2 adsorbed onto particulate matter such as soot (Seinfeld and Pandis, 1998).

The analytical distinction between the OC and EC fractions is currently not well defined. This is because the very low volatilities and solubilities of the high molecular weight organic constituents of particulate organic carbon (POC) make such compounds behave increasingly like EC in analytical procedures (Seinfeld and Pankow, 2003).

5.1 Elemental Carbon (EC)

Carbonaceous particles are by-product of the incomplete combustion of solid (coal), liquid and gaseous fuels, in addition to particles escaping during coal mining, transport and industrial activities. Individual elemental carbon particles range in size from 0.05 to 0.12 μm. They are roughly spherical and can agglomerate to form what is known “soot” particles which have a range size < 10 μm (Seinfeld and Pandis, 1998).

Soot may contain organic carbon particles because the ability of EC particles to adsorb OC particles onto its surface. Besides carbon, soot contains up to 10 mol% of hydrogen as well as traces of other elements.When adsorbed OC particles are water-soluble, it increases the hygroscopicity of EC particles which are originally hydrophobic. This leads to longer lifetime for EC particles inside urban fog (Seinfeld and Pandis, 1998).

The composition of soot that has been aged in high-temperature region of a flame is typically C_8H, but soot contains usually more hydrogen earlier in the flame (Seinfeld and Pandis, 1998).
Soot may contain small amounts of other elements such as oxygen and nitrogen incorporated in its structure.

5.2 Organic Carbon (OC)

The organic component of ambient particles in both polluted and remote areas is a complex mixture of hundreds of organic compounds which are formed from natural and anthropogenic sources.
OC concentration is expressed by carbon concentration in $\mu g\ C/m^3$ and does not include the contribution to the aerosol mass of the other elements (oxygen, hydrogen and nitrogen) of the organic aerosol compounds. The concentration of total organic matter (OM) is determined by

multiply the measured OC values with an empirical factor in the range 1.3-2.2 depending on the location (Salam et al., 2003). Organic carbon is divided into two categories:

Primary Organic Carbon (POC)
Primary organic carbon consists of numerous organic compounds which are a cumulative result of a variety of primary sources. Polycyclic aromatic hydrocarbons, carboxylic acids and phenols are classified as primary organic carbon.

Secondary Organic Carbon (SOC)
Secondary organic aerosol is formed in the atmosphere by the mass transfer to the aerosol of low vapour pressure products of oxidation of organic gases. As organic gases such as volatile organic compounds (VOCs) are oxidised in the gas phase by species such as hydroxyl radical (OH), ozone (O_3) and the nitrate radical (NO_3), their oxidation products accumulate. Some of these products have low volatilities and condense on the available particles (Seinfeld and Pandis, 1998). PAHs are likely less oxygenated with atmospheric radicals, but they tend to be adsorbed onto carbonaceous particles.

The mass transfer of these products to the aerosol phase *f,* will be proportional to the difference between their gas phase concentration c_g, and their concentration in the gas phase at the particle surface c_{eq}:

$$f \sim c_g - c_{eq}$$

If the two concentrations are equal, the organic compound will be in equilibrium and there will be no net transfer between the two phases. If $c_g > c_{eq}$ then the gas phase is supersaturated with the compound and some of it will condense on the available aerosol (Seinfeld and Pandis, 1998). The equilibrium concentration c_{eq}, depends not only on the properties of the species but also on its ability to form solutions with compounds already present in the aerosol phase (other organics, water, etc).

5.3 Physical Properties of OC and EC Aerosols

OC aerosols are mostly hydrophilic and light scattering except for some absorption in the ultra violet (UV) and visible region. Thus OC can minimize the visibility in a polluted area. OC particles play a significant role in formation of cloud condensation nuclei, and in formation of photochemical smog.

EC aerosols are hydrophobic but can be hydrophilic when they get coated with other particles as they age. However, unlike OC, EC is mostly absorbing in the visible and UV region. This absorbing property of EC and its effectiveness in warming the atmosphere could potentially partly compensate the cooling caused by the other aerosols. Although EC particles are estimated to have a small total global forcing effect of 0.4 to 1 W m^{-2}, their efficacy as a forcing agent can be high mainly due to their effects on snow albedo (Menon, 2004).

Absorbing and scattering of light by EC and OC are expressed by the term “Extinction” which is the attenuation of light along a beam by scattering and absorption due to particles present in the beam. Extinction is proportional to particle size. Large particle size causes high extinction

which leads to low visual range (Brausseur et al., 1999). Computations by Mallet et al (2002) indicate that 90% of the light extinction is due to anthropogenic aerosol and only 10% is due to natural aerosol. 20% of the extinction is due to EC and 21% to OC.

5.4 Black Carbon Emissions in China

Roughly one-fourth of global anthropogenic BC emissions is believed to originate in China (1). Streets et al. (2001) calculated that BC emissions in China in 1995 were 1342 Gg, about 83 % being generated by the residential combustion of coal and biofuels. The same authors estimated that BC emissions could fall to 1224 Gg by 2020 (Streets et al., 2001). This 9 % decrease in BC emissions can be contrasted with the expected increase of 50 % in energy use; the reduction will be obtained because of a transition to more advanced technology, including greater use of coal briquettes in place of raw coal in cities and towns.

The increased use of diesel vehicles in the future will result in a greater contribution from the transport sector to total BC emissions (Streets et al., 2001). Spatially, BC emissions are predominantly distributed in an east-west swath across the agricultural heartland of China, where BC is preferentially emitted from domestic coal-fired stoves. This is in contrast to the emissions of most other anthropogenically derived air pollutants, which are closely tied to population and industrial centers.

Emissions of BC are difficult to determine under the best of circumstances, because of uncertainty in the fraction of elemental carbon of less than 1 μm or so in diameter. This fraction is very sensitive to fuel type and combustion conditions, where larger particles, organic compounds, and ash can confound measurements. Such problems are compounded when dealing with China, where no statistics are available on types of combustor and particulate controls- neither the prevalence nor performance of each type of device (Streets et al., 2001).

Efforts to Decrease Coal Consumption in China

Chinese rapid economic growth and its enormous population (about 1.3 billion) make China the largest coal consumer in the world.

According to Becker (2003), China has ambitious plans to cut its reliance on coal to about 55 % of its energy needs. By 2030 coal is expected to provide 62 %, oil 18 %, natural gas 8 %, hydropower 9 %, and nuclear power 3 % of China's energy consumption. By 2050 Chinese planners believe coal consumption should be down to 35 % of consumption, with oil and natural gas accounting for 40-50 % and primary energy sources such as nuclear, solar and wind power accounting for 15-20 % (Becker, 2003).

Beijing has built two transcontinental gas pipelines and half a dozen smaller ones that would supply the big cities with clean energy for heating and cooking. In many cities such as Beijing and Taiyuan, people are already installing new gas-fired boilers to replace coal-fired ones (Becker, 2003).

Growth in Chinese coal consumption should slow somewhat in 2007, where China starts building three Gorges dams which are going to provide considerable additional electricity for

China's national grid by that year (Bradsher, 2003). These projects can minimize coal consumption, by contributing 20 % of China's electricity consumption from non-polluting energy that is vastly preferable to coal.
Some experts from International Energy Agency, warned that with no further large hydroelectric projects, coal consumption is going to increase again after 2007 (Becker, 2003).

In June 2000 provincial leaders in Shanxi managed to close nearly 10000 polluting enterprises. This was one-seventh of the total shut down nationwide. Other enterprises made investments to reduce their emissions. For example, Taiyuan Iron and Steel (Taigang), which with annual steel output of 300000 tons is one of the city's main pollution sources, reportedly invested US$ 39.5 million in 2000 on pollution control, more than in the previous 10 years combined (U.S. embassy Beijing, 2001).This campaign was not entirely efficient because of local corruption and government inefficiency. Some of the smaller mines have reopened secretly (SCMP, 2004).

Abatement measures

The emission of carbonaceous species can be abated by (Aunan et al., 2001):

1- Improving the combustion technique of coal.
2- Converting coal to less pollutant fuel (coal gasification)
3- Coal briquetting
4- Using alternative energy sources, such as, wind, power, and hydroelectric power.

5.5 Polycyclic Aromatic Hydrocarbons (PAHs)

5.5.1 Characterizations

There are large numbers of PAHs species that have been identified by different studies. They consist of two or more fused benzene rings in linear, angular, or cluster arrangements, and by definition, they contain only carbon and hydrogen (Seinfeld and Pandis, 1998). The largest PAHs, with five, six, and seven aromatic rings, are found in the atmosphere predominantly as particles such as coronene (seven fused rings), while two ring species such as naphthalene exist exclusively in the gas phase (Wayne, 2002). Some of them are distributed in both the gas and aerosol phases such as pyrene and anthracene. Generally, the partitioning of PAHs between gas and aerosol phases depends on their vapor pressures, where a certain PAH with a vapor pressure greater than (10^{-6} Torr) at the ambient air temperature will exist mainly in the gas phase in the atmosphere, while a certain PAH with a vapor pressure (less than 10^{-6} Torr) will exist in the particle phase (Atkinson and Arey, 1994).

Airborne-PAHs particles consisting of more than three condensed aromatic rings can be adsorbed onto the surfaces of other aerosol particles generated in combustion processes such as elemental carbon aerosols , and products more polar and reactive than the parent PAHs can be formed (Letzel et al., 1999). It was proved by Mastral et al., (2003) that the higher the PAHs boiling point, the higher the PAHs adsorption capacity.

The importance of PAHs resides largely in their impact on human health. Some of them are carcinogenic or mutagenic, such as benzo(a)pyrene (Wayne, 2002).

5.5.2 Atmospheric Transformation

Polycyclic aromatic hydrocarbons can be transformed in the troposphere by gas phase or particle phase reactions with atmospheric OH radical, and NO_2 and O_3 gases.

The major gas phase reactions for PAHs are believed to be reaction with OH radicals and then with NO_2 at day and reaction with NO_3 radicals at night. The major product of the reactions are nitro-PAHs. Also photodecomposition of PAHs can take place in gas phase reaction.

In particle phase reaction, the dominant reactions for PAHs are likely photochemical reactions with minor contributions by heterogeneous reactions with O_3, NO_2, N_2O_5 and HNO_3. The photochemical reaction rate of particulate PAHs increases as a function of relative humidity (Feilberg, 2000).

5.6 The Atmospheric Chemistry of Elemental Carbon

EC particles play a significant role in enhancing the oxidation of SO_2 to sulfate (De Santis and Allegrini, 1992), HNO_3 to NO_2 and NO_2 to NO, and O_3 to O_2 (Lary et al., 1997). Therefore they can contribute in reducing atmospheric constituents.

EC particles can catalyze SO_2 oxidation in the presence of effective oxidants such as O_3 and NO_2, and relative humidity of 65 % (Cofer et al., 1981). Oxidation rate increases with higher concentrations of the oxidants. The presence of water vapor, formed during coal combustion, helps in the partial hydration of the surface of freshly generated soot (Chughtai et al., 1998). Water molecules may be hydrogen-bonded to polar adsorption sites on the carbon. These adsorption sites may be chemisorbed oxygen in the case of pure carbons, or, probably, polar surface functional groups or mineral centers in less pure carbons. Also the hydration process increases with soot aging where this is attributed to physisorbed oxygen (Chughtai et al., 1996). The mechanism of SO_2 oxidation includes the adsorption of SO_2 onto soot particles, the surface hydration of SO_2 to $SO_2.H_2O$ (H_2SO_3), followed by air oxidation to sulfate (Chughtai et al., 1996).

6. Environmental Effects of Carbonaceous Particles

6.1 Effects of Carbonaceous Particles on Climate

The effect of aerosols on climate is expressed by climate forcing which is defined as imposed perturbation of the Earth's energy balance. It is measured in W m^{-2} (Environmental protection agency, 2001). Every 1 W m^{-2} forcing can produce about 0.75 °C change in temperature (Menon, 2004).

6.1.1 Direct Effect

Carbonaceous particles can affect climate directly by absorption and scattering light. Absorption of light increases the atmospheric temperature and can play a role in global warming, while scattering light reduces the visibility and the amount of solar energy that reaches the ground. This can cause global cooling (Menon, 2004). A model simulation by (Menon, 2004) suggested forcing values of OC ranging from – 0.29 to – 0.82 W m^{-2} (for sulphate column burden of 1.14 to 3.3 mg m^{-2}). One can expect that the values of OC are similar to that for sulphates because they are both mainly reflective in the visible spectrum. The direct forcing for EC produced from fossil fuel was estimated to range from 0.17 to 0.42 W m^{-2} for column burdens of 0.13 to 0.16 mg m^{-2} (Menon, 2004).

6.1.2 Indirect Effect

Carbonaceous particles can indirectly affect climate by acting as cloud condensation nuclei (CCN) and thereby determine the initial cloud droplet number concentration, precipitation formation and lifetime of warm clouds.

Any change in the availability of CCN may change nucleated droplet number concentrations. When droplet number concentrations increase for fixed water content, the mean droplet size decreases and the reflectivity (albedo) of the clouds increases (Brausseur et al., 1999). Small droplets tend to inhibit rainfall, thus increasing cloud lifetime and the average cloud cover on Earth, causing global cooling. Climate models that incorporate the aerosol-cloud physics suggest that indirect effects may produce a negative global forcing of the order of 1 W m^{-2} or larger (Environmental protection agency, 2001).

6.1.3 Semidirect Effect

The evaporation of clouds by absorbing aerosols such as EC (Menon, 2004) and soot forcing are semidirect effects.

Soot forcing is important for snow albedo. By using general circulation model and empirical data on soot amount in snow, Hansen & Nazarenko (Menon, 2004) estimated that soot effects on snow and ice albedos result in a forcing of ~0.3 W m^{-2} for the Northern Hemisphere and find the efficiency of this forcing to be approximately twice as effective as CO_2 in altering

global surface air temperatures. Furthermore, they suggest that this soot effect may have contributed to the past century's global warming by 25 %, melting land ice and permafrost, early arrival of spring in the northern hemisphere, and thinning Arctic sea ice (Menon, 2004).

BC particles are estimated to have a total global forcing effect of 0.4 to 1 W m^{-2}, their efficiency as a forcing agent can be high mainly due to their effects on snow albedo (Menon, 2004). Fig 6.1 illustrates the climate forcing of EC, OC and greenhouse gases.

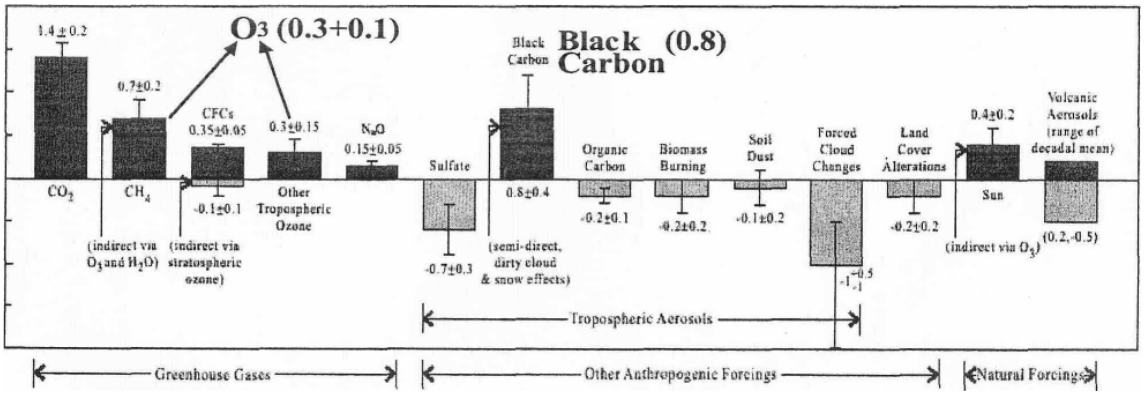

Fig 6.1 Estimated change of climate forcings beween 1850-2000 (Hansen and Sato, 2001)

Other studies suggested different values for net BC forcing, such as 0.25 W/m^2 by IPCC (2001), 0.5 W/m^2 by Jacobson (2002) and 0.0-1 W/m^2 by Hansen and Sato (2001), but all these values are uncertain.

The uncertainties of aerosol effects on climate are large. This is due not only to the heterogeneous spatial and temporal distribution of tropospheric aerosol particles, their different origins (natural and anthropogenic), their physical and chemical behaviour in the free troposphere, but also to the lack of knowledge of optical and microphysical properties of the aerosol particles (Mallet et al., 2002).

The uncertainty of BC is very high because BC emission is not easy to estimate. As a product of incomplete combustion, the emitted amount depends on how efficiently the fuel is burned in addition to the fuel amount. Thus, the mass of EC emitted per unit weight of fuel (emission factor) depends on fuel type and other factors that influence the combustion efficiency.

Black Carbon or Soot Contributes to Droughts and Floods in China

A study by "NASA climate" has found that large amounts of black carbon or soot particles and other pollutants are causing changes in precipitation and temperatures over China and may be at least partially responsible for the tendency toward increased floods and droughts in those regions over the last several decades (NASA, 2002).

When soot absorbs sunlight it heats the air and reduces the amount of sunlight reaching the ground. The heated air makes the atmosphere more unstable, creating rising air (convection) which forms clouds and brings rainfall to regions that are heavily polluted.

The increase of rising air in southern China is balanced by an increase of sinking air (subsidence) and drying in northern China. When air sinks, clouds and thus rain, cannot form, creating dry conditions. For example, deserts are places where subsidence occurs.
In recent years, northern China has suffered from an increased severity of dust storms, while southern China has had increased rainfall that is thought to be the largest change in precipitation trends since the year 950 (NASA, 2002).

A. Soot changes ground temperatures in Asia

Soot blocks the sun's energy from reaching the ground and cools the surface. Fig 6.2, derived from the GISS climate computer model, and aerosol data from 46 ground stations in China, shows black carbon's effect in lowering surface temperatures during the summer months (June, July and August). Cooler temperatures are denoted by the blue colorations. This map shows cooling of 0.5 to 1.0 ºC occurring over China, and warming temperatures throughout the rest of the world (in yellow). As soot heats the lower atmosphere over China some of this warm air can get transported to the other regions of the world and can cause surface warming at distant locations (NASA, 2002).

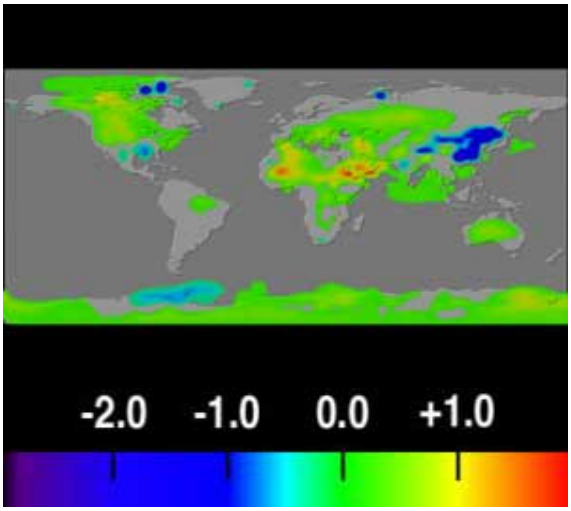

Fig 6.2 Black carbon's effect in lowering surface temperatures in areas in China during the summer months (June, July and August).

B. Soot intensifies flooding and droughts in Asia

Soot intensifies rainfall in polluted regions. The black carbon aerosols soak up the sun's rays heating up the atmosphere. Air rises and creates rain clouds over polluted areas. Rising air is balanced by an increase in sinking air and drying in neighboring regions. When air sinks, clouds and thus, rain, cannot form, creating dry condition (NASA, 2002).
Fig 6.3, derived from the GISS climate computer model, and aerosol data from 46 ground stations in China, shows how black carbon can change rainfall patterns over the northern and southern regions of china during the summer months (June, July and August). The blue colors indicate regions in which the simulations yield a tendency for increased rainfall by as much as 10 inches over the summer. Other regions (brown colors) have decreased rainfall by as much as several inches or more (NASA, 2002).

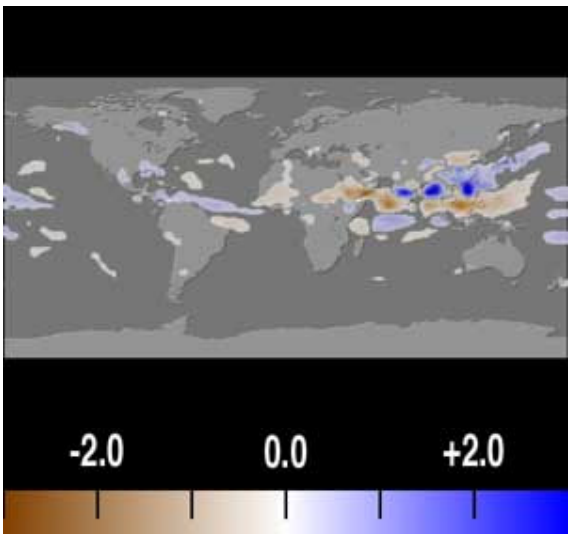

Fig 6.3 The effect of black carbon on rainfall patterns

C- Sunblock reduces crop yields

Soot can block the sun's energy from the ground and reduce crop yields. Fig 6.4, derived from NASA Goddard institute for space studies (GISS) climate computer model and aerosol data from 46 ground stations in China, shows the decrease in solar energy reaching the ground (in black) during the summer months (June, July and August). Yellow colors show where the sunlight has increased (NASA, 2002).

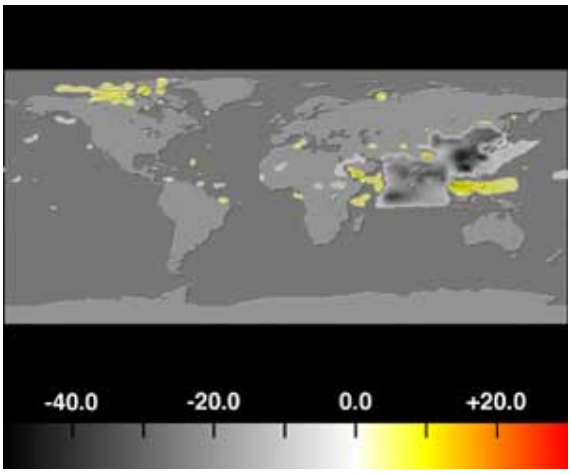

Fig 6.4 Solar energy reaching the ground

Slowing global warming

A study by Jacobson (2002), presents a quantitative analysis on controls of EC and OC versus greenhouse gases in controlling warming and the time period over which measures would be effective. He finds that reduction in emissions of fossil fuel EC and associated OC may slow warming more than any reductions in CO_2 and CH_4 for a specific period. To eliminate 20%-45% of net warming within 3-5 years, all fossil fuel EC and OC would have to be eliminated. A similar reductions in warming can be obtained by eliminating approximately one third of CO_2 emissions. However the reduced warming would not come into effect for 50-200 years (Jacobson, 2002).

6.2 Effects of Carbonaceous Particles on Human Health

Particles are often classified in three categories: ultrafine, fine and coarse (Fig 6.5). Carbonaceous particles are within the ultrafine and fine categories. The ultra and fine particles are predominantly of anthropogenic origin and are deposited with high probability in the lower parts of the human respiratory system and thus have the larger impact. While coarse particles are often of natural origin (dust, seaspray, pollen, insect debris…etc). Their health impacts are modest, because they are deposited in the upper airways (Fig 6.5), and because they may be less toxic (Austin et al., 2002).

Adults: Breathing fine and ultrafine particles can adversely affect individuals with heart disease, emphysema, asthma, chronic bronchitis by causing additional medical treatment. Inhaling fine particulate matter may cause increased hospital admissions, emergency room visits and premature death among sensitive population.

Children: Breathing fine and ultrafine particles affects children with increased respiratory symptoms and reduced lung function, including symptoms such as aggravated coughing and pain in the affected children (PCAQ, 2004).

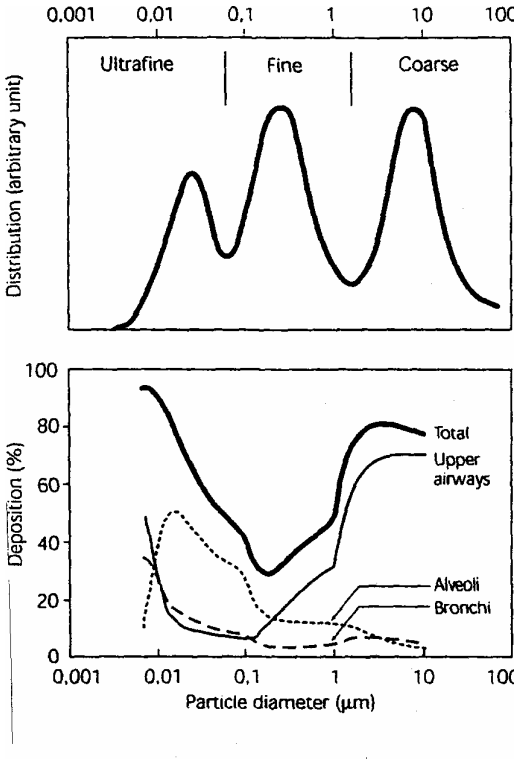

Fig 6.5 Schematic size distribution of particulate matter in the atmosphere and the corresponding deposition in the human respiratory system (Austin et al., 2002)

Some polycyclic aromatic hydrocarbons have carcinogenic or mutagenic effects. Benzo(a)pyrene is identified as a strong mutagen, while other compounds such as benzo[k]fluoranthene are identified as moderate mutagens (Wornat et al., 2001). Mono- and di-nitro derivatives of PAHs have direct, powerful and mutagenic properties. They can be formed directly from combustion sources or from atmospheric chemical reactions of PAHs with OH and NO_2 radicals (Fig 6.6) (Wayne, 2002).

Many Chinese provinces are using unvented residential coal stoves. Emissions of soot and PAHs particles from residential coal combustor are of particular concern because they are 3-4 orders of magnitude greater than that from other sources. Thus human exposure to PAH-coated soot is high by either inhalation of particles that remain air-borne or by ingestion of particles that deposit on food and food-preparation surfaces within the home (Wornat et al., 2001).

Table 6.1 shows the burden of disease for major causes in different parts of the world. The numerical values correspond to the percentage of total disability adjusted life years' (i.e. DALY) which is a standard measure for the burden of disease. The concept of DALYs combines life years lost due to premature death and fractions of years of healthy life lost as a result of illness or disability. Thus the higher the figures, the greater the detrimental health impact of the cause. The table highlights the severity of the problem of urban and especially indoor air pollution in developing countries (EEB, 2000).

Table 6.1 Burden of diseases from major environmental risks for several country groups

Environmental health group	Percent of total DALY's in each country group							
	Africa	India	**China**	Asia&Pacific	Latin America	FSE	LDCs	EME
Water supply&sanitation	13	11	4.5	10	7	2	9	1.5
Malaria	9	0.5	0	1.5	0	0	3	0
Indoor air pollution	**5.5**	**6**	**9.5**	**4**	**0.5**	**0**	**5**	**0**
Urban air pollution	**1**	**2**	**5**	**2**	**3**	**3**	**2**	**1**
Agro-industrial waste	1	1	1.5	1.5	2	2	1	2.5

Note: FSE-former socialist economies of Europe (does not include Central Asia); LDCs-(less developed countries) comprise all regions/countries in the first six columns; EME-established market economies. Note that Asia and Pacific includes countries from East and South Asia, except for China, India and Pakistan (EEB, 2000).

The Environmental Protection Agency uses its Air Quality Index to provide general information to the public about air quality and associated health effects (Wunderground, 2004). An air quality index (AQI) of 100 for any pollutant corresponds to the level needed to violate the federal health standard for that pollutant. For $PM_{2,5}$ an AQI of 100 corresponds to 40 $\mu g/m^3$ (averaged over 24 hours), the current federal standard. An AQI of 100 for PM_{10} corresponds to 150 $\mu g/m^3$ (averaged over 24 hours).

Table 6.2 Particulate matter health hazards according to Enviromental Protection Agency

EPA air quality index	Levels of health concern	Cautionary statements for PM_{10}
0-50	Good	None
51-100	Moderate	None
100-150	Unhealthy for sensitive groups	People with respiratory disease, such as asthma, should limit outdoor exertion
151-200	Unhealthy	People with respiratory disease, such as asthma, should avoid outdoor exertion; everyone else, especially the elderly and children, should limit prolonged outdoor exertion
201-300	Very unhealthy	People with respiratory disease, such as asthma, should avoid any outdoor activity; everyone else, especially the elderly and children, should limit outdoor exertion
301-500	Hazardous	Everyone should avoid outdoor exertion; people with respiratory disease, such as asthma, should remain indoors

A World Bank report estimates that air pollution costs the Chinese economy $25 billion a year in health expenditure and lost labour productivity alone (Becker, 2003). As many as 700,000 premature deaths per year are attributed just to indoor air pollution from burning coal for heating and cooking. Throughout China, respiratory diseases are blamed for a quarter of all early deaths, a figure that has increased by nearly 25 % over the past decade. Then there are the 10000 miners who lose their lives each year, largely from coal-mining accidents (Becker, 2003).

6.3 Soiling

Carbonaceous particles may coat building materials, damaging the appearance of homes, public buildings, and historic landmarks (Menon, 2004).

7. Analytical Methods

7.1 Carbonaceous Particles Analysis

7.1.1 Modified Walkley-Black Method

7.1.1.1 Theory

A modified Walkley-Black method is often used to determine OC content in soils. It is a titrimetric procedure based on oxidation-reduction reactions. Filtered aerosols samples are much smaller than soil samples, but are richer in the OC and EC fractions. The mix of organic compounds is also different from that in soil, and includes many reduced carbon compounds, resulting in an average oxidation number of carbon which is lower than zero (Chan et al., 1995).

The method consists of two procedures:

1- Digestion procedure: Samples were digested with 1ml (1N)potassium dichromate and 5 ml concentrated sulphuric acid at room temperature and 145°C for one hour, by using a block digestor (Tecator, 2012 Digestor)
2- Titration procedure: Digested samples were titrated by 0.05M ferrous sulfate.

Essentially, particles are oxidized with excess dichromate in sulfuric acid and the residual dichromate back titrated with ferrous (II) sulfate.

The reactions involved are:

1- Oxidation of carbon by dichromate:

$$2\,Cr_2O_7^{2-} + 3\,C + 16\,H^+ \rightarrow 4\,Cr^{3+} + 3\,CO_2 + 8\,H_2O$$

2- Reduction of excess dichromate by Fe^{2+}:

$$2\,Cr_2O_7^{2-} + 12\,Fe^{2+} + 28\ H^+ \rightarrow 4\,Cr^{3+} + 12\,Fe^{3+} + 14\ H_2O$$

$$3\,C \leftrightarrow 12\,Fe$$

7.1.1.2 Experimental

7.1.1.1.1 Equipment

1- Block digester (Tecator, 2012 Digestor)
2- 50 ml conical flasks
3- 50 ml beakers
4- Pipettes
5- 50 ml burette
6- 10 cm length test tubes
7- Magnetic stirrer
8- Desiccator
9- Blank glass fiber filters
10- Double surface condensers
11- Volumetric flasks

7.1.1.1.2 Reagents

1- 0.05M $FeSO_4.7H_2O$ 99 %(rectapur)
2- 1N $K_2Cr_2O_7$ (pro analysi)
3- (95-97%) H_2SO_4 (pro analysi)
4- Ferroin indicator (1,10 phenanthroline, {pro analysi} + ferrous sulfate)

7.1.1.1.3 Reference Materials

1- Sucrose: (aristar) Extra pure, $C_{12}H_{22}O_{11}$ (342.30 g/mol), carbon fraction = 42.11 %
2- Activated Charcoal: (purum) In powder form, particle size 40 % ≤ µm. Contents 5 % ash and 3.5 % moisture.

7.1.1.1.4 Type of Used Water

Milli-Q plus Reagent Grade Water Purification System was used to produce high level purity water (18.2 Ωohm.cm, < 10ppb TOC, and particle-free to 0,22 µm).

7.1.1.1.5 Preparation of Solutions

1. 0.05M $FeSO_4.7H_2O$

An amount of $FeSO_4.7H_2O$ was weighed and dissolved in 500 ml milliQ water in 1L volumetric flask, then 10 ml (95-97%) H_2SO_4 was added (Schulte, 1995), and the mixture was diluted with water to the mark. The solution was stored in a dark bottle. Table A1 in the appendix, shows the preparation of ferrous sulfate solution during analysis.

2. 1N $K_2Cr_2O_7$ 6 g of $K_2Cr_2O_7$ was placed in a crucible and warmed in an oven at 105 ºC for 30 minutes. Then 4.9033 g was weighed and dissolved in 50 ml milliQ water in 100 ml volumetric flask, and the mixture was diluted with water to the mark.

3**.** *Indicator (Ferrion)*

1.484 g 1,10-phenanthroline (Monohydrate) ($C_{12}H_8N_2.H_2O$) and 0.6952 g $FeSO_4.7H_2O$ were weighed and dissolved in 100 ml milliQ water (2).

7.1.1.1.6 Standardization of $FeSO_4.7H_2O$ Solution

0.05M $FeSO_4.7H_2O$ solution is not stable in air. Therefore a standardization was carried out to determine the concentration of the solution. A mixture containing 1 ml 1N $K_2Cr_2O_7$, 5 ml (95-97%) H_2SO_4 and 5 ml of milliQ water was used for this purpose. This mixture was poured into three 50 ml conical flasks. The flasks were cooled down because of the heat of dilution. Then two drops of ferroin indicator were added to each flask and a magnetic stirrer was run (Schulte, 1995). The three replicates were titrated with 0.05M $FeSO_4.7H_2O$.

Consumed volume of the titrant (ml)

20.1
19.8 Mean = 19.9 ml
19.8

$$N = \frac{1ml * 1N}{19.9ml} = 0.0502 \text{ meq/ml} = 0.0502 \text{ M} = 0.0502\text{N}$$

During titration the color of the solution at the beginning was yellow-orange changing to dark green, depending of the amount of unreacted $Cr_2O_7^{2-}$ remaining. At this point ferrous sulfate was added drop by drop until the color shifts sharply from blue-green to wine red.

7.1.1.1.7 Maximum Oxidation Temperature

Because of high digestion temperature, some dichromate may be lost as chromic acid vapour, the first step in this method was to determine the maximum temperature for the oxidising mixture. Oxidising mixtures of potassium dichromate solution and sulphuric acid were heated at different temperatures for fifteen minutes up to 225°C on a block digester (table1 and Fig 1), then titrated with ferrous sulfate solution to determine the fraction of dichromate remaining(Chan et al., 1995).

Table 7.1 and Fig 7.1 show the fraction of dichromate remaining after heating at different temperatures. Evident loss in the remaining amount of dichromate was observed above 150°C (the reported boiling point of chromic acid). Therefore a temperature of 145°C was used as a maximum oxidation temperature during analysis.

Table 7.1 Digestion of blank reagents at different heating conditions for 15 minutes and remaining dichromate % after titration

Digestion temperature °C	Consumed volume of $FeSO_4$ during titration (ml)	Mean (ml)	Remaining dichromate %
Room	20.00 19.80 19.85	19.88	99.80*
100	19.80 19.85 19.90	19.85	99.65
125	19.85 19.80 19.85	19.83	99.55
150	19.55 19.45 19.55	19.52	97.99
175	18.65 18.85 18.95	18.82	94.48
200	17.60 16.60 17.40	17.20	86.34
225	11.90 12.70 13.00	12.53	62.90

* Remaining dichromate = $\frac{19.88ml * 0.0502N}{1ml * 1N} * 100 = 99.80\ \%$

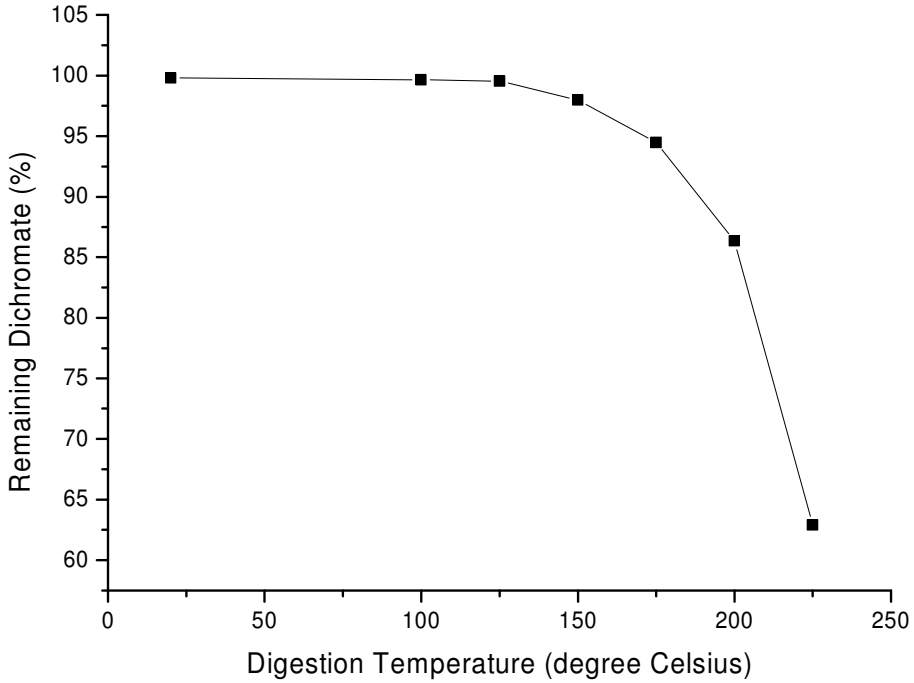

Fig 1.Fraction of acidic dichromate remaining after heating for 15 minutes

7.1.1.1.8 Reference Materials Recovery

Two materials, sucrose (extra pure, aristar) and powdered activated charcoal (purum) were used as a reference materials for OC and EC in analysis to find the optimum oxidation conditions. 0.45 mg of sucrose carbon (as 2.4% sucrose solution) or 1 mg of charcoal, were treated with oxidizing mixtures at different temperatures and for different periods of time to find out the fraction of sucrose and charcoal left under different heating conditions (Chan et al., 1995).

The same amounts of the reagents used in standardization and maximum oxidation temperature procedures were also used in determining the recovery or the fraction of oxidized sucrose carbon and charcoal carbon.
2.4% sucrose solution was prepared by dissolving 13.9100 g of sucrose in 100 ml of MilliQ water in a volumetric flask. Then a secondary sucrose solution containing 0.454 mg C/ml was prepared by adding 4.5 ml of the first solution in a 100 ml volumetric flask and dilute to the mark. Three replicates containing oxidizing mixtures and 1 ml of secondary sucrose solution were oxidized under a certain digestion conditions. After digestion the mixtures were transferred to 50 ml conical flasks and after cooling down, 5 ml water was added to each flask and titrated with 0.0506M $FeSO_4$ (Table 7.2). The same procedure was carried out with mixtures of blank reagents.

Table 7.2 The oxidized fraction of sucrose-carbon

Digestion condition	Consumed volume of $FeSO_4$ (ml) for blank reagents during titration	Mean (ml)	mmole of $FeSO_4$	Consumed volume of $FeSO_4$ (ml) for sucrose during titration	Mean (ml)	mmole of $FeSO_4$	Fraction of sucrose carbon Oxidized (%)
At room temperature for 60 minutes	19.75 19.75 19.75	19.75	0.9993	16.65 16.80 17.20	16.88	0.8541	0.96±0.04
At 100 °C for 10 minutes	19.70 19.80 19.75	19.75	0.9993	16.80 16.90 16.80	16.83	0.8516	0.98±0.004
At 100 °C for 20 minutes	19.75 19.70 19.65	19.70	0.9968	16.95 17.00 16.75	16.90	0.8551	0.94±0.02
At 100 °C for 30 minutes	19.80 19.70 19.75	19.75	0.9993	16.85 16.80 16.60	16.75	0.8475	1.00±0.02
At 100 °C for 40 minutes	19.70 19.70 19.75	19.72	0.9978	17.10 17.00 16.90	17.00	0.8602	0.91±0.03
At 145 °C for 60 minutes	19.30 19.50 19.40	19.40	0.9816	16.6 16.5 16.3	16.47	0.8334	0.98±0.05

The same procedure was carried out by using 1 mg charcoal instead of sucrose and the results are shown in Table 7.3 The concentration of ferrous sulfate, after standardization, was 0.0504 mmol/ml at room temperature and 145°C and 0.0495 mmol/ml at the other heating conditions.

Table 7.3 The oxidized fraction of charcoal-carbon

Digestion condition	Consumed volume of $FeSO_4$ (ml) for blank reagents during titration	Mean (ml)	mmole of $FeSO_4$	Charcoal mass in the replicates (mg)	Consumed volume of $FeSO_4$ (ml) for charcoal during titration	Mean (ml)	mmole of $FeSO_4$	Fraction of charcoal carbon Oxidized (%)
At room temperature for 60 minutes	19.85 19.85 19.80	19.83	0.9994	0.92 1.37 1.1 1.19	18.45 17.55 18.10 18.05	18.04	0.9092	0.24±0.01
At 100 °C for 10 minutes	20.20 20.40 20.00	20.20	0.9999	1.1 1.01 0.92	16.80 16.80 16.90	16.80	0.8316	0.46±0.03
At 145 °C for 10 minutes	20.20 20.00 20.20	20.13	0.9964	0.92 1.1 0.92	14.30 15.95 14.85	15.03	0.7440	0.73±0.2
At 145 °C for 20 minutes	20.20 20.20 20.10	20.17	0.9984	1.01 1.01 1.01	13.60 15.20 12.50	13.77	0.6816	0.89±0.19
At 145 °C for 60 minutes	18.80 18.75 18.80	18.78	0.9465	1.1 1.01 1.19 1.01	11.3 11.65 10.6 12.3	11.46	0.5776	1.02±0.05

The mass of carbon oxidized was calculated according to the following formula:

Mass of carbon oxidized (mg)

= (mmoles of $FeSO_4$ in blank titration - mmoles of $FeSO_4$ in sample titration) * $\frac{12}{4}$ ..(1)

From Table 7.3, the fraction of charcoal oxidized at room temperature is 0.24 ± 0.01, and 1.02 ± 0.05 at 145°C. From table 7.2, the fraction of sucrose oxidized at room temperature is 0.96± 0.04, and at 145 °C is 0.98 ± 0.05.

Equations for EC and OC can be derived as follows:

$$M_1 = 0.96\ OC + 0.24\ EC \ldots\ldots(2)$$

Where M_1 mass of carbon oxidised at room temperature, 0.96 carbon fraction oxidised in sucrose, and 0.24 average carbon fraction oxidised in charcoal.

$$M_2 = 0.98\ OC + 1.02\ EC \ldots\ldots (3)$$

Where M_2 mass of carbon oxidised at 145 °C, 0.98 carbon fraction oxidised in sucrose, and 1.02 carbon fraction oxidized in charcoal.

By multiplying (1) with (0.98), and (2) with (0.96), and subtracting (2) from (1), the following equations were obtained:

$$EC = 1.24\ M_2 - 1.27\ M_1 \ldots\ldots (4)$$

$$OC = 1.02\ M_2 - 1.07\ EC \ldots\ldots (5)$$

Chan et al., (1995) found other expressions for EC and OC:

$$M_1 = 1.0\ OC + 0.24\ EC$$

$$M_2 = 1.0\ OC + 1.0\ EC = TC$$

$$EC = 1.32\ (M_2 - M_1)$$

$$OC = M_2 - EC$$

7.1.1.1.9 Method Validation

The method was validated by two ways. Firstly, by determining the recovery of 1 mg OC (in the form of a sucrose solution) and about 1 mg EC (as charcoal) spiked onto glass fibre filters. Secondly, by using thermal optical transmittance carbon analyzer to determine the concentrations of OC, EC and TC, and compare them with measured concentrations by the modified Walkley-Black method (see 7.2).

1 ml of standard sucrose solution (1.1 mg/ml sucrose carbon) and an amount of charcoal around 1.1 mg were spiked into blank filters (ten pieces with an area of 1.96 cm^2) (Chan et al., 1995). A block digester was used (Tecator) and seven replicates were prepared by adding 5 ml sulfuric acid and 1 ml potassium dichromate into 7 tubes. Three of them were for blank filters, and four for spiked filters.

Digestion was performed at room temperature for one hour. After the digestion was finished, the mixtures were cooled and then 5 ml MilliQ water was added to the replicates. A titration with (0.0503mM)$FeSO_4.7H_2O$ solution and two drops indicator was proceeded (Table 7.4 and 7.5). The same procedure was repeated on another seven replicates, but the digestion temperature was 145°C (Table 7.6 and 7.7).

Table 7.4 Digestion and titration at room temperature for 1 hour for blank filters

Sample	Consumed volume of ferrous sulfate (ml)	Mean (ml)	Average mmoles of ferrous sulfate
1	19.90	19.85	0.9985
2	19.80		
3	19.95		

Table 7.5 Digestion and titration at room temperature for 1 hour for spiked filters :

Sample	Charcoal content/mg	Sucrose carbon content/mg	Reacted volume of ferrous sulfate/ml	mmoles of reacted ferrous sulfate
1	0.92	1.0998	11.0	0.5533
2	1.1	1.0998	10.30	0.5181
3	1.19	1.0998	10.15	0.5105
4	1.01	1.0998	10.70	0.5382

Table 7.6 Digestion and titration at 145 ℃ for 1 hour for blank filters

Replicates	Consumed volume of ferrous sulfate (ml)	Mean (ml)	Average mmoles of ferrous sulfate
1	19.60	19.63	0.9874
2	19.60		
3	19.70		

Table 7.7 Digestion and titration at 145 ℃ for 1 hour for spiked filters

Sample	Charcoal Content (mg)	Sucrose carbon content (mg)	Reacted volume of ferrous sulfate(ml)	mmoles of ferrous sulfate
1	1.1	1.0998	6.4	0.3217
2	1.01	1.0998	6.65	0.3343
3	1.19	1.0998	5.55	0.2788
4	1.28	1.0998	5.8	0.2914

Equation 1 was used to determine masses of carbon oxidized at room temperature and at 145 ℃ (Table 7.8):

Table 7.8 The masses of oxidized carbon during digestion and titration procedures

Sample	Mass of carbon oxidized at room temperature/mg (M_1)	Mass of carbon oxidized at 145 ℃/mg (M_2)
1	1.3356	1.9971
2	1.4412	1.9593
3	1.464	2.1258
4	1.3809	2.0880

Because there are different amounts of charcoal in the samples during analysis at room temperature and 145℃, carbonaceous species are determined by the following equations:

1- 1.3356 = 0.96 OC + 0.24 EC & 1.9971 = 0.98 OC + 1.02 (1.1/0.92) EC

2- 1.4412 = 0.96 OC + 0.24 EC & 1.9593 = 0.98 OC + 1.02 (1.01/1.1) EC

3- 1.464 = 0.96 OC + 0.24 EC & 2.1258 = 0.98 OC + 1.02 EC

4- 1.3809 = 0.96 OC + 0.24 EC & 2.0880 = 0.98 OC + 1.02 (1.28/1.01) EC

Table 7.9 The masses of OC, EC and TC

Sample	OC	EC	TC
1	1.26	0.68	2.13
2	1.32	0.71	1.91
3	1.33	0.81	2.11
4	1.27	0.65	2.29

Table 7.10 The accuracy % for OC, EC and TC measurement

Species	1	2	3	4	Average %
OC	+ 15	+ 20	+ 21	+ 15	+ 18
EC	- 25	- 35	- 32	- 49	- 35
TC	+ 5	- 13	- 8	+ 9	+ 2

Table 7.11 The average content of carbon in charcoal and sucrose

Sample	Charcoal content/mg	Sucrose content/mg	Total carbon content/mg
1	1.01	1.0998	2.1998
2	1,05	1.0998	2.2498
3	1,19	1.0998	2.3998
4	1,14	1.0998	2.3498

The samples contain different amount of charcoal carbon. Average amount of charcoal carbon in the samples = 1.1 mg, but to calculate the precision (relative standard deviation), it is necessary to take this into account.

Adjusted values for EC are (0.68*, 0.77, 0.75, 0.56)

$$* \frac{0.68 * 1.1}{1.1} = 0.68 \text{ mg}$$

Then the precision was calculated (Table 7.12):

Table 7.12 The precision of OC, EC and TC measurement

Species	Mean (mg)	Standard deviation (mg)	Precision (RSD %)
OC	1.3	0.04	± 3
EC	0.69	0.09	±13
TC	2.11	0.16	± 8

7.1.1.1.10 Determination Limit of Detection (LOD)

Field blank filters were not available, therefore laboratory blank filters were used in determining the limit of detection of modified walkley-Black method.

Limit of detection was determined by digestion of 10 samples of blank filters (10 punched pieces of a glass fibre filter for each sample = 1.96 cm^2). The blank filters were digested at two different temperatures for one hour. The same procedure was repeated for blank reagents.

After digestion at room temperature and at 145°C the samples were cooled down and 5 ml of MilliQ water was added to each sample. Blank filter samples were titrated with 0.0501N $FeSO_4$, and blank reagents samples were titrated with 0.0497N $FeSO_4$.
A magnetic stirrer was used occasionally during digestion, and a continuous,vigorous swirling was carried out during titration.

LOD Results

Table 7.13 Titration results of digested blank reagents samples and blank filter samples at room temperature

Consumed volume of $FeSO_4.7H_2O$ at room temperature for blank reagents	mmoles $FeSO_4.7H_2O$	Consumed volume of $FeSO_4.7H_2O$ at Room temperature for blank filters	mmoles $FeSO_4.7H_2O$
19.90	0,9890	19.80	0,9920
19.95	0,9915	19.80	0,9920
19.95	0,9915	19.70	0,9870
20.10	0,9990	19.90	0,9970
19.90	0,9890	19.75	0,9895
19.85	0,9865	19.70	0,9870
20.05	0,9965	19.85	0,9945
19.95	0,9915	19.80	0,9920
19.80	0,9841	19.70	0,9870
19.90	0,9890	19.80	0,9920

Table 7.14 Titration results of digested blank reagents samples and blank filter samples at 145 °C

Consumed volume of $FeSO_4.7H_2O$ at room temperature for blank reagents	mmoles $FeSO_4.7H_2O$	Consumed volume of $FeSO_4.7H_2O$ at 145 °C for blank filters	mmoles $FeSO_4.7H_2O$
19.65	0,9766	19.35	0,9694
19.50	0,9691	19.25	0,9644
19.75	0,9816	19.40	0,9719
19.55	0,9716	19.30	0,9669
19.65	0,9766	18.45	0,9243
19.45	0,9666	19.20	0,9619
19.65	0,9766	18.30	0,9168
19.70	0,9791	19.40	0,9719
19.65	0,9766	18.50	0,9269
19.60	0,9741	18.40	0,9218

The mass of carbon oxidized at room temperature and 145°C was calculated by using equation 1, Masses of EC, OC and TC per area unit were calculated by using equation 4 and 5 (Table 7.15).

Table 7.15 The masses of carbon oxidized at room temperature, and the masses of OC, EC and TC per area unit

Mass of carbon oxidised at room temperature(mg/cm^2) (M_1)	Mass of carbon oxidised at 145°C (mg/cm^2) (M_2)	OC (mg/cm^2)	EC (mg/cm^2)	TC (mg/cm^2)
-0,009	0,0216	0,0382	0,0317	0,0699
-0,0015	0,0141	0,0194	0,0159	0,0354
0,0135	0,0291	0,01894	0,0152	0,0342
0,006	0,0141	0,0099	0,0080	0,0178
-0,0015	0,1569	0,1965	0,1616	0,3581
-0,0015	0,0141	0,0194	0,0160	0,0354
0,006	0,1794	0,2148	0,1766	0,3914
-0,0015	0,0216	0,0287	0,0236	0,0523
-0,0087	0,1491	0,1959	0,1614	0,3573
-0,009	0,1569	0,2060	0,1697	0,3757

Limit of detection is determined by using the following equation:

$$LOD = S_B * k \ldots. (6)$$

Where S_B is blank standard deviation and k is a factor equal to 3 (2).

Table 16: The blank standard deviation and limit of detection for carbonaceous species

Species	S_B (mg/cm^2)	LOD (mg/cm^2)
OC	0.08	0.24
EC	0.09	0.27
TC	0.17	0.51

As it was mentioned field blank filters are not available, thus it was not possible to find LOD in mg/m^3.

7.1.1.1.11 Sample Analysis

Sampling Location

Samples were collected in Taiyuan city on the roof of a 4-floor building near the city centre.

Sample Collection

Two groups of samples were collected. The first group were collected in daytime and nighttime for 6-24 hours from 3 March to 15 March, 2004. A medium volume (100 L/min) sampler (wuhan Tianhong Intelligent Instrument Plant) was used with an impactor cutoff of 10 μm (aerodynamic diameter). Particles were sampled on Millipore glass fibre filters without binder AP40 and with a diameter of 90 mm.

The second group were in daytime and nighttime for 5-24 hours from 2 March to 16 March, 2004 (Table 7.25). A medium volume (100 L/min) sampler (wuhan Tianhong Intelligent Instrument Plant) was used with an impactor cutoff of 10 μm (aerodynamic diameter). Particles were sampled on Fluoropore (PTFE) membrane filters with a pore size of 3 μm and a diameter of 90 mm.

Mass and concentration of PM_{10}

The filters were weighed before sampling. After sampling, filters were placed folded in plastic bags and kept in a freezer. Before analysis they were taken out of the freezer and placed in a desiccator for 24 hours to remove any moisture. Mass concentration of PM_{10} were determined by calculating the ratio of the net mass of particulates to the standard air volume. Table 7.17 and 7.18 show the mass concentration and sampling conditions.

Table 7.17 The weights of unloaded and loaded filters and PM_{10} masses

Filter number	Unloaded filter weight (g)	Loaded filter weight (g)	PM_{10} mass (mg)	PM_{10} concentration ($\mu g/m^3$)
3	0.4725	0.5420	69.50	514
6	0.4705	0.5818	111.30	957
7	0.4672	0.5601	92.90	1552
8	0.4670	0.4818	14.80	215
9	0.4696	0.5141	44.50	732
10	0.4644	0.5254	61.00	631
12	0.4650	0.4980	33.00	915
13	0.4691	0.5648	95.70	852

Table 7.18 Sampling information for glass fiber filters

Sample	Apparent color	Date of sampling	Start time	Finish time	Collection duration	Wind speed (m/s) and direction	Weather	Temperature (daily average)
3	Black	3-4 Mar,2004	16:52	16:52	24 hrs	3.85 North-west[1]	Sunny	1
6	Black	8-9 Mar,2004	16:55	15:01	22 hrs and 6 min	2.95 Northwest	Sunny to cloudy	9
7	Soil	10 Mar,2004	8:08	18:09	10 hrs	4.2 Northwest	Sunny, to cloudy[2]	12
8	Gray with grid shape	11 Mar,2004	8:30	19:59	11 hrs and 29 min	2.5 North	Sunny to cloudy	8
9	Black	12 Mar,2004	8:37	18:44	10 hrs and 1 min	3.1 Northwest	Cloudy[3]	7
10	Black	12-13 Mar,2004	23:59	16:07	16 hrs and 8 min	2.95 South	Sunny to cloudy	7
12	Black	14 Mar,2004	12:45	18:46	6 hrs and 1 min	2.6 Southeast	Sunny to cloudy	8
13	Black	14-15 Mar,2004	23:59	18:44	18 hrs and 45 min	2.85 North	Sunny to cloudy	11

[1] In the eastern neighborhood of the sampling site, there is a chimney of a bathing house emitting black smoke.
[2] From 8 to 10 o'clock, there were many suspended particles in the air, around 18 o'clock, the emitted black smoke from the chimney of the bathing house was very heavy.
[3] Heavy black smoke was emitted from the chimney of the bathing house.

Air flow through sampling instrument was 100 λ/min in order to entrap only PM_{10} (Table 7.19).

Table 7.19 The volume and flow of air passed through the filters during sampling procedure

Filter number	Air volume (λ)	Air flow (λ/min)
3	135227	94
6	116309	88
7	59872	100

8	68691	100
9	60770	100
10	96639	100
12	36062	100
13	112288	100

Three replicates for blank filter and four replicates for sample filter were prepared in seven glass tubes. The filters were cut up by a punch tool which has an internal diameter of 0.5 cm. Then 10 punched pieces which have an total area of 1.96 cm^2 were placed in each tube, and 1 ml of 1N $K_2Cr_2O_7$ and 5 ml of (95-97%)H_2SO_4 was added to each tube. The mixtures were digested at room temperature for one hour. After digestion and cooling down, 5 ml of milliQ water and two drops of ferroin indicator were added and the mixtures titrated with ferrous sulfate solution (table 7.20).
Another three replicates for blank filter and four replicates for sample filter were analysed in the same manner at 145°C.

Table 7.20 Titration results

Consumed volume of ferrous sulfate during Standardization (ml)	Ferrous sulfate concentration (mmol/ml)	Filter type	Consumed volume of ferrous sulfate after digestion for 1 hr at room temperature (ml)	mmoles of ferrous sulfate	Consumed volume of ferrous sulfate after digestion for 1 hr at 145 ºC	mmoles of ferrous sulfate
20.25 20.25 19.95	0.0496	Blank	20.25 20.20 20.10	1.0010	19.50 19.55 19.35	0.9657
	0.0496	Sample 3	18.55 18.65 18.55 18.35	0.9201 0.9250 0.9209 0.9102	15.95 15.55 15.45 15.30	0.7911 0.7713 0.7663 0.7589
20.00 20.30 20.20	0.0496	Blank	19.90 20.05 19.90	0.9895	18.85 18.95 19.15	0.9414
	0.0496	Sample 6	16.45 15.80 15.85 16.55	0.8159 0.7837 0.7862 0.8209	12.40 11.15 12.40 12.10	0.6150 0.5530 0.6150 0.6002
20.05 20.00 20.00	0.0499	Blank	20.55 20.20 20.10	1.0120	19.35 19.40 19.75	0.9730
	0.0499	Sample 7	18.45 18.35 18.40 18.40	0.9206 0.9157 0.9182 0.9182	15.70 16.15 15.90 15.75	0.7834 0.8059 0.7934 0.7859
20.15 20.15 20.10	0.0497	Blank	19.95 20.10 20.00	0.9950	20.10 19.50 19.45	0.9781
	0.0497	Sample 8	19.75 19.60 19.60 19.70	0.9816 0.9741 0.9741 0.9791	18.70 18.45 18.80 19.15	0.9294 0.9170 0.9344 0.9518
20.00 19.90 20.25	0.0499	Blank	19.85 19.70 19.80	0.9870	19.40 19.00 18.95	0.9541
	0.0499	Sample 9	18.75 18.70 18.60 18.50	0.9356 0.9331 0.9281 0.9231	16.35 16.30 16.55 16.30	0.8159 0.8134 0.8258 0.8134

Table 7.20 contined.

Consumed volume of ferrous sulfate during Standardization (ml)	Ferrous sulfate concentration (mmol/ml)	Filter type	Consumed volume of ferrous sulfate after digestion for 1 hr at room temperature (ml)	mmoles of ferrous sulfate	Consumed volume of ferrous sulfate after digestion for 1 hr at 145 ℃	mmoles of ferrous sulfate
20.10 20.15 20.25	0.0496	Blank	20.15 19.90 19.95	0.9920	19.00 19.10 18.90	0.9424
	0.0496	Sample 10	18.70 18.60 18.45 18.40	0.9275 0.9226 0.9151 0.9126	15.40 15.55 15.35 15.60	0.7638 0.7713 0.7614 0.7738
20.20 20.35 20.60	0.0491	Blank	21.40 19.45 20.55	1.0051	19.05 19.30 19.20	0.9417
	0.0491	Sample 12	19.85 19.40 19.50 19.95	0.9746 0.9525 0.9574 0.9795	17.85 17.90 17.80 17.80	0.8764 0.8789 0.8740 0.8740
20.15 20.05 20.10	0.0497	Blank	20.00 20.05 20.00	0.9950	19.50 18.90 19.95	0.9667
	0.0497	Sample 13	17.60 17.50 17.40 17.50	0.8747 0.8697 0.8648 0.8697	15.35 14.90 15.15 15.80	0.7629 0.7405 0.7529 0.7853

The surface of sample filters was not totally covered with particles, so filter area covered with particles was calculated for all the samples (Table 7.22).

Table 7.22 The diameter and area of sample filter covered with particles, and the area correction factor

Filter sample	Filter diameter covered with particles (cm)	Filter area covered with particles (cm^2)
3	8.0	50.26
6	7.8	47.78
7	8.1	51.53
8	8.0	50.26
9	7.8	47.78
10	7.8	47.78
12	7.8	47.78
13	7.8	47.78

Table 7.23 Carbon mass oxidized at room temperature and 145 ºC in (mg)

Sample	Carbon mass oxidized at room temperature (M_1) in (mg)	Carbon mass oxidized at 145 ºC (M_2) in (mg)
3	6,2235	13,4317
	5,8466	14,9549
	6,1620	15,3395
	6,9851	15,9088
6	1,6958	23,8705
	15,0507	28,4047
	14,8679	23,8705
	12,3302	24,9529
7	7,2089	14,9542
	7,5954	13,1796
	7,3982	14,1655
	7,3982	14,7570
8	1,0328	3,5616
	1,6063	4,7003
	1,6063	3,1959
	1,2239	1,9234
9	3,7590	10,1069
	3,9418	10,2898
	4,3075	9,3829
	4,6732	10,2898
10	4,7171	13,0615
	5,0754	12,5130
	5,6239	13,2370
	5,8067	12,3302
12	2,2305	4,7756
	3,8468	4,5927
	3,4884	4,9511
	1,8722	4,9511
13	8,7978	14,9044
	9,1635	16,5426
	9,5219	15,6358
	9,1635	13,2663

The masses of OC are overestimated if the oxidation number is not equal to 0 as it was during analysis of reference materials. A value of an oxidation number of (- 0.45) was used to correct for OC (Chan et al,. 1995). The overestimation of OC aerosol is 4.45/4 or 11%. Thus the mass of OC in aerosols is:

$$\text{aerosol OC} = \text{OC}/1.11$$

$$\text{aerosol OC} = 0.9\ \text{OC} \quad \ldots\ldots (7)$$

$$\text{aerosol TC} = \text{aerosol OC} + \text{EC}$$

Results are given in section 8.1.

7.1.1.1.12 Uncertainty

There are various sources of uncertainties during analysis by the modified Walkley-Black method:

7.1.1.1.12.1 Carbonaceous Aerosols Sampling Artifacts

The organic aerosols consist of a complex mixture of many compounds with a wide range of vapor pressure, sorption properties, and chemical stabilities. Therefore the sampling process has the potential for several sampling artifacts (Tsitouridou, 2004). These may include the following :

1- A portion of the organic vapour phase may sorb onto the filter surface or on the deposited particulate matter. This is often called the "positive" artifact because the apparent mass that would be collected and measured is greater than the aerosol mass that existed in the volume of the atmosphere sampled.
2- The sampling process may change the gas-solid distribution of the sample being collected, which results in volatilization of some of the particulate organic compounds. This produces a negative artifact.
3- The collected particulate matter may chemically react with vapour components (e. g. O_3 and NO_2) that pass through the filter during sampling to change the chemical composition of the deposit. This can result in positive or negative artefacts, especially if individual chemical compounds or chemical functionalities are being measured.

These sampling artifacts complicate the organic aerosol measurements, and it is difficult to separate the different competing artifact processes (Roy et al., 1994)..
An adsorbant material can be added inside the impactor like Al_2O_3 to minimize negative artifacts as much possible (Pitts and Pitts, 1986).

7.1.1.1.12.2 Oxidation Number

The oxidation number is another source of uncertainty. A value of - 0.45 was used (Chan et al., 1995). This value is the average oxidation number of 66 organic compounds. The source of these compounds is not coal combustion but car exhaust. This may cause uncertainty because the oxidation number for organic compounds from coal combustion is definitely different.

7.1.1.1.12.3 Interference possibility

There are some elements in the aerosols such as Fe may interfere the measurements (Chow, 2004). Chlorides, if present, reduce $Cr_2O_7^{2-}$ and lead to the overestimation of carbon matter (Chan et al., 1995).

7.1.2 Thermal Optical Transmittance (TOT) Method

7.1.2.1 Theory

The modified Walkley-Black method was validated by comparing with results obtained using thermal optical transmittance carbon analyzer. The thermal/optical OC/EC analysis method was performed using a Sunset Laboratory Instrument. The instrument follows the thermal protocol, NIOSH, (National Institute of Occupational Safety and Health) with a change in maximum temperature in the first analysis procedure (620°C rather than 850°C), and adopts the transmittance method to determine the particulate OC and EC collected on quartz or glass fiber filters (Chow et al., 2001).

The method consists of two procedures:

1- A certain area often 1-0.5 cm^2 of a sample filter is inserted in the instrument and heated stepwise up to 620°C in a non-oxidizing He-atmosphere. Some of the organic carbon is pyrolized to black carbon, resulting in darkening of the filter. Red light from a He-Ne laser was monitors the darkening and measures the transmittance.

Evolved carbon is catalytically oxidized to CO_2 gas in a bed of granular manganese dioxide (MnO_2). The CO_2 is swept out of the oxidizing oven in the helium stream and mixed with hydrogen gas.

This mixture then flows through a heated nickel catalyst where it is quantitatively converted to methane. The methane is subsequently measured using a flame ionization detector (FID).

2- Two per cent oxygen is added to He. The temperature is increased stepwise up to 890°C. The original and pyrolized black carbon is combusted and the transmittance returns to its original value.

The point at which the transmittance is reduced to its original value is called “split point”. Any EC detected before this point is said to have been formed pyrotically by charring of the organic carbon. This carbon is subtracted from the EC area observed during the oxidizing phase of the analysis and is assigned as OC.

The instrument is calibrated with known quantities of CH_4 every day.
The minimum limit of detection of sunset laboratory instrument is 0.2 $\mu g/cm^2$ and the maximum is 200 $\mu g/cm^2$. Fig 7.2 shows the analysis profile for the thermal optical transmittance carbon analyzer.

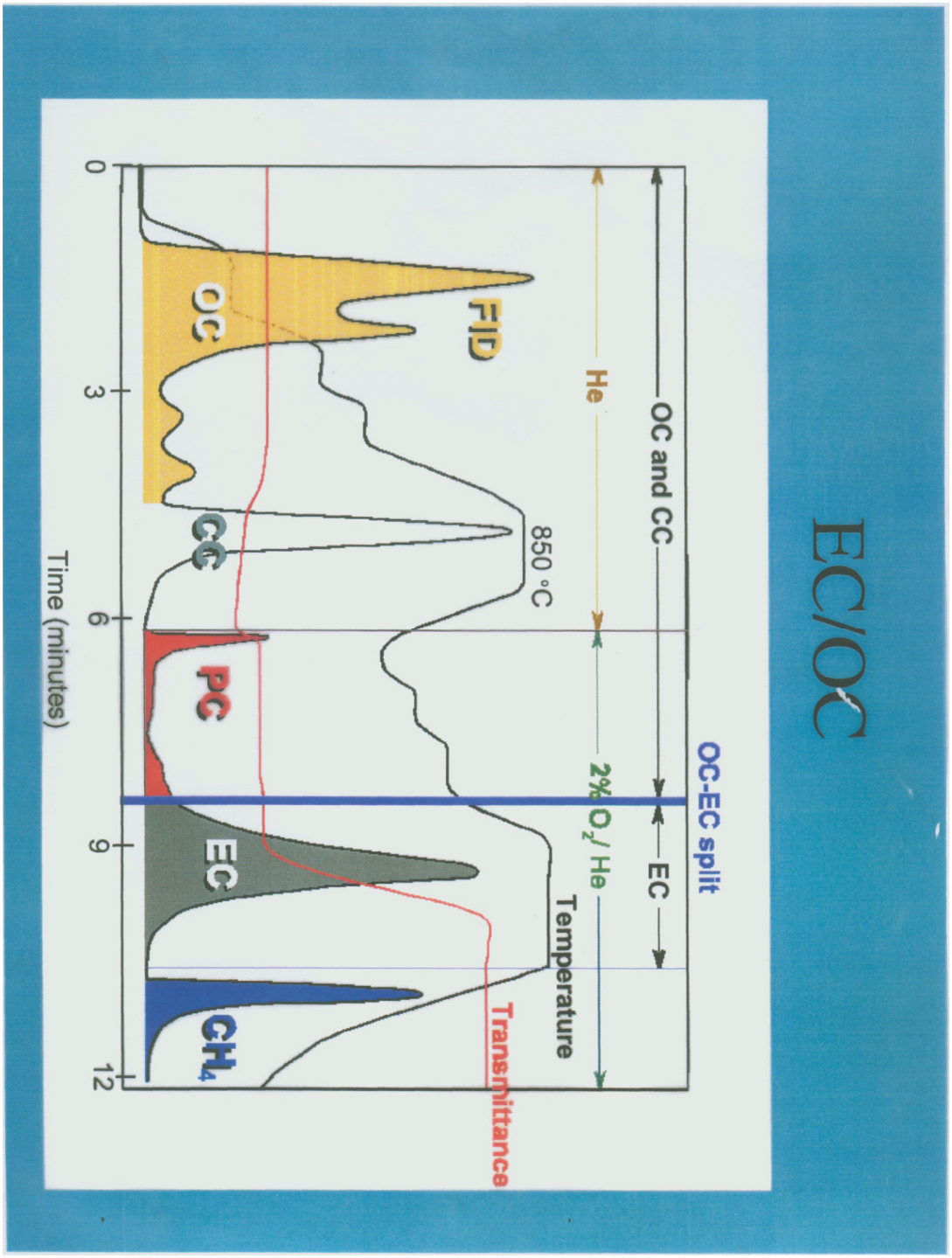

Fig 7.2 Analysis profile for thermal optical transmittance carbon analyzer

Flame Ionization Detector (FID)

The produced methane gas in the carbon analyzer is mixed with hydrogen. The gaseous mixture enters the detector and undergoes combustion in an atmosphere of excess air. Ions and free electrons are formed in the reducing part of the flame. A voltage is applied between a positive electrode (Collector) and a negative electrode (flame tip). A small current which is proportional with the amount of combusted carbon is generated. This signal is amplified in an electrometer (Greibrokk et al., 1998).

7.1.2.2 Experimental

A punch was used to cut an 1 cm^2 area from a quartz filter. The piece was placed on a platform. Then the platform was inserted inside a quartz oven. A cleaning procedure was run by purging the oven with helium, a stepped temperature ramp increased the oven temperature to 620 °C . Then the oven was cooled down to 340 °C and a new stepped temperature ramp increased the oven temperature to 890 °C. This step was achieved to clean the quartz piece from any background amount of OC or EC.

Then one piece with an area of 1 cm^2 was cut up from a blank glass fibre filter and placed on the cleaned quartz punch onto the platform and the same procedure mentioned above was repeated.

Sucrose solutions with concentration of 200 μg and 300 μg carbon were used to know the performance of the instrument. 20 μL from each solution was injected onto a separated cleaned piece of quartz filter and placed in the instrument and run by the same procedure.

The samples were analyzed also by the same. The operating temperature of the glass fiber filter was 550°C. It was preferable to put a glass fiber piece on a quartz punch to prevent the smelted glass fiber to stick on the platform.

7.2 Elemental Analysis

Mass and concentration of PM_{10}

The filters were weighed before sampling. After sampling, filters were placed folded in plastic bags and kept in a freezer. Before analysis they were taken out of the freezer and placed in a dessicator for 24 hours to remove any moisture. Mass concentrations of PM_{10} were determined by calculating the ratio of the net mass of particulates to the standard air volume. Table 7.24 and 25 show the mass concentration and sampling conditions.

Table 7.24 The weights of unloaded and loaded Teflon filters and PM_{10} masses and concentrations

Sample	Unloaded filter weight (g)	Loaded filter weight (g)	PM_{10} mass (mg)	PM_{10} concentration ($\mu g/m^3$)
2	0.20878	0.23001	21.23	151
6	0.21645	0.24264	26.19	188
7	0.20788	0.25068	42.80	301
8	0.20683	0.24801	41.18	462
9	0.19124	0.24117	49.93	914
10	0.20644	0.21979	13.35	208
3	0.21301	0.22952	16.51	374
11	0.21946	0.23600	16.54	807
12	0.20381	0.22199	18.18	624
13	0.20879	0.23826	29.47	545
14	0.18105	0.20935	28.30	979

Table 7.25 Sampling information for Teflon filters

Sample	Apparent color	Date of sampling	Start time	Finish time	Collection duration	Wind speed (m/s) and direction	Weather	Temperature daily) (average
2	Dark gray	2-3 Mar,2004	15:41	15:41	24 hrs	3.85 Northwest	Sunny [1]	0
6	Dark gray	4-5 Mar,2004	9:41	9:41	24 hrs	4.75 Northwest	Sunny	0
7	Dark gray	5-6 Mar,2004	9:59	9:59	24 hrs	4 Northwest	Sunny to cloudy	-2
8	Black	8-9 Mar,2004	16:55	15:03	22 hrs and 8 mins	2.95 Northwest	Sunny to cloudy	9
9	Light brown with grid shape	10 Mar,2004	8:08	18:08	10 hrs	4.2 Northwest	Sunny, sometimes cloudy	12
10	Light gray	11 Mar,2004	8:31	19:58	11 hrs and 27 mins	2.5 North	Sunny to cloudy	8
3	Dark gray	13 Mar,2004	7:52	16:03	8 hrs and 11 mins	2.8 South	Sunny to cloudy	8
11	Dark gray	14 Mar,2004	8:25	12:28	3 hrs and 58 mins	2.6 Southeast	Sunny to cloudy	8
12	Dark gray	14 Mar,2004	12:45	18:10	5 hrs and 25 mins	2.6 Southeast	Sunny to cloudy	8
13	Dark gray	15 Mar,2004	8:30	18:42	10 hrs and 45 mins	2.8 North	Sunny to cloudy [2]	14
14	Dark gray	16 Mar,2004	10:42	17:42	7 hrs	3.4 Southeast	Sunny to cloudy [3]	13

[1] At 16:30 of March 2, snowfall lasted 15 minutes with strong wind. The wind seemed to be more than 6 grade.

[2] There was large amount of re-suspended dust in air

[3] There was large amount of re-suspended dust in air

Air flow through sampling instrument was 100 λ/min in order to entrap only PM_{10} (Table 7.26).

Table 7.26 The volume and flow of air passed through the Teflon filters during sampling procedure

Filter number	Air volume (λ)	Air flow (λ/min)
2	140580	100
6	139556	97
7	142361	100
8	89060	73
9	54641	100
10	64207	101
3	44116	100
11	20492	96
12	29125	100
13	54078	100
14	28920	78

7.2.1 Microwave Digestion

7.2.1.1 Theory

The purpose of using a microwave oven is to dissolve elemental particles present in a sample and obtain a homogeneous solution prior to instrumental analysis.
The microwave oven contains a magnetron that produces microwaves. A vessel containing a mineral acid or a mixture of mineral acids with the sample of interest, is subjected to the microwaves. The mineral acids have the ability to convert microwave energy to heat and thus can dissolve the sample to a homogeneous solute

7.2.1.2 Experimental

Digestion by microwave oven is a good technique to get a complete sample dissolution prior to analysis. Microwave digestion can be achieved without any loss of volatile analyte species, and the chance of contamination is small.

Airborne particles were digested by using a 5 ml digestion mixture consisting of HNO_3 + HF at 172 °C in closed PTFE bombs. Nitric acid is useful to decompose organic compounds and to oxidize metals. Hydrofluoric acid is added to dissolve some minerals, such as alumsilicates and Ti compounds

A standard reference material (SRM1648) is used as a control material to evaluate the methods used in the analysis of atmospheric particulate matter. It consists of natural atmospheric particulate matter collected at an urban location. The certified values are based on measurements of 6 to 30 samples by several modern analytical methods (NIST, 1998). To

determine the accuracy and precision of our measurements, recovery experiments were conducted by comparing the observed results with the certified values.

Blank filters and blank reagents were used during digestion to check the background concentration and any possible contamination. HNO_3 (65%) and HF (40%) were Suprapur (Merck, Germany). Milli-Q plus Reagent Grade Water Purification System was used to produce high level purity water (18.2 Ωohm.cm, < 10ppb TOC, and particle-free to 0,22 μm).

All containers and vessels are made of PTFE or PFA materials. They were immersed in 10% HNO_3 acid overnight and rinsed with Milli-Q water prior use.

The samples were digested by using a Milestone microwave oven (ETHOS PLUS), equipped with temperature sensor and controlled by a personal computer. Filters loaded with airborne particles (6-41 mg) or equivalent SRM 1648 were placed in closed PTFE vessels with 5 ml of HNO_3 + HF (5+1) and digested in the microwave oven according to the following programme:

Step	Temperature (°C)	Time (min)	Power(W)
1	172	15	1000
2	172	15	1000
3, ventilation		10	0

After cooling, the vessels were opened and the digested solutions were diluted with 50 ml water. Then the vessels were closed again and kept at room temperature overnight to dissolve the fluorides completely.

7.2.2 Inductively Coupled Plasma-Atom Emission Spectrometry (ICP-AES)

7.2.2.1 Theory

ICP-AES is an analytical technique used in simultaneous multielement determination for about 70 elements at concentration levels below one ppm. It is based on using a high temperature plasma in atomization or ionization of a sample present in an aqueous or organic solution. Plasma is a mixture of atoms, ions and electrons (in case of Ar-plasma, the temperature ranges 6000-10000 K and consists of Ar-atoms > 99 % and Ar-ions < 0.1 %). The concentrations of ions and electrons are such that the net charge approaches zero (Skoog et al., 1998).
Fig 7.3 shows a schematic diagram of ICP-AES instrument (Varian Vista AX CCD)

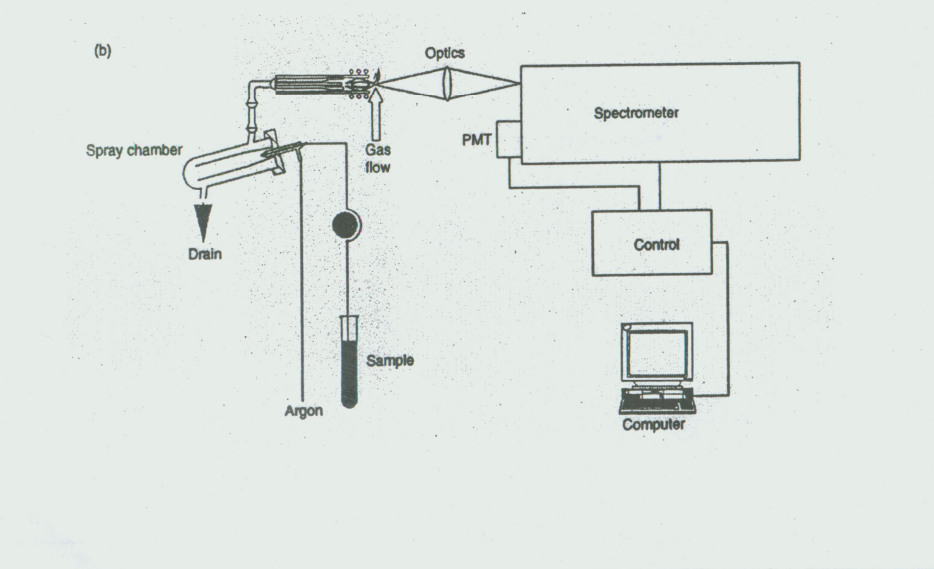

Fig 7.3 Schematic diagram of ICP-AES instrument (Varian Vista AX CCD)

Plasma Formation

A stream of Ar-gas is directed in a torch consisting of three concentric tubes made of quartz. A copper coil, called the load coil, surrounds the top end of the torch and is connected to a radio frequency (RF) generator.
When RF power (typically 700-1500 watts) is applied to the load coil, an alternating current oscillates at a rate corresponding to the frequency of the generator (frequency ranges from 27 to 40 MHz). This RF oscillation of the current in the coil causes RF electric and magnetic fields to be set up in the area at the top of the torch. With Ar-gas being swirled through the torch, a spark is applied to the gas causing some electrons to be stripped from their Ar-atoms. These electrons are then caught up in the magnetic field and accelerated by them. Adding energy to the electrons by the use of a coil in this manner is known as inductive coupling. These high-energy electrons in turn collide with other Ar-atoms, stripping off still more electrons. This collisional ionization of the argon gas continues in a chain reaction, breaking down the gas into a plasma consisting of argon atoms, electrons, and argon ions, forming what is known as an inductively coupled plasma (ICP) discharge. The ICP discharge is then sustained within the torch and load coil as RF energy is continually transferred to it through the inductive coupling process (Boss and Fredeen, 1999). Fig 7.4 shows the principle of plasma formation.

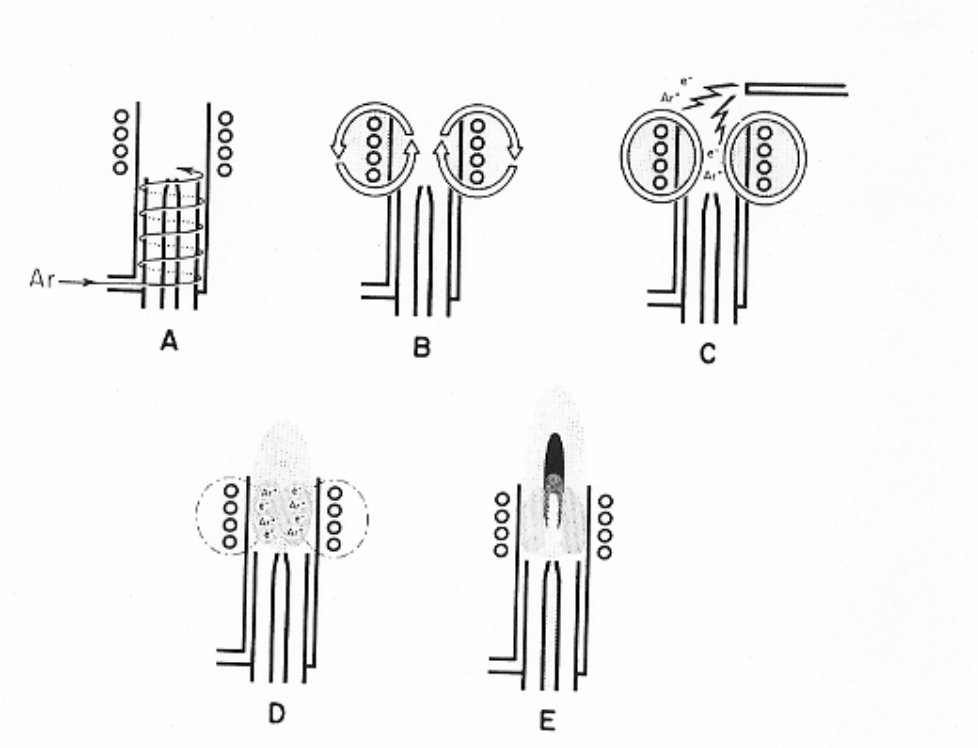

Fig 7.4 Cross section of an ICP torch and load coil depicting an ignition sequence. **A**- Argon gas is swirled through the torch. **B**- RF power is applied to the load coil. **C**- A spark produces some free electrons in the argon. **D**- The free electrons are accelerated by the RF fields causing further ionization and forming a plasma. **E**- The sample aerosol-carrying nebulizer flow punches a hole in the plasma.

Sample Introduction

The sample is usually fed into the instrument as a stream of liquid sample. Inside the instrument, the liquid is converted into an aerosol through a process known as nebulization. The sample aerosol is then transported to the plasma where it is desolvated, vaporized, atomized, and excited and/or ionized by the plasma. The excited atoms and ions emit their characteristic radiation which is collected by a polychromator that sorts the radiation by wavelength. The radiation is detected by charge-coupled device (CCD) and turned into electronic signals that are converted into concentration data (Boss and Fredeen, 1999).

Charge-Coupled Device (CCD) Detector

Charge-coupled device (CCD) is based on the light sensitive properties of solid-state silicon and belongs to the broad class of silicon-based devices called charge transfer devices (CTD). CTD contains a block of very high purity crystalline silicon. The silicon-silicon bond may be broken by energy of sufficient strength such as photons with visible or ultraviolet wavelength, (photons are emitted when excited atoms or ions from an analyte return back to their ground state). When the bond is broken, an electron is released within the lattice structure and a subsequent hole in the crystalline structure is formed. This is called an electron-hole pair.

This electron and hole can move within crystalline lattice by applying a voltage and create a current which is proportional to the amount of photons impinging on the structure.

7.2.2.2 Experimental

Major and minor elements such as Al, Ca, Fe, K, Mg, Na, Pb, Ti, Zn were measured by using Inductively Coupled Plasma- Atomic Emission Spectrometer.
ICP-AES instrument was calibrated by the external calibration method. A multielement standard solution was used to prepare three standard solutions. The multielement standard solution consists of the following elements; Al, B, Ca, Cr, Co, Cu, Fe, Pb, Mg, Ni, P, K, Si, Na, Sn, Ti, V, Zn and Zr. The concentration of each element is 50 µg/ml. Three standard solutions were prepared with elemental concentrations of 16,667 ppm, 8,333 ppm, 4,545 ppm and 3% HNO_3 acid was used during standard preparation. Sample, standard solution, blank reagents and blank filter replicates were analyzed in three batches.

Table 7.34 ICP-AES Operating Conditions

Insrument	Varian Vista AX CCD
RF power	1250W
Plasma flow	15 L/min
Auxiliary flow	1 L/min
Nebulizer flow	0,7 L/min
Replicate read time	4s
Instrument stabilization delay	15s
Sample uptake delay	15s
Pump flow rate	1 ml/min
Rinse time	15s
Replicates	3
Calibration method	External
Type of detector	CCD
Type of nebulizer	V-groove

For each element a proper analytical wavelength was chosen to determine the concentration of the element (Table 7.35).

Table 7.35 Analytical wavelength used for each element

Element	Wavelength (nm)
Al	396.152
Ca	317.933
Fe	259.940
K	766.491
Mg	280.270
Na	588.995
Pb	220.353
Ti	334.941
Zn	213.857

7.2.3 Inductively Coupled Plasma-Mass Spectrometry (ICP-MS)

7.2.3.1 Theory

ICP-MS is another analytical technique for simultaneous multielement determination at concentration levels below one ppb or ppt. In this instrument, the ICP torch, which operates at atmospheric pressure, is coupled with the mass spectrometer that requires a pressure of less than 10^{-4} torr. This coupling is achieved by using a series of cones.

In this technique, the principle is based on the separation of ions formed in the ICP torch according to their mass/charge ratios (m/z), where m is the mass of the ion in atomic mass units and z is its charge, and counting the number of ions of each type or measuring the ion current produced when the ions formed from the sample strike a suitable transducer. The ions are usually singly charged positive ions, so that the m/z ratio is simply equal to the mass of the ion (Skoog et al., 1998).

When a sample is atomized and ionized in the ICP-torch, the formed ions enter a quadrupole mass spectrometer, where the positive ions are separated from electrons and molecular species by an applied negative potential, then they are accelerated towards a quadrupole filter which allows only ions with one particular mass-to-charge ratio to reach the detector. By varying the applied potential, ions of different masses are selected to reach the detector. The detector converts the beam of selected ions to an electrical signal proportional to the concentration (Skoog et al., 1998).

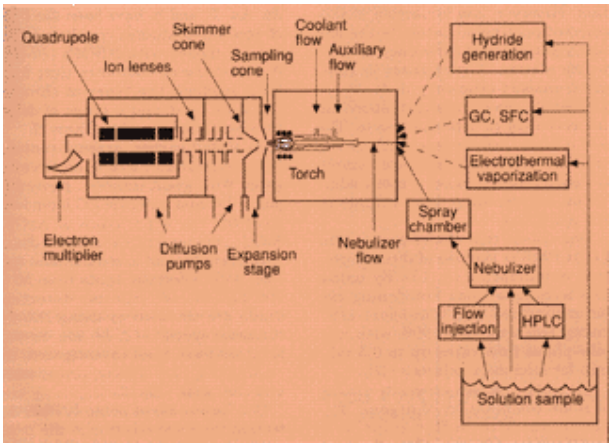

Fig 7.5 Schematic diagram of an ICP-MS system

7.2.3.2 Experimental

Trace elements such as As, Co, Cu, Mn, Ni, Sb, Se, V, Bi, Sn were measured by using Inductively Coupled Plasma-Mass Spectrometer.
ICP-MS was calibrated by the standard addition method. A multielement standard solution was used to prepare three standard solutions. The multielement standard solution consists of the following elements; As, Bi, Ga, Ge, In, Pb, Sb, Se, Sn, Te, Ti and V. The concentration of each element is 50 µg/ml. Three standard solutions were prepared with elemental concentration of 50 ppb, 5 ppb and 3% HNO_3 acid was used during standards preparation.

Table 7.36 ICP-MS Operating Conditions

Instrument	Perkin-Elmer SCIEX Elan Model 5000
Forward power	1000W
Plasma flow	Ar 15 L/min
Nebulizer flow	~ 0,91 min^{-1}
Sample uptake rate	1 ml/min
Scanning mode	Peak hop
Operating pressure	$1{,}25.10^{-5}$
Dwell time	100ms
Replicate time	200ms
Ion lenses	Optimized on ^{24}Mg, ^{103}Rh and ^{208}Pb
Sweeps/Reading	2
Readings/Replicate	1
Number of replicates	3
Points across peak	1
Baseline time	0ms
Polarity	+
Calibration method	External
Type of mass spectrometer	Quadrupole

Table 7.37 Masses of selected elemental isotopes and the analytical ratio (m/z) used

Element	Isotope mass	m/z
As	75	75
Co	59	59
Cu	63	63
Mn	55	55
Ni	58	58
Sb	121	121
Se	80	80
V	51	51
Bi	209	209
Sn	120	120
Pb	208	208

Where m is the mass of the selected elemental isotope, z is the charge of the elemental ion, equal to 1 in all cases.

8. Results and Discussion

8.1 Comparison of modified Walkley-Black method and Thermal Optical Transmittance Carbon Analyzer

Table 8.1 Table 8.2 show respectively the concentrations of OC, EC and TC measured by the modified Walkley-Black method, and by the thermal optical carbon analyzer. The results are compared in Tables 8.3 and 8.4.

Table 8.1 Concentration of PM_{10}, OC, EC, TC and the ratios EC/TC, OC/EC and TC/ PM_{10} obtained by the modified Walkley-Black method

Sample	OC $\mu g/m^3$	EC $\mu g/m^3$	TC $\mu g/m^3$	OC/EC	EC/TC	TC/PM_{10} %
3	26.57±3.86	77.50±8.59	104.08±7.48	0.34	0.74	20
6	84.44±13.26	119.47±20.52	203.91±17.53	0.71	0.59	21
7	32.90±4.82	69.19±17.33	102.09±13.46	0.48	0.68	7
8	8.13±5.34	47.56±15.02	55.68±12.04	0.17	0.85	26
9	43.37±8.58	94.98±12.84	138.35±6.94	0.46	0.69	19
10	36.31±6.78	68.76±9.70	105.07±4.39	0.53	0.65	17
12	59.91±33,08	65.71±36.94	125.62±5.31	0.91	0.52	14
13	62.69±4.16	62.99±14.96	125.68±11.88	1.00	0.50	15
Average	44.29±23.94	75.77±22.15	120.06±42.05	**0.58**	**0.63**	**17**

Table 8.2 Concentrations of OC, EC,TC obtained using the thermal optical carbon analyzer

Sample	Species	$\mu g/cm^2$	Mean $\mu g/cm^2$	µg	$\mu g/m^3$
3	OC	106.36 102.27	[1] 101,855	5224,1429	37.86±1.07
	EC	124.90 119.66	122.28	6271.7412	45.45±1.38
	TC	231.26 221.93	[2] 224,135	11495,8841	83.30±2.45
6	OC	256.28 221.62	236,645	11538,8102	97.15±10.07
	EC	191.37 176.98	184.175	8980.373	75.66±4.18
	TC	447.65 398.61	420,67	20511,8692	172.81±14.25
7	OC	141.31 76.30	106.345	5479.9578	91.53±39.56
	EC	128.71 120.59	124.65	6423.2145	107.28±4.94
	TC	270.02 196.89	230.995	11903.1723	198.81±44.51

Table 8.2 continued

8	OC	22,31 16.24 17,25	16,14	827,8206	12.11±2.44
	EC	23.45 16.81 19.90	20.05	1028.3645	15.04±2.49
	TC	45.77 33.05 37.15	38.66	1982.8714	27.15±4.87
9	OC	89.34 82.84 73.06	79.2867	3788.3185	62.34±6.44
	EC	68.89 80.45 70.33	73.2233	3498.6009	57.57±4.95
	TC	158.23 163.29 143.39	152.51	7286.9278	119.91±8.13
10	OC	94.98 106.93 99.73	98.0867	4686.5825	48.50±2.97
	EC	87.31 68.17 94.31	83.2633	3978.3205	41.17±6.70
	TC	182.29 175.09 194.04	181.3467	8664.7453	89.66±4.73
12	OC	48.92 48.43 48.82	46.2633	2210.4605	61.30±0.34
	EC	44.37 46.06 47.48	45.97	2196.4466	60.91±2.06
	TC	93.29 94.49 96.29	92.23	4406.7494	122.20±2.00
13	OC	167.83 203.53 180.26	181.4133	8667.9275	77.19±7.71
	EC	86.46 74.80 92.53	84.5967	4042.0303	36.00±3.83
	TC	254.29 278.34 272.79	266.0133	12710.1155	113.19±5.36

[1] Mean value was subtracted from the OC content in (2.46 μg/cm^2) in the blank filter.

[2] Mean value was subtracted from the OC content in the blank filter.

Table 8.3 Comparison of results between the modified Walkley-Black method and thermal/optical transmittance method

Sample	Thermal/optical transmittance (TOT) carbon analyzer			Modified Walkley-Black (MWB) method		
	OC μg/m^3	EC μg/m^3	TC μg/m^3	OC μg/m^3	EC μg/m^3	TC μg/m^3
3	37.86	45.45	83.30	26.57	77.50	104.08
6	97.15	75.66	172.81	84.44	119.47	203.91
7	91.53	107.28	198.81	32.90	69.19	102.09
8	12.11	15.04	27.15	8.13	47.56	55.68
9	62.34	57.57	119.91	43.37	94.98	138.35
10	48.50	41.17	89.66	36.31	68.76	105.07
12	61.30	60.91	122.20	59.91	65.71	125.62
13	77.19	36.00	113.19	62.69	62.99	125.68
Average	**61.00**	**54.89**	**115.88**	**44.29**	**75.77**	**120.06**

Table 8.4 Comparison of the ratios OC/EC, EC/TC, TC/ PM_{10} between the modified Walkley-Black method and thermal/optical transmittance method

Sample	Thermal/optical transmittance (TOT) carbon analyzer			Modified Walkley-Black (MWB) method		
	OC/EC	EC/TC	TC/PM_{10} %	OC/EC	EC/TC	TC/PM_{10} %
3	0.83	0.55	16	0.34	0.74	20
6	1.28	0.44	18	0.71	0.59	21
7	0.85	0.54	13	0.48	0.68	7
8	0.81	0.55	13	0.17	0.85	26
9	1.08	0.48	17	0.46	0.69	19
10	1.18	0.46	15	0.53	0.65	17
12	1.01	0.5	14	0.91	0.52	14
13	2.14	0.32	13	1.00	0.50	15
Average	**1.14**	**0.48**	**15**	**0.58**	**0.63**	**17**

The variation in carbonaceous species concentrations (Table 8.3) may be due to many factors:

a- Fluctuation in emission sources (Yu et al., 2004)
b- Stagnation period (temperature inversion) (Salam et al., 2000)
c- Variation in mixing height (planetary boundary layer thickness) (Salama et al., 2004)
d- Variation in wind speed and direction (Yu et al., 2004)
e- Long-range transport (Na, 2004)
f- Different atmospheric lifetimes of OC and EC (Dan et al., 2004)
g- Variation in wet and dry deposition
h- Inhomogeneous distribution of particles on the filter surface.

From Table 8.3, one can see that the carbonaceous species are an important component of particles in Taiyuan urban area. The mass percentage of OC, EC and TC to the total

suspended particles (PM_{10}) measured by thermal optical transmittance method are averagely accounting for 8 ± 1 %, 7 ± 1 % and 15 ± 2 % respectively.

8.1.1 Underestimation and Overestimation

The methods give quite similar TC values. However, the modified Walkley-Black method gives lower OC-concentrations and higher EC-concentrations in comparison with the results obtained by thermal transmittance method.

The EC and OC fractions are not well defined and it is to be expected that two methods that are so different give somewhat different results. Underestimation of OC may be due to loss in the particles during cutting of the sample filters. This applies to both methods. An actual oxidation number less than our chosen value (- 0.45) may cause underestimation of OC in the W-B method. There is a slight loss of dichromate at 145 °C. If the loss is different in analyses of samples and blanks, this will cause an error. We found it very difficult to find a correction for this effect. Also underestimation of OC may occur due to the presence of organic oxygen according to the following reaction (Schulte, 1995):

$$RCOOH \xrightarrow{Dissociation} RH + CO_2$$

Overestimation of EC in the W-B method may due to interferences from the aerosols such as Fe, presence of chlorides in the samples, and oxidation of the indicator by sulphuric acid if the digested mixtures were not cooled down sufficiently. Chlorides in the samples may react with dichromate and produce Chlorine and Cr^{+3}.

8.1.2 PM_{10} and TSP

The PM_{10} fraction in total suspended particles (TSP) is about 70 % (Aunan et al., 2005), and the average measured mass concentration of (PM_{10}) is 796 $\mu g/m^3$. So the average mass concentration of TSP is about 1137 $\mu g/m^3$ in Taiyuan city during sampling time. This is 47 % higher than the average mass concentration in 1998 of 600 $\mu g/m^3$ (U.S. embassy Beijing, 2001). This may be a result of increase in anthropogenic activities in the urban area or that the selected period had higher concentrations than the rest of the year.

In Taiyuan city the background level of total suspended particles (TSP) has been estimated to 200 $\mu g/m^3$ in winter and 110 $\mu g/m^3$ in summer. With a PM_{10} fraction of 70 % this gives a background PM_{10} level of 140 $\mu g/m^3$ in winter and 77 $\mu g/m^3$ in summer (Aunan et al., 2005). Comparison of this value with the average measured mass concentration of PM_{10}, 796 $\mu g/m^3$, indicates that a large part of PM_{10} is produced by anthropogenic sources, mainly coal combustion. This value is much higher than the PM_{10} standards suggested by US Environmental Protection Agency which are 150 $\mu g/m^3$ for 24 hours exposure and 50 $\mu g/m^3$ for annual average (EPA, 2001).

Background level of TSP may originate from natural sources or long-range transport from anthropogenic sources. The prevailing wind direction is northwest during sampling time. This can bring pollutants from Northern Shanxi and its economic centre "Datong". Datong is the second largest city in Shanxi. Northern Shanxi is one of the main coal mining regions in China, and mining and coking are major air pollution sources in the area. The city of Datong also has machine-building and building-materials industries, as well as a substantial cement production (Aunan et al., 2004).

Fig 8.1 and 8.2 show mass concentration of TC and PM_{10} measured by the modified Walkley-Black and thermal optical transmittance methods

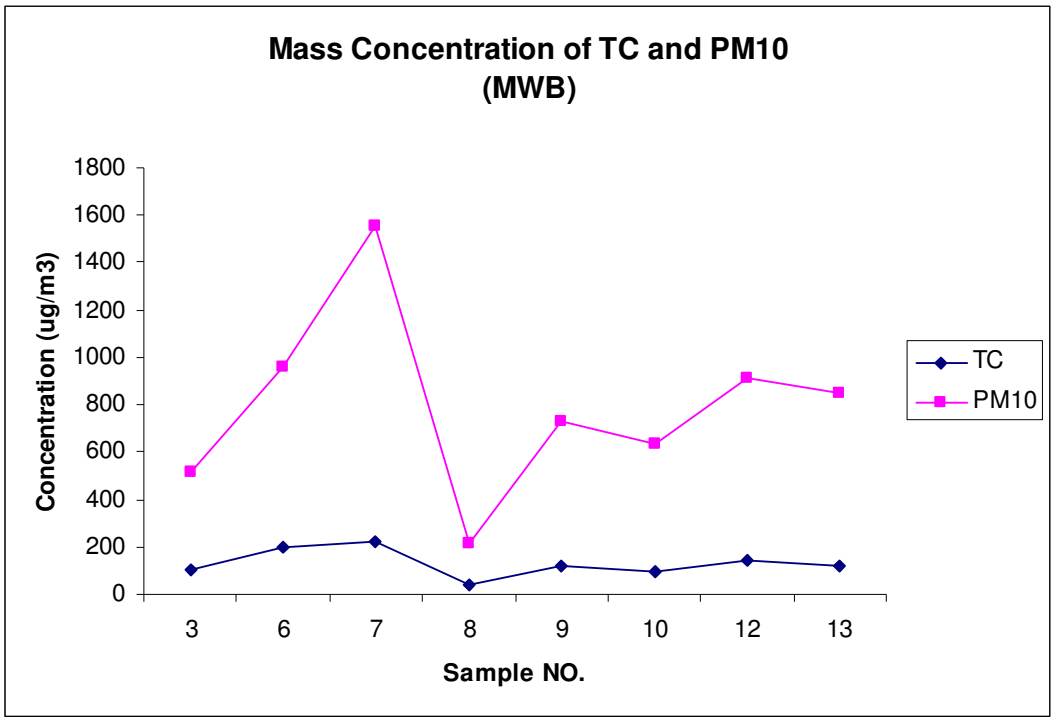

Fig 8.1 Mass concentration of PM_{10} and TC measured by modified Walkley-Black method

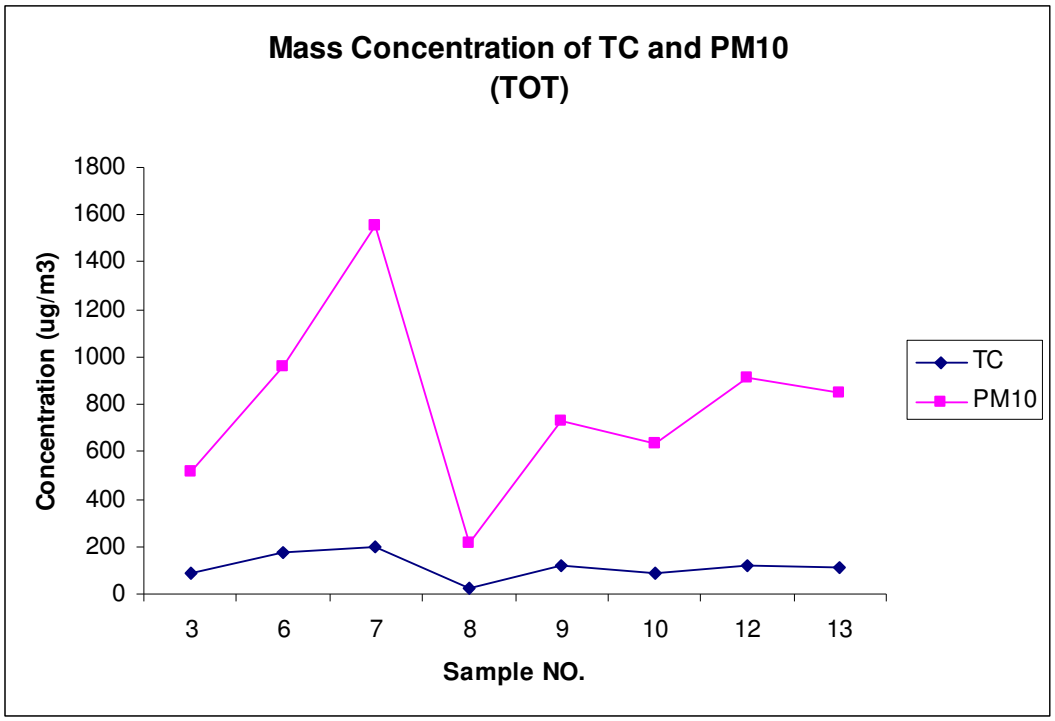

Fig 8.2 Mass concentration of PM_{10} and TC measured by thermal optical transmittance method

8.1.3 EC/TC Ratio

When there are many sources of EC-emissions, EC/TC ratios are normally in the range 0.6-0.7 (Salam, 2003). The average value of EC/TC ratio is 0.48 by the thermal optical transmittance method (Table 8.4). This value is consistent with the presence of primary sources of carbonaceous species mainly related to coal activities (Tsitouridou, 2004).

The average ratio of EC/TC is 0.63 by modified Walkley-Black method, which does not seem consistent with the situation in Taiyuan.

There is no international air quality standard for EC, but there is a tentative guideline value of 8 $\mu g/m^3$ in Germany (Salam et al., 2003). The average EC-concentration in Taiyuan urban area is about 7 times higher than the threshold, indicating a high load of black smoke.

8.1.4 OC/EC Ratio

The average OC/EC ratio is 1.14 by thermal optical transmittance method (and as low as 0.58 by the W-B method), indicating high emission of EC, while in other Chinese cities this ratio is generally larger than 2 (Dan et al., 2004), see Table 8.5. High emissions of EC are attributed to high consumption of coal, inefficient PM collection devices in the power sector and non-controlled residential coal stoves (Streets et al., 2001). Low emissions of OC can be attributed to sampling technique, where no procedure was used to entrap volatile organic compounds which caused negative artefacts. Also there is a possibility of sample loss during storage.

8.1.5 Correlation Between OC and EC

Fig 8.3 and 8.4 show clearly that OC-concentrations correlate closely with EC-concentrations in both methods, except for samples nr.12 and 13 in MWB and samples nr. 7 and 13 in TOT. The regression coefficient R is ~ 0.66 for modified Walkley-Black and 0.8 for thermal optical transmittance (Fig 8.5 and 8.6). This indicates that there is a dominant primary source of carbonaceous species emissions, represented by coal combustion (Na, 2004).

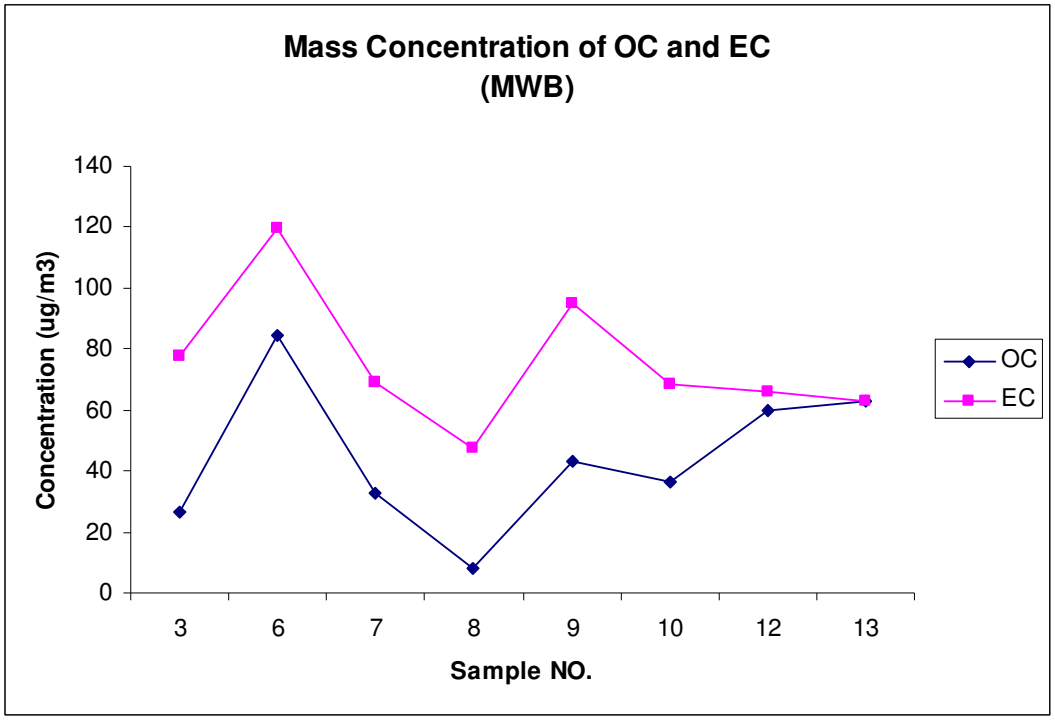

Fig 8.3 Mass concentration of OC and EC measured by MWB method

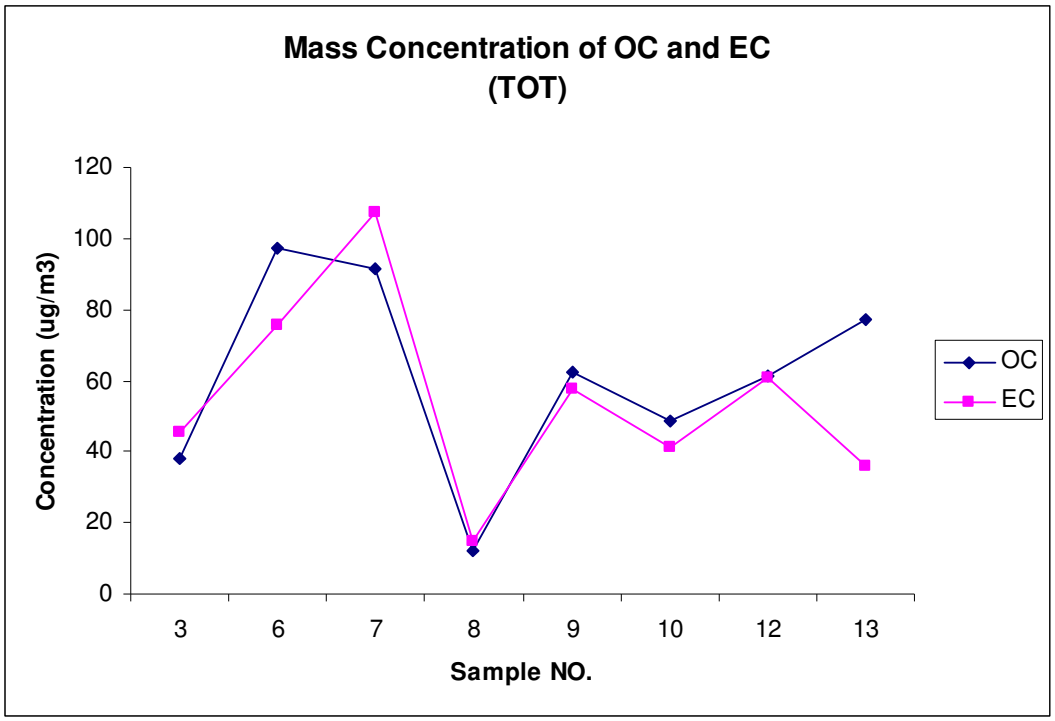

Fig 8.4 Mass concentration of OC and EC measured by TOT method

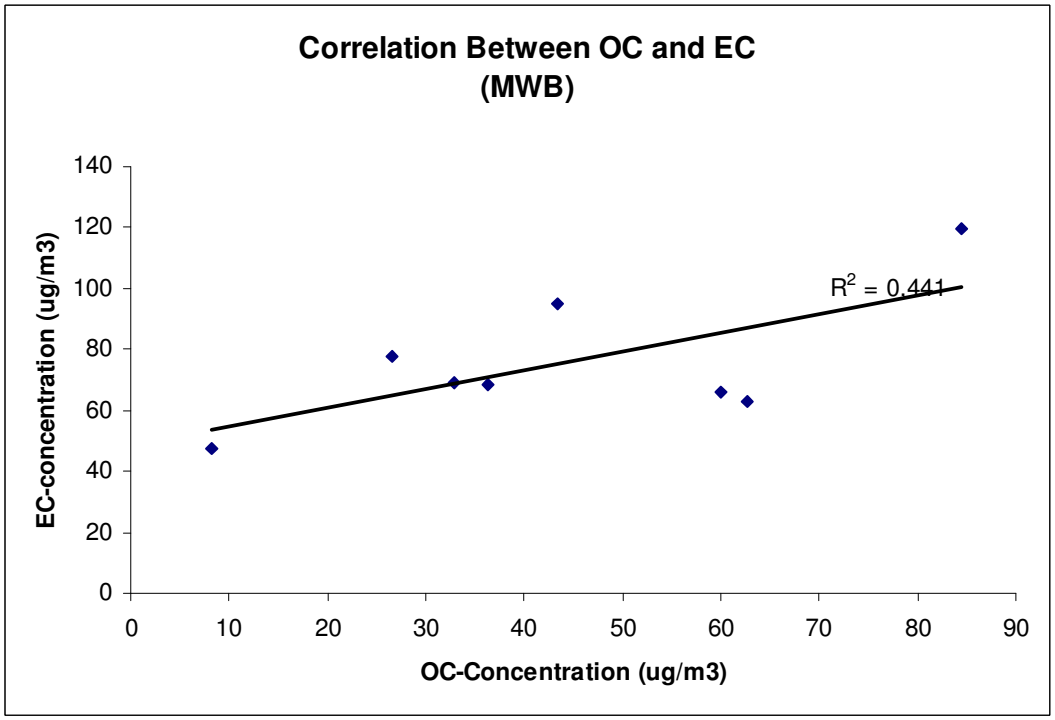

Fig 8.5 Correlation between OC and EC-concentrations measured by MWBmethod

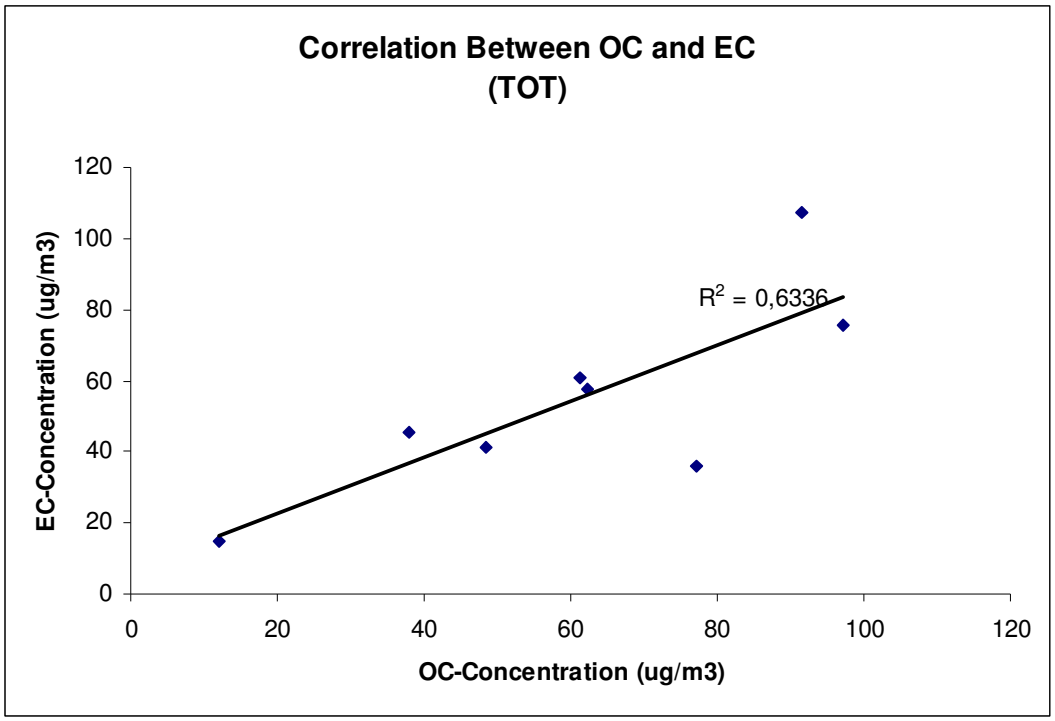

Fig 8.6 Correlation between OC and EC-concentrations measured by method TOT

8.1.6 Correlation of Carbonaceous Species Between the Two Methods

Fig 8.7, 8.8 and 8.9 illustrate good correlation for OC and TC-concentrations, and weak correlation for EC-concentrations measured by the modified Walkley-Black method and thermal optical transmittance method.

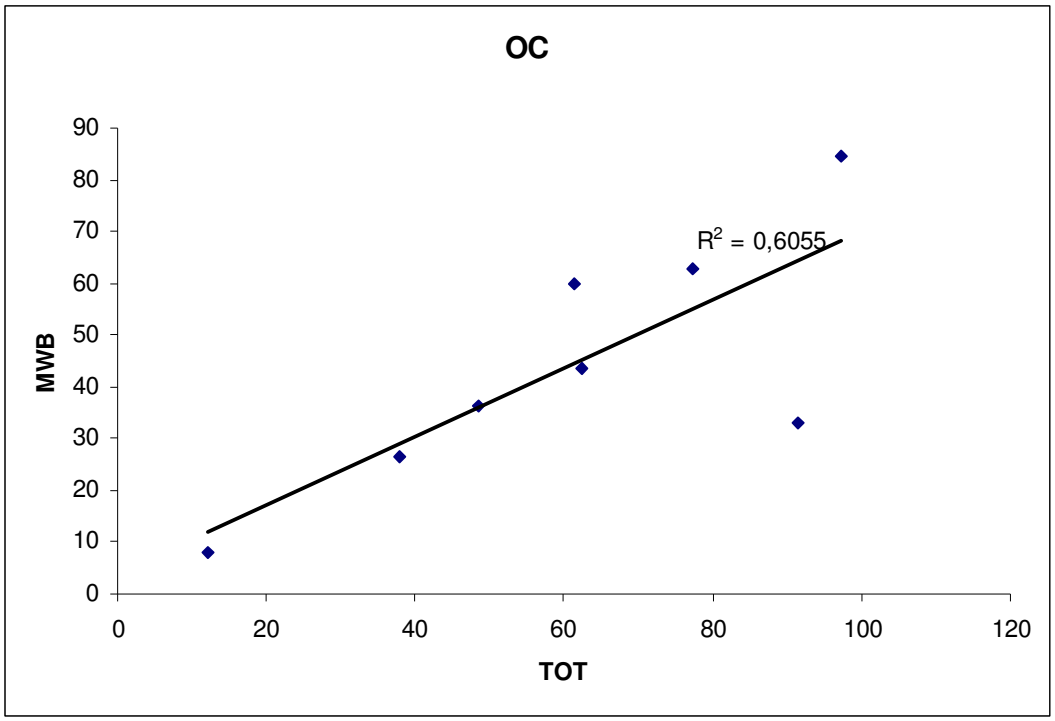

Fig 8.7 Correlation modified Walkley-Black method (MWB) and Thermal optical transmittance method (TOT) for measured OC-concentrations

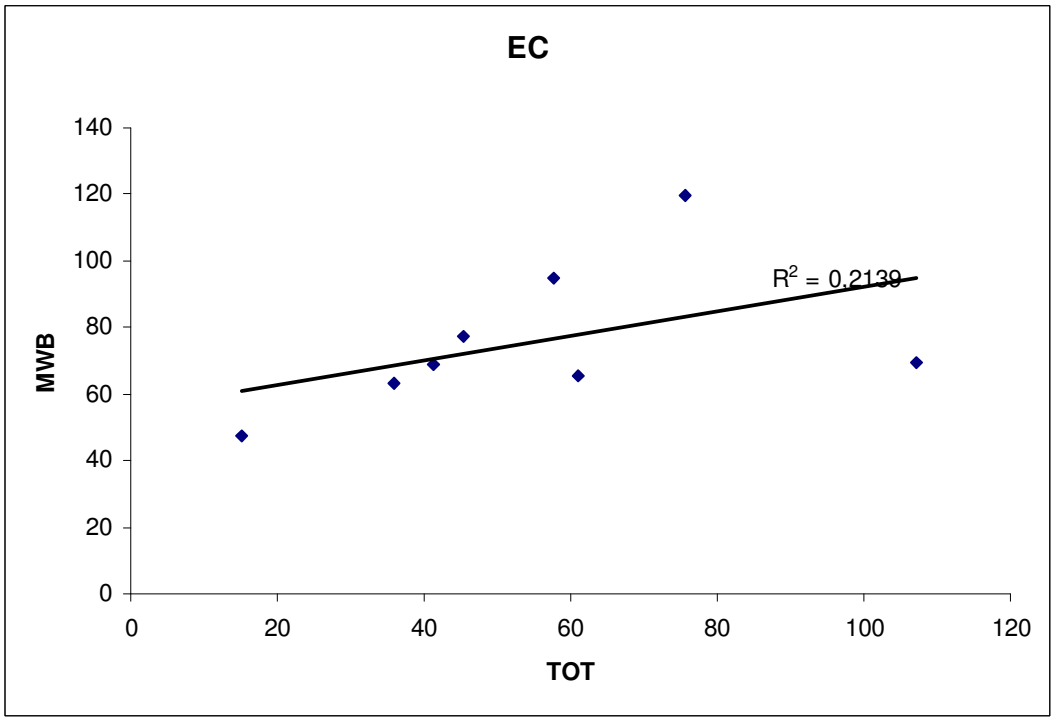

Fig 8.8 Correlation modified Walkley-Black method (MWB) and Thermal optical transmittance method (TOT) for measured EC-concentrations

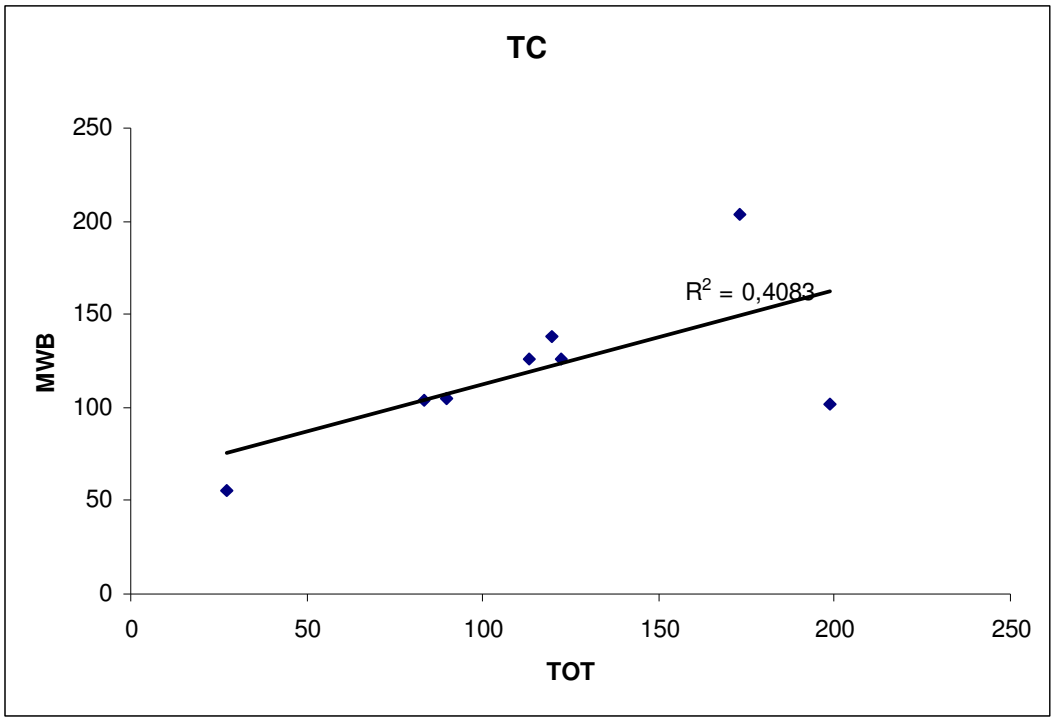

Fig 8.9 Correlation modified Walkley-Black method (MWB) and Thermal optical transmittance method (TOT) for measured TC-concentrations

8.1.7 Comments on some of the Filter Samples

8.1.7.1 Modified Walkley-Black Method

Sample filter nr.3 and 7: The apparent colour of sample filter nr.7 was light brown. Many visible suspended particles were observed between 8-10 o'clock caused by high wind speed bringing dust particles which increases PM_{10}-concentration.

Sample filter nr.6: The air flow is less than 100 λ/min which allows particulate matter > 10 μm (such as pollen and insect debris) to deposit on the filter and increase OC/EC ratio.

Sample filter nr. 8: The apparent colour of the filter was grey, and it could be seen that the particles accumulated differently over the filter surface giving a grid-like distribution. This indicates that a part of sampling device was very near to the filter surface which led to deposition of the particles in the shape mentioned above. The very low PM_{10}-concentration found may thus be a result of sampling problems.

Sample filter nr. 13: High value of OC/EC ratio. This indicates large production of OC, either from its sources directly primary organic carbon (POC) or from photochemical reactions that produce secondary organic carbon (SOC). One factor that may enhance the formation of (SOC) is the relatively high temperature and sporadic sunlight.

8.1.7.2 Thermal Optical Transmittance Method

The total carbon amounts in samples 3, 6, 7 and 13 exceed the instrument maximum limit of detection 200 μg/cm^2 (Table 8.2). This may give uncertianties in the distribution of OC and EC because the instrument can not give the exact split point between original EC and EC formed from organic components pyrolysis. Where the transmittance is too low the instrument is not able to distinguish differences in carbon blackness.

Sample filter nr. 7: Four measurements for sample 7 were taken. The relative standard deviations were very high and they were 42 % for OC, 65 % for EC and 48 % for TC. The first and third measurements were taken into account and better relative standard deviations have been obtained for EC 5 % and TC 22 %, but there was only slight change in case of OC 43 %. The reason was that the filter was badly folded and there were white, empty spots on the filter surface.

8.1.8 Carbonaceous Species in Other Cities

It is obvious by comparing the concentrations of carbonaceous species with those in other Chinese cities (Table 8.5), that there are extremely high emissions of carbonaceous species in Taiyuan. So Taiyuan city is considered to be one of the most polluted city not only in China but in all over the world (Table 8.6).

Table 8.5 Concentrations of TC, OC and EC concentrations (μg/m^3) in some Chinese cities (Yu, 2004 & Cao, 2001)

	Hong Kong	Guangzhou	Shenzhen	Zhuhai
OC	8.90	29.40	16.40	14.50
EC	4.70	10.40	7.30	6.00
TC	13.60	39.80	23.70	20.50
PM_{10}	73.9	161.7	83.7	84.1
OC/EC	1.89	2.83	2.25	2.42
EC/TC	0.35	0.26	0.31	0.29
Measurement Period	1998-2001	8 Jan-8 Feb 2002	8 Jan-8 Feb 2002	8 Jan-8 Feb 2002
Collection Duration	24 h	24 h sampling every 3 days	24 h sampling every 3 days	24 h sampling every 3 days

Table 8.6 Concentrations of carbonaceous particles ($\mu g/m^3$) in different cities

	Taiyuan-China	Vienna-Austria	Uji-Japan	Barcelona-Spain
OC	61	5.7	2.03	8.00
EC	54.89	3.5	6.25	3.00
TC	115.88	9.2	8.28	11.00
OC/EC	1.14	1.63	0.32	2.67
EC/TC	0.48	0.38	0.75*	0.27
Measurement Period	3 Mar-15 Mar 2004	Jun 1999- Mar 2000	Jun 1998-Nov 1999	June 1999
Collection Duration	6 h- 24 h	24 h	24 h	12 h- 24 h
Reference		Salam, 2000	Høller, 2002	Querol, 2001

* High value of EC/TC ratio indicates to long-range transport of pollutants from the Asian continent.

The high concentration of carbonaceous species in Taiyuan (Table 8.6) indicates the intensive use of coal in coal-fired power plant, industry, domestic stoves and coke making. Besides there are other sources which might add some carbonaceous particles, such as diesel vehicles and biomass burning.

Precipitation

During sampling period, there was no precipitation. Therefore there was no possibility of wet deposition for water-soluble organic particles.

8.2 Elemental Analysis

8.2.1 Precision and accuracy

The accuracy of ICP-AES and ICP-MS analytical methods during elemental determination was < 10.7 % and < 28.1 % respectively (Table 8.7). Cr had low recovery and is not listed in the table. Low Cr and Si-recovery is due to digestion problems. Ca, Bi and Sn have no certified values in the reference material, so they are not listed in the table. Values above 100 % for Co may be attributed to contamination during digestion especially the first and third values, where the reference material samples were digested twice.

Table 8.7 Recovery of elements by ICP-AES and ICP-MS methods (n = 8)

		Recovery %								Average	SD
ICP-AES	Al	98,1	101,9	98,8	100	104,2	101,3	99,9	98,5	100,3	2,1
	Fe	105,4	108,7	104,9	105,8	108,3	108,2	107,8	106,6	106,9	1,5
	K	92,6	95,1	95,5	89,2	98,9	92,8	90,2	80,5	91,8	5,5
	Mg	108,8	112,7	107,3	110,7	111,3	111,4	111,0	112,5	110,7	1,8
	Na	99,3	104,0	100,5	100,4	105,7	100,9	100,3	98,3	101,2	2,5
	Pb	107,3	117,2	105,6	109,5	106,5	106,0	109,9	111,0	109,1	3,8
	Ti	101,7	90,7	97,4	100,0	95,4	102,5	103,3	105,8	99,6	4,9
	Zn	99,4	107,3	101,2	105,5	105,5	108,3	106,6	108,6	105,3	3,3
ICP-MS	As	92,0	108,2	90,6	105,9	105,8	103,3	109,1	111,0	103,2	7,7
	Co	162,1	119,5	161,3	108,9	115,5	114,9	123,9	118,7	128,1	21,2
	Cu	89,5	95,5	89,6	96,1	92,0	92,7	91,3	90,5	92,2	2,5
	Mn	114,1	102,2	92,4	103,0	103,7	104,6	103,5	100,9	103,1	5,9
	Ni	97,4	95,3	101,2	94,3	100,5	101,3	84,9	73,7	93,6	9,7
	Sb	70,2	86	70,5	90,8	90,6	99,2	98,6	92,4	87,4	11,3
	Se	109	129	118	119	71	87	124	104	107,6	19,8
	V	94	95	96	106	95	106	101	96	98,6	5,0

8.2.2 Elements Concentration

Measured elemental concentrations by ICP-AES and ICP-MS methods were given in µg/ml or ng/ml respectively. Then elemental concentrations were calculated in $\mu g/m^3$ or ng/m^3 (Table 8.8 and 8.9). There were large differences in the concentrations of some elements. Therefore geometric mean (GM) and geometric standard deviation (GSD) were calculated (See appendix for definitions or expressions).

In our samples Zn is the most abundant element with anthropogenic sources followed by Mn, Pb and Cu while Al and Ca were the most abundant crustal elements.

Table 8.8 Elemental concentration (μg/m^3) measured by ICP-AES

Sample	Elemental concentration (ug/m3)								
	Al	Ca	Fe	K	Mg	Na	Pb	Ti	Zn
2	5,86	9,4	4,82	2,56	1,48	1,18	0,2	0,44	0,4
6	9,94	15,1	7,42	2,52	3,22	1,46	0,18	0,58	0,38
7	15,3	23,62	11,04	3,16	4,46	2,04	0,16	0,9	0,36
8	22,05	32,71	13,42	7,2	6,1	4,6	0,69	1,16	1,02
9	59,54	48,86	34,52	17,16	18,52	14,98	0,2	3,06	0,26
10	11,46	17,74	8,4	2,54	3,54	2	0,32	0,76	0,28
3	19,22	32,9	17,54	4,76	6,44	3,14	0,42	1,18	0,76
11	34,48	67,38	28,63	10,24	11,33	4,83	1,34	2,11	2,74
12	31,19	47,98	20,79	10,89	13,55	8,81	0,43	1,8	0,99
13	26,59	38,6	17,26	8,69	7,96	4,4	0,68	1,43	1,18
14	55,12	76,94	34,44	17,1	17,74	11,18	0,84	2,86	2,44
Mean	26,43	37,38	18,03	7,89	8,58	5,33	0,50	1,48	0,98
SD	17,67	21,46	10,54	5,52	5,90	4,47	0,36	0,89	0,86
GM	21,28	31,47	15,13	6,18	6,68	3,90	0,39	1,25	0,71
GSD	1,98	5,45	1,85	2,05	2,12	2,22	1,97	1,82	2,64

Table 8.9 Elemental concentration (ng/m^3) measured by ICP-MS

Sample	Elemental concentration (ng/m^3)									
	As	Co	Cu	Mn	Ni	Sb	Se	V	Bi	Sn
2	17,34	2,46	63,3	208,92	1,83	4,36	25,42	10,24	5,7	6,42
6	14,92	4,16	312,92	265,62	3,48	2,84	12,08	13,58	2,02	4,82
7	11,98	6,1	99,98	297,48	8,69	2,9	9,5	19,68	1,66	4,94
8	30,7	13,02	1843,45	338,84	17,19	9,76	39,33	27,09	28,26	10,3
9	17,56	16,76	198,1	652,26	19,83	2,22	5,18	70,06	1,38	5,86
10	5,1	4,46	56,54	126,44	5,5	0,62	0,8	14,06	0,62	4,14
3	23,36	9,36	228,9	735,56	50,97	5,34	30,34	30,8	3,72	10,76
11	82,55	30,13	408,28	1195,93	123,9	32,13	126,36	53,99	50,28	33,75
12	44,26	21,13	153,36	757,08	20,42	6,34	55,12	44,58	23,1	15,05
13	31,57	15,38	152,61	439,2	41,59	6,85	35,65	33,78	19,78	10,24
14	73,22	19,78	228,22	1207,64	23,39	13,96	101,52	62,72	12,04	23,78
Mean	24,62	12,98	340,51	565,91	28,80	7,94	40,12	34,60	13,51	11,82
SD	25,14	8,650589	509,43	378,41	35,11	8,86	40,32	20,68	15,64	9,28
GM	15,58	6,49	199,94	452,52	15,57	5,01	21,07	28,84	6,15	9,40
GSD	2,44	2,41	2,5	2	3,24	2,69	3,99	1,87	3,98	1,92

Fig 8.11, 8.12 and 8.13 show the concentration of crustal, minor and trace elements.

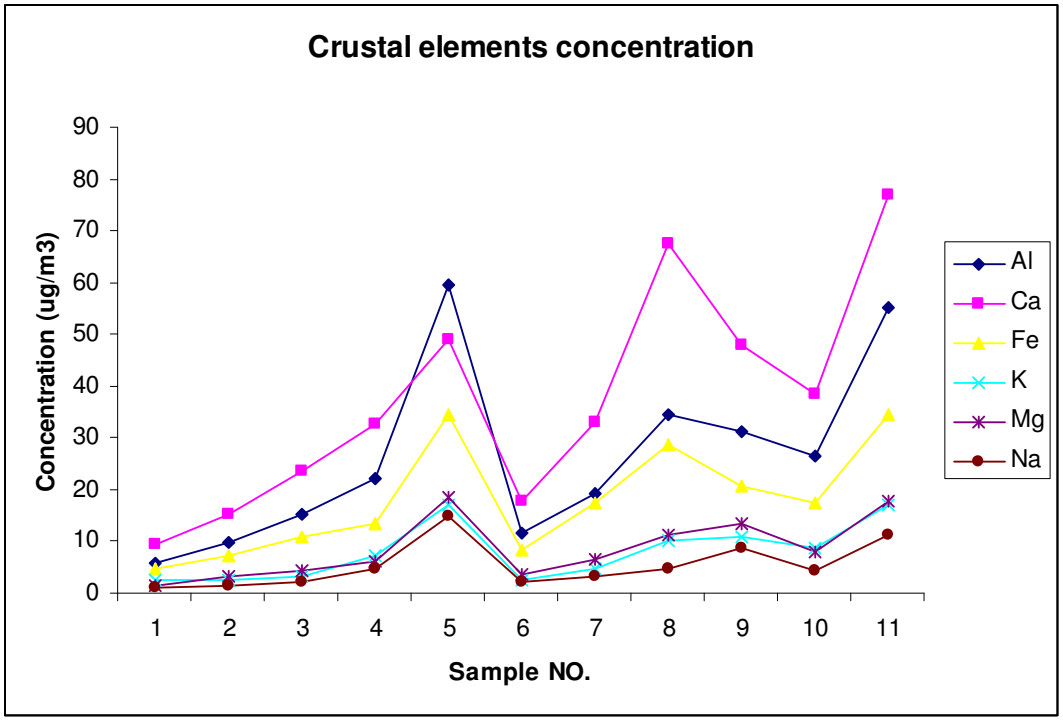

Fig 8.11 The concentrations of crustal elements

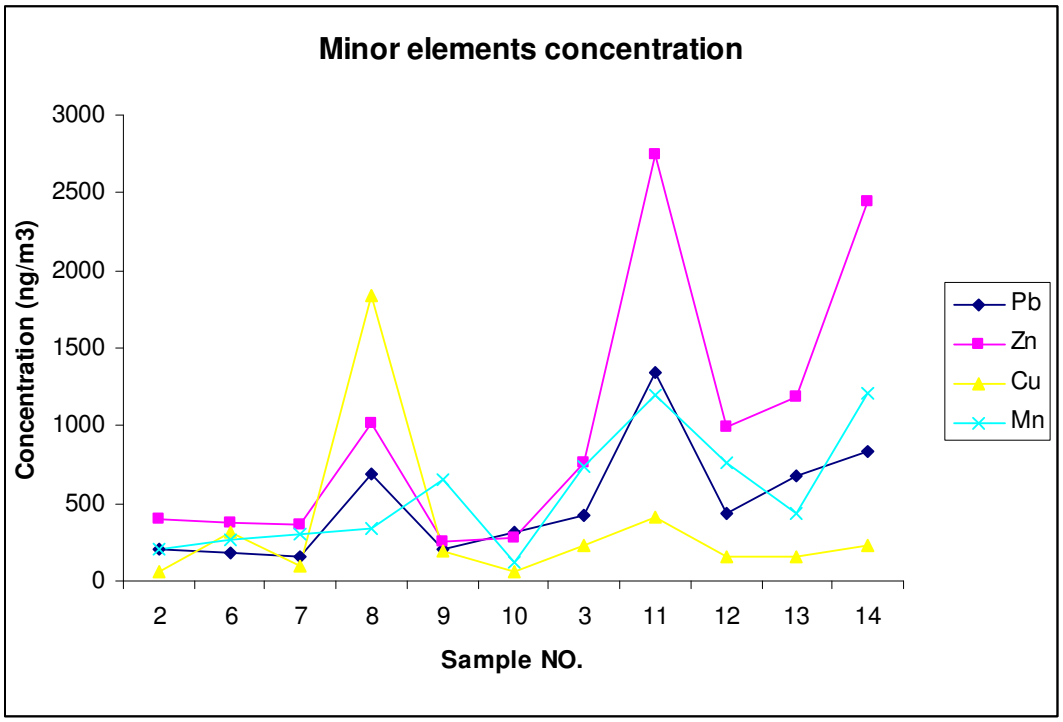

Fig 8.12 The concentrations of minor elements. Log-values for the concentrations were used because there were large variations in elemental concentrations.

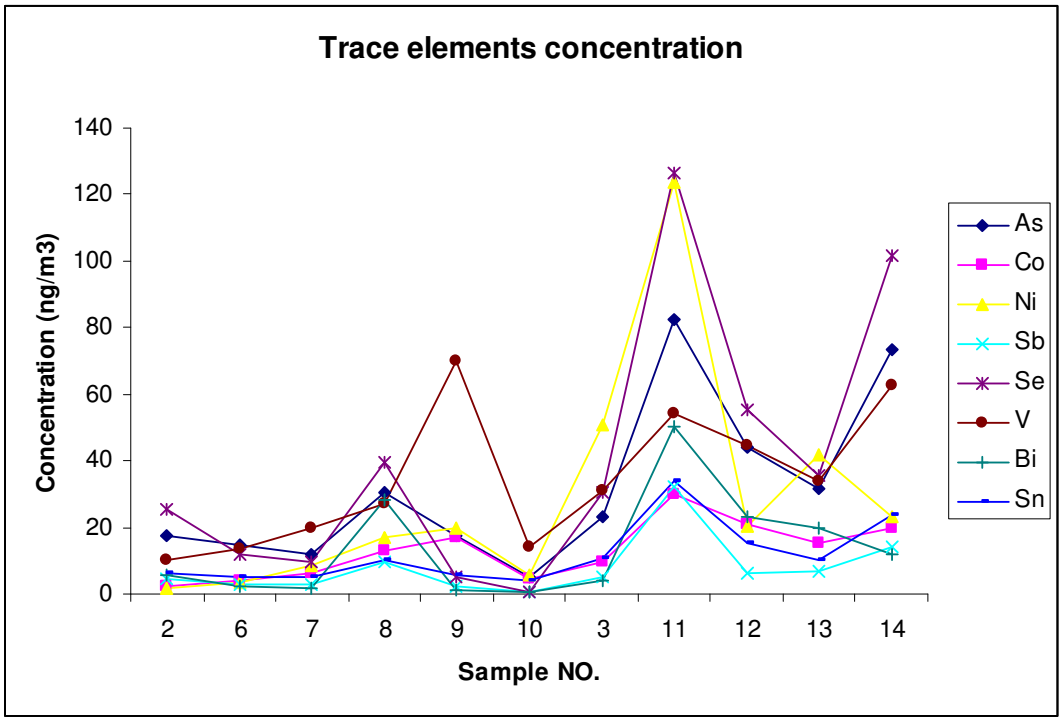

Fig 8.13 The concentrations of trace elements

8.2.3 Enrichment Factors

Enrichment factors were calculated to estimate the contribution of anthropogenic sources other than natural crust to the ambient element level. Ti was used as a reference element. Other elements can be used as reference element such as Al, Si and Fe, where they are considered to be crustal matters. Selected reference element should be least affected by other sources. Using an element as a reference element may hide the contribution from anthropogenic sources containing this element.
Enrichment factor is calculated from the following formula:

$$E.F. = [(X/Ti)_{Aerosol} / (X/Ti)_{Crust}]$$

Where X is the concentration of element of interest, Ti is the concentration of element Ti, $(X/Ti)_{Crust}$ is the ratio derived from the concentrations of element X and Ti in background crustal matter.

There is no detailed data about crust composition in Taiyuan city. The calculation of the enrichment factor is based on the global average elemental concentrations (Table A4). Values larger than 3 will be considered enriched. Table 8.10, and Fig 8.14 and Fif 8.15 show enrichment factors for elements.

Table 8.10 Enrichment Factor (%) (Ti as reference)

Sample	Enrichment Factors									
	Al	Ca	Fe	K	Mg	Na	Pb	Ti	Zn	
2	0,92	2,93	1,11	1,59	0,82	0,65	207,27	1	74,03	
6	1,19	3,58	1,30	1,18	1,36	0,61	141,52	1	53,35	
7	1,18	3,60	1,24	0,96	1,21	0,55	81,07	1	32,57	
8	1,32	3,87	1,17	1,69	1,29	0,96	271,24	1	71,6	
9	1,35	2,19	1,14	1,53	1,48	1,18	29,8	1	6,92	
10	1,04	3,21	1,12	0,91	1,14	0,64	192	1	30	
3	1,13	3,83	1,50	1,10	1,34	0,64	162,3	1	52,45	
11	1,13	4,39	1,37	1,32	1,31	0,55	289,59	1	105,74	
12	1,20	3,66	1,17	1,65	1,84	1,18	108,93	1	44,79	
13	1,29	3,71	1,22	1,66	1,36	0,74	216,84	1	67,19	
14	1,33	3,69	1,22	1,63	1,52	0,94	133,93	1	69,47	
Mean	1,19	3,52	1,23	1,38	1,33	0,79	166,77	1	55,28	
SD	0,13	0,57	0,12	0,30	0,25	0,24	78,72	0	26,69	
GM	1,18	3,47	1,23	1,35	1,31	0,76	143,92	0	46,54	
GSD	1,12	1,19	1,09	1,25	1,21	1,32	1,85		2,01	
Sample	Enrichment Factors									
	As	Co	Cu	Mn	Ni	Sb	Se	V	Bi	Sn
2	124,80	1,27	14,91	2,85	0,32	282,41	6586,09	0,98	434,36	41,58
6	81,46	1,64	55,91	2,78	0,46	139,55	2374,35	0,99	116,8	23,68
7	42,15	1,55	11,51	1,98	0,73	91,83	1203,33	0,92	61,84	15,64
8	83,81	2,56	164,70	1,75	1,13	239,79	3865,19	0,99	816,85	25,31
9	18,17	1,25	6,71	1,28	0,49	20,68	192,98	0,97	15,12	5,46
10	21,25	1,338	7,71	1,00	0,55	23,25	120	0,78	27,35	15,52
3	62,69	1,81	20,10	3,74	3,28	128,97	2931,15	1,10	105,70	25,99
11	123,89	3,26	20,05	3,40	4,46	433,98	6827,03	1,08	798,99	45,59
12	77,86	2,68	8,83	2,52	0,86	100,38	3490,93	1,05	430,29	23,83
13	69,91	2,45	11,06	1,84	2,21	136,52	2842,03	1,00	463,78	20,41
14	81,07	1,58	8,27	2,53	0,62	139,11	4046,60	0,93	141,15	23,70
Mean	71,55	1,94	29,98	2,33	1,37	157,86	3134,52	0,98	310,20	24,25
SD	35,04	0,68	46,80	0,85	1,36	120,44	2218,45	0,09	297,59	11,31
GM	61,49	1,84	16,61	2,18	0,95	114,54	1926,05	0,98	165,32	21,49
GSD	1,84	1,37	2,52	1,47	2,27	2,45	3,61	1,09	3,62	1,71

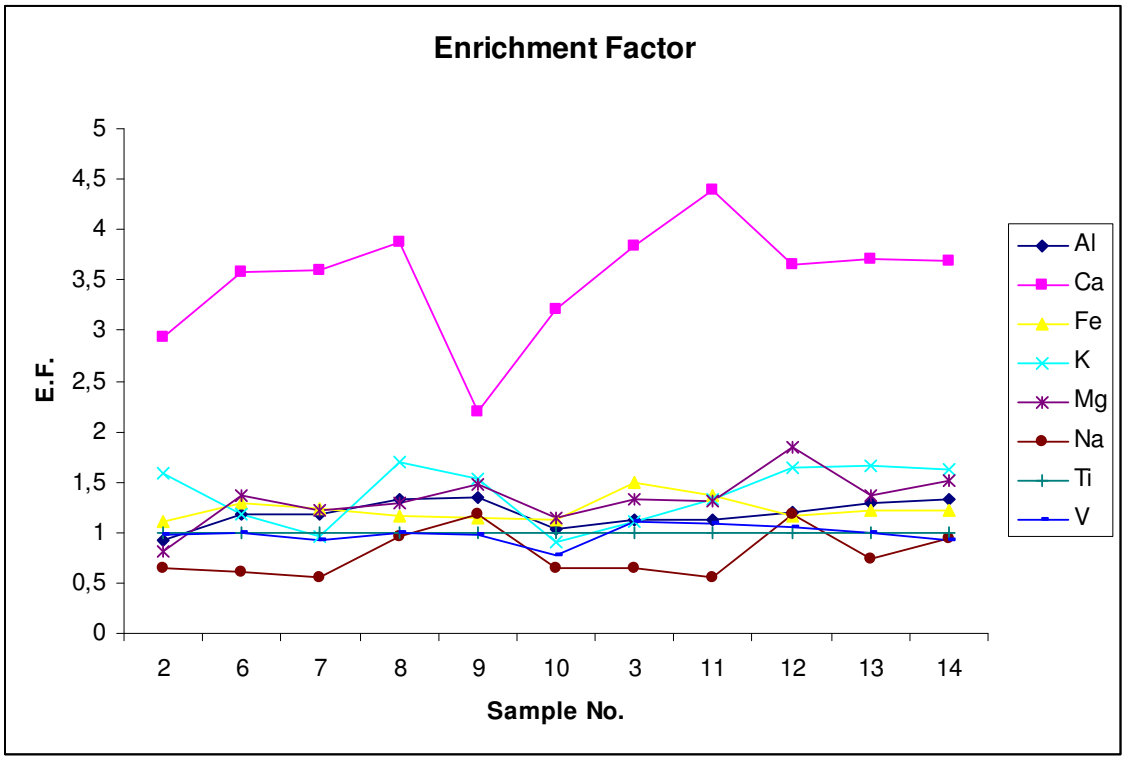

Fig 8.14 Enrichment factors for Al, Ca, Fe, K, Mg, Na, Ti and V.

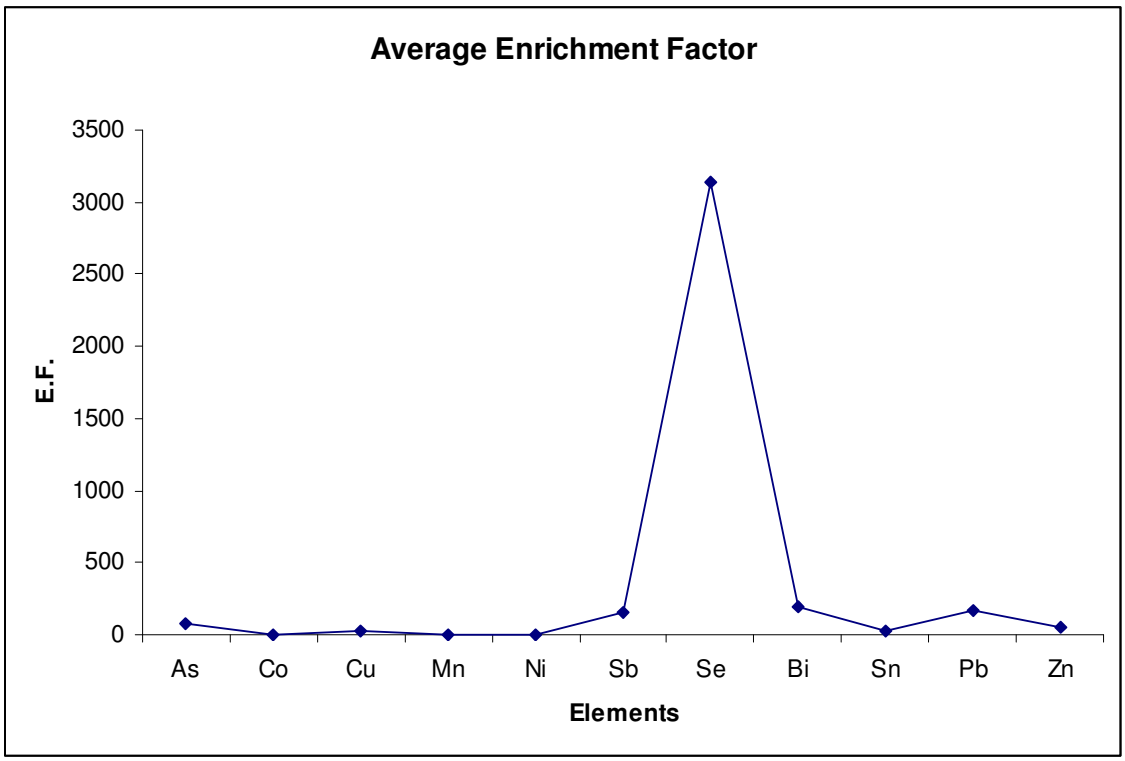

Fig 8.15 Average enrichment factors for As, Co, Cu, Mn, Ni, Sb, Se, Bi, Sn, Pb and Zn

From table 8.10, the small variations in the values for Al and Fe (close to 1), show that the enrichment factors would not be much different if Al and Fe were used as reference.

Since E.F. value of potassium (K) is not larger than 3, K is not considered to be enriched. The enrichment factor of K is near unity, indicating that the main source of K is soil dust. There is indication of some biomass burning. The average ratio K/EC for three samples collected on fiber glass filters and three samples collected on Teflon filters was 0.14 (Table 8.11). In case there is a minor contribution from biomass burning the value of this ratio should be 0.07 (Salam et al., 2003).

Table 8.11 K/EC ratios for different type of filters

Fibre glass filter sample	EC measured by TOT($\mu g/m^3$)	Teflon filter sample	K ($\mu g/m^3$)	Date of sampling	Collection duration	K/EC
6	75.66	8	7.2	8-9 Mar,2004	22 hrs and 8 mins	0.1
7	107.28	9	17.16	10 Mar, 2004	10 hrs	0.16
8	15.04	10	2.54	11 Mar, 2004	11 hrs and 27 mins	0.17

Emissions of As and Se may be used as a marker for coal combustion activities, where they have large enrichment factors. The ratio of As/Se is often ~ 1 in most atmospheric particulate material and in aged coal combustion aerosols (Park and Kim, 2004). It can be seen from Table 8.12 that this is true, except for sample 9 and 10, where the ratio is larger than one which indicates the presence of other sources. Also there is good correlation between As and Se (Fig 8.12).

Table 8.12 As/Se ratios

Sample	As ng/m^3	Se ng/m^3	As/Se
2	17,34	25,42	0,68
6	14,92	12,08	1,23
7	11,98	9,5	1,26
8	30,7	39,33	0,78
9	17,56	5,18	3,39
10	5,1	0,8	6,37
3	23,36	30,34	0,77
11	82,55	126,36	0,65
12	44,26	55,12	0,80
13	31,57	35,65	0,86
14	73,22	101,52	0,72

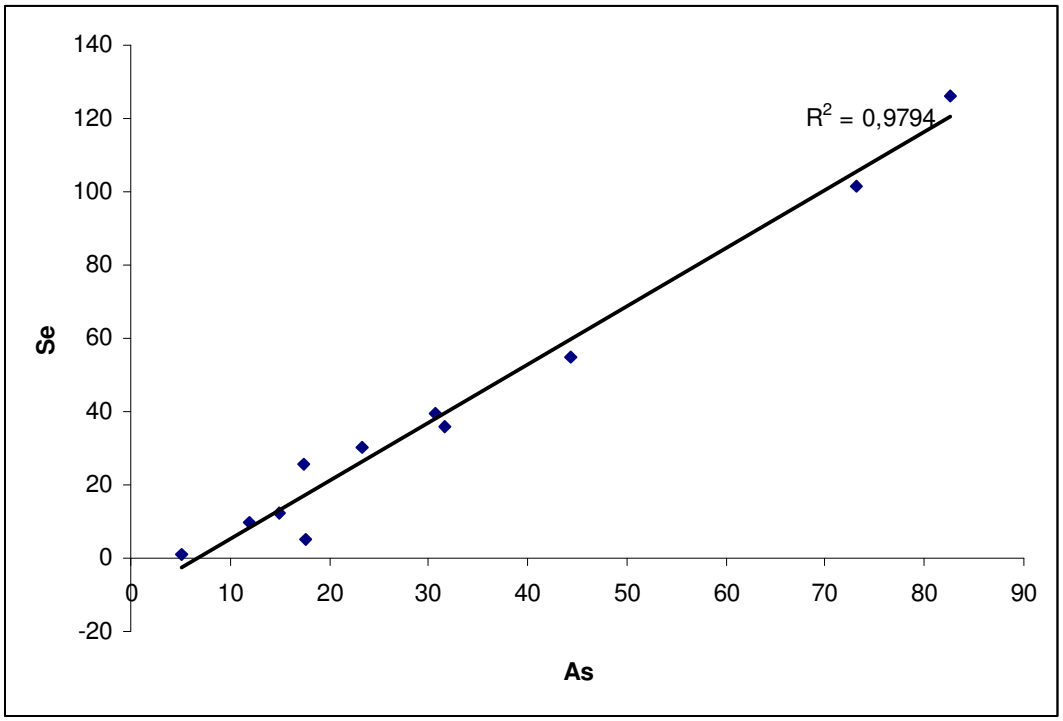

Fig 8.12 Correlation between Se and As

Table 8.10 shows that Al, Ca, Fe, Mg, Na and Ti have small enrichment factors because they are mostly crustal (Chan et al., 1997). The slight enrichment of Ca may reflect that Chinese cities look like big construction sites because of the growing economy and the mismanagement of the environment. Fig 8.13 and 8.14 show good correlation between Al as a crust tracer and other crustal elements. Emissions of V and Co are considered to be produced from heavy oil combustion (Xie, 2002). They have enrichment factor less than 3. This is consistent with that Taiyuan do not use heavy oil as an energy source for space heating, industry or power generating. Also there is good correlation between V and Co (Fig 8.15).

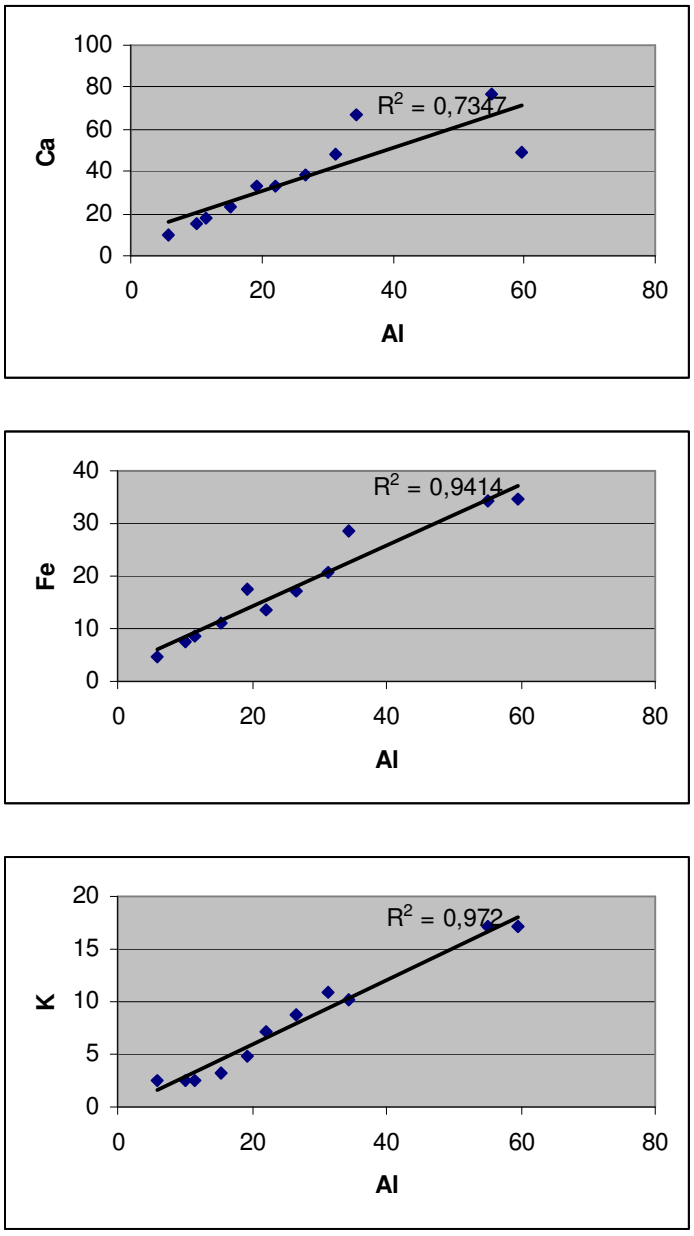

Fig 8.13 Correlation between Al and other crustal elements

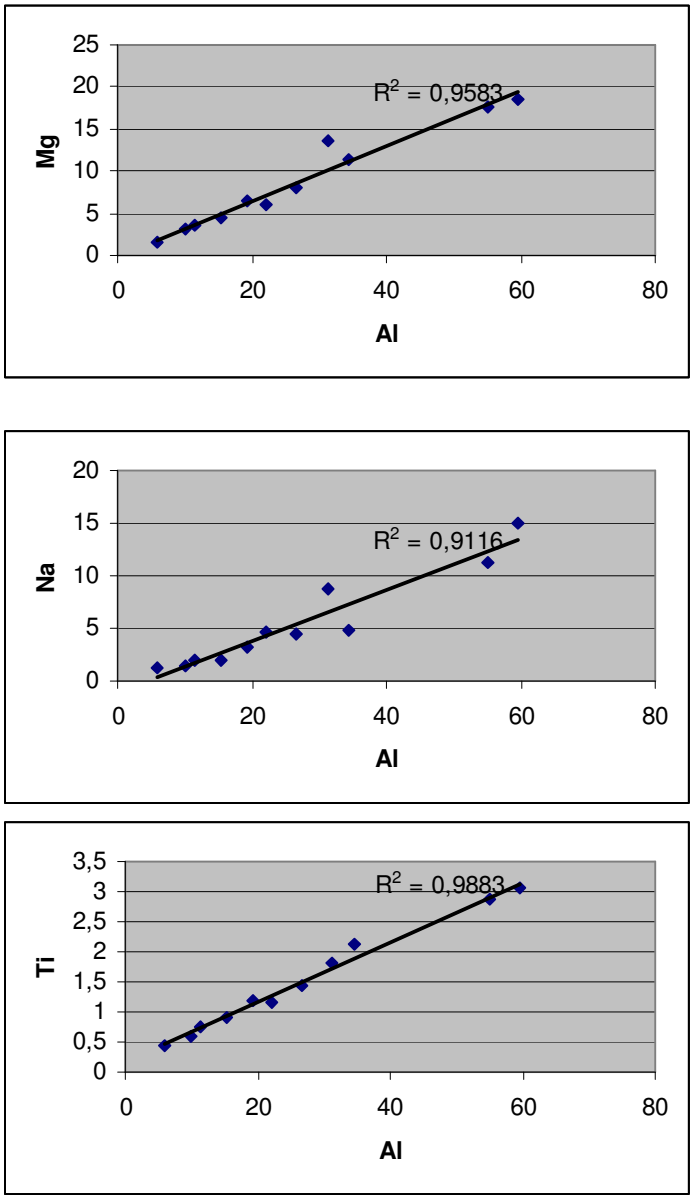

Fig 8.14 Correlation between Al and other crustal elements

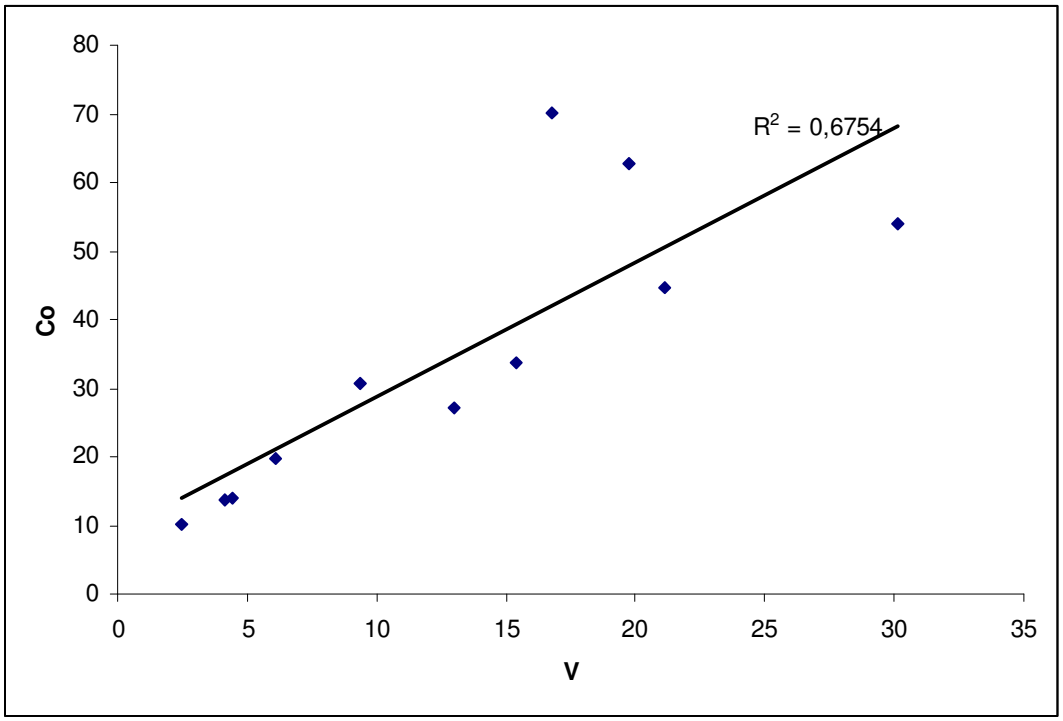

Fig 8.15 Correlation between V and Co

Enrichment factors for Pb, Zn, Cu, Sb, Bi, Sn and Se are high. This indicates the contribution of anthropogenic emission sources. Pb, Zn, Cu, Mn and Ni may originate from many sources, including waste incinerator, smelters and coal combustion. Sb comes from various industrial sources, especially non-ferrous smelters. Bi and Sn come mainly from non-ferrous refinery (Chiaradia and Cupelin, 2000). The highest enrichment factor is for Se which indicates the contribution of many sources such as coal combustion, non-ferrous smelters, waste incineration (Oddabbasi et al., 2002) and electronic industries.

One can see from Table 8.13 that there are high correlations between many elements. This may imply either that the elements are from the same source(s) and/or that they share similar emission and transport pattern(s) (Xie et al., 2005).

Table 8.13 Correlation between the measured aerosol components at urban area of Taiyuan

	Al	Ca	Fe	K	Mg	Na	Pb	Ti	Zn	As	Co	Cu	Mn	Ni	Sb	Se	V	Bi
Ca	0.73																	
Fe	0.94	0.86																
K	0.97	0.76	0.9															
Mg	0.96	0.76	0.92	0.55														
Na	0.91	0.52	0.78	0.91	0.92													
Pb	0.13	0.54	0.97	0.17	0.13	0.02												
Ti	0.99	0.79	0.27	0.96	0.97	0.88	0.18											
Zn	0.23	0.71	0.38	0.27	0.24	0.07	0.88	0.28										
As	0.3	0.77	0.46	0.36	0.34	0.14	0.8	0.36	0.95									
Co	0.51	0.82	0.66	0.56	0.58	0.35	0.66	0.59	0.66	0.76								
Cu	0	0	0	0	0	0	0.09	0	0.02	0.01	0.02							
Mn	0.53	0.89	0.74	0.55	0.59	0.34	0.53	0.61	0.72	0.81	0.74	0						
Ni	0.08	0.35	0.23	0.07	0.08	0	0.7	0.13	0.54	0.51	0.57	0	0.48					
Sb	0.1	0.47	0.24	0.12	0.1	0.01	0.88	0.15	0.82	0.8	0.63	0.05	0.55	0.77				
Se	0.19	0.66	0.34	0.24	0.23	0.06	0.83	0.25	0.96	0.98	0.67	0.02	0.75	0.54	0.85			
V	0.95	0.82	0.98	0.93	0.95	0.84	0.23	0.99	0.32	0.42	0.68	0	0.68	0.2	0.21	0.3		
Bi	0.04	0.31	0.11	0.08	0.06	0.06	0.78	0.07	0.59	0.6	0.64	0.18	0.3	0.6	0.78	0.63	0.12	
Sn	0.22	0.69	0.4	0.26	0.26	0.08	0.85	0.29	0.94	0.96	0.74	0.01	0.79	0.67	0.3	0.97	0.35	0.65

Table 8.14 shows elemental concentrations in Taiyuan and other different cities. The elemental concentrations are the highest in Taiyuan except for some elements, such as Al and Ca in case of Izmir.

Table 8.14 Elemental concentrations ($\mu g/m^3$) in PM_{10} samples in different cities

Element	China			Korea	Spain	Turkey
	Taiyuan [a]	Guiyang [b]	Beijing [c]	Taejon [d]	Barcelona [e]	Izmir [f]
Al	18.41	1.12	3.5			23.50
Ca	27.18	4.03	8.5		2.25	40.202
Fe	12.65	1.57	5.5	1.577	0.89	3.438
K	5.63	1.31				
Mg	6.06	0.77			0.29	3.89
Na	3.69	0.19				
Pb	0.39	0.13	0.43	0.195	0.149	0.111
Ti	1.03	0.13	0.47	0.0304		
Zn	0.76	0.44	0.77	0.277	0.25	0.733
As	0.02462	0.0174	0.048	0.012		
Co	0.01011	0.00065	0.0046	0.00135		
Cu	0.28652	0.03125	0.11	0.0324	0.074	0.154
Mn	0.40709	0.17495	0.24	0.0418	0.024	0.135
Ni	0.0288		0.022	0.0426	0.007	0.039
Sb	0.00647	0.02623	0.033	0.0033		
Se	0.03172		0.01	0.00173		
V	0.02455	0.00413	0.013	0.0137		
Bi	0.00675	0.00159				
Sn	0.00906	0.00598				

[a] This study

[b] Samples were collected from September 2001 to August 2003 and the collection duration was 24 h (Xie, 2002).

[c] Samples were collected in late June 2001 to July 2001 for 5 consecutive days (Okuda, 2004).

[d] Values are an annual average for 1999 and the collection duration was 24 h- 48 h (Kim et al., 2002)

[e] Samples were collected in June 1999 and the collection duration was 12 h- 24 h (Querol et al., 2001).

[f] Samples were collected from November 2000 to April 2001 and the collection duration was 24 h (Oddabbasi et al., 2002).

9. Conclusion

High concentrations of carbonaceous species (OC, EC and TC) were observed in Taiyuan city. These high concentrations indicate high level of anthropogenic activities; coal combustion, coke industry and diesel-fired vehicles. The concentrations are exceptionally high even compared with other Chinese cities, and that puts Taiyuan as the most polluted city in China.

The modified Walkley-Black method was developed as a cost-effective method (Chan et al., 1995). It is a cheap method to determine OC, EC and TC in aerosol samples collected on glass fibre filters. The analysis can be achieved without need for complicated laboratory equipment. However, the method gives higher EC and lower OC values than the thermal optical transmittance method. This may be due to different operational definitions of the fractions and/or weaknesses in the method such as dichromate loss during heating.

Thermal optical transmittance method is a good method with 5 % accuracy (Chow et al., 2001). It is fast and easy to run.

To get a better profile of airborne carbonaceous particles:

1- Long term measurements combined with intensive campaigns (24 h a day) should be done.
2- Establishing a network for air quality monitoring consisting of many stations covering as much as the whole urban area of the city.

References

Anderson J.E. Coal Dirty Cheap Energy. RFF (Resources for the future) winter 2005, Issue 156. www.rff.org

ARB, Air Resources Board. March, 2005. Atmospheric persistence VI. www.arb.ca.gov

Atkinson R and Arey J. Atmospheric chemistry of gas-phase polycyclic aromatic hydrocarbons: formation of atmospheric mutagens. Environmental health perspectives **102**, supplement 4, October 1994

Aunan, Fang J, Vennemo H, Oye K, and Seip H.M. 2004. Co-benefits of climate policy-lessons learned from a study in Shanxi, China. Energy policy **32**, 567-581.

Aunan K, Mestl H.E.S, Fang J, and Li Y. Household fuel use and indoor air pollution in Shanxi. Master plan against air pollution in Shanxi province, Final seminar and workshop 17-18 March, 2005, Taiyuan, Shanxi

Austin J, Brimblecombe P and Sturges W. 2002. Air pollution science for the 21th century. Elsevier science Ltd.

Becker J.China, part 3. 28th Aug, 2003. China in an energy quandary. Asia Times. http://www.atimes.com/atimes/China/EH28Ad01.htm

BPs statistical review of world energy for 2004. www.bp.com

Boss C.Bb. and Fredeen K.J. 1999. Concepts, instrumentation, and techniques in inductively coupled plasma optical emission spectrometry. Second edition. Perkin Elmer publishing. U.S.A

Bradsher Keith. China burning more coal.China's boom adds to global warming problem. October 22, 2003. http://healthandenergy.com/china_more_coal.htm

Brasseur G.P., John J. Orlando and Geoffery S. Tyndall. 1999. Atmospheric chemistry and climate change. Oxford

Cao. J.J. , S.C. Lee, K.F. Ho, X.Y. Zhang, S.C. Zou, Kochy Fung, Judith C. Chow, John G. Watson, 2001. Characteristics of carbonaceous aerosol in Pearl River Delta Region, China during 2003 winter period. Atmospheric Environment **37**, 1451-1460

Chagger H.K., Jones J.M, Pourkashanian M, Williams A, Owen A, Fynes G. 1999. Emission of volatile organic compounds from coal combustion. Fuel **78**, 1527-1538

Chan Y.C., Vowles P.D., McTainsh G.H., Simpson R.W., Cohen D.D. and Bailey G.M. (1995). Use of a modified Walkley-Black method to determine the organic and elemental carbon content of urban aerosols collected on glass fibre filters. Chemosphere, **31,** 4403-4411

Chan Y.C., Simpson R.W., McTainsh G.H., and Vowels P.D. (1997). Characterisation of chemical species in $PM_{2.5}$ and PM_{10} aerosols in Brisbane, Australia. Atmos. Environ. **31**, 3773-3785

Chiaradia M and Cupelin F. (2000). Gas-to-particle conversion of mercury, arsenic and selenium through reactions with traffic-related compounds (Geneva)? Indications from lead isotopes. Atmos. Environ. **34**, 327-332

Chow J.C., Watson J.G., Crow D, Lowenthal D.H., and Merrifield T. (2001). Comparison of IMPROVE and NIOSH carbon measurements. Aerosol science and technology, **34**, 23-34

Chughtai A.R., Brooks M.E., and Smith D.M. 1996. Hydration of blach carbon. Journal of geophysical research, **101**,No.D14, 19505-19514

Chughtai A.R., Atteya M.M.O, Kim J, Konowalchuk B.K. and Smith D.M.. 1998. Adsorption and adsorbate interaction at soot particle surfaces. Carbon, **36**. 1573-1589.

CIEPCP, Chinese-Italian environmental protection cooperation project. Dec, 2003. Sustainable energy planning for Taiyuan.

Cofer III W.R., Schryer D.R. and Rogowski R.S. 1981. The oxidation of SO_2 on carbon particles in the presence of O_3, NO_2 and N_2O. Atmospheric Environment, **15**, No. 7, 1282-1286

Cslforum, Carbon sequestration leadership forum. 8 July, 2004. An energy summery of China. www.cslforum.org/china.htm

Dan M, Zhuang G, Li X, Tao H and Zhuang Y. (2004). The characteristics of carbonaceous species and their sources in $PM_{2.5}$ in Beijing. Atmos. Environ. **38,** 3443-3452

De Santis F and Allegrini I. 1992. Heterogeneous reactions of SO_2 and NO_2 on carbonaceous surfaces. Atmospheric Environment **26A**, 3061-3064

EEB, European Environmental Bureau. 2000. The case for real co-reductions. www.eeb.org/publication

EPA, Environmental Protection Agency .March 2001. Air Quality criteria for particulate matter, vol 1 Second external review. www.epa.gov/

Feilberg A. 2000. Atmospheric chemistry of polycyclic aromatic compounds with special emphasis on nitro derivatives. Risø national laboratory, Roskilde

Greibrokk T, Lundanes E and Rasmussen K.E. (1998). Kromatografi. Universitetetforlaget
Hansen J.E. and Sato M. 2001. Trends of measured climate forcing agents. PANS, Vol. 98, 14778-14783

Harrison R.M. 1999. Understanding our environment. Third edition, RS.C.

Høller R, Tohno S, Kasahara M, and Hitzenberger R. (2002). Long-term characterization of carbonaceous aerosol in Uji, Japan. Atmos. Environ. **36,** 1267-1275

IPCC, Intergovernmental Panel on climate Change. 2001. Climate Change 2001, eds. Houghton J.T, ding Y, Griggs D.J, Noguer M, van der Linden P.J, Dai X, Maskell K, & Johnson C.A. (Cambridge Univ. Press, Cambridge, U.K)

Jacobson M.Z. 2002. Control of fossil-fuel particulate black carbon and organic matter, possibly the most effective method of slowing global warming. Journal of geophysical research, Vol. 107, NO. D19

Kim, H.Y., Lee, J.H., Jang, M.S., 2002. Metals in airborne particulate matter from the first and second industrial complex area of Taejon city, Korea. Environmental pollution 118, 41-51

Lary D.J., Lee A.M., Toumi R, Newchurch M.J., pirre M, and Renard J.B. 1997. Carbon aerosols and atmospheric photochemistry. Journal of geophysical research, **102**, No. D3, 3671-3682.

Lee S. C., Ho K. F., Cao J. J. 2002. Characteristics of organic and elemental carbon in $PM_{2.5}$ of Pearl river delta region, Better air quality in Asian and Pacific rim cities. Hong Kong SAR.

Letzel T, Rosenberg E, Wissiack R, Grasserbauer M and Niessner R. 1999. Separation and identification of polar degradation products of benzo[a]pyrene with ozone by atmospheric pressure chemical ionization-mass spectrometry after optimized column chromatographic clean-up. Journal of chromatography A, **855**, 501-514

Mallet M, Roger J.C., Despiau S, Dubovik O, Putaud J.P. 2002. Microphysical and optical properties of aerosol particles in urban zone during ESCOMPTE. Atmospheric research 69, 73-97

Mastral A.M., Garcia T, Murillo R, Callen M.S., Lopez J.M. and Navarro M.V. Pollution control technology for atmospheric PAH. http://ejeafche.uvigo.es/2(2)2003/002222003F.htm

Menon S. 2004. Current uncertainties in assessing aerosol effects on climate. Annual review of environmental and resources, vol. 29, 1-30.

Mestl H.E.S., Aunan K, Fang J, Seip H.M, Skjelvik J.M, Vennemo H. 2005. Cleaner production as climate investment- integrated assessment in Taiyuan City, China. Journal of Cleaner Production **13**, 57-70

Miller J.N and Miller J.C. (2000).Statistics and chemometrics for analytical chemistry.Chapter 5, Calibration methods in instrumental analysis: regression and correlation

Na K, Sawat A.A., Song C and Cocker III D.R. (2004). Primary and secondary carbonaceous species in the atmosphere of Western Riverside County, California. Atmos Environ. **38**, 1345-1355

NASA. 26, September 2002. Top story, Goddard space flight center. Black carbon contributes to droughts and floods in China. www.gsfc.nasa.gov

NIST, 1998. Certificate of Analysis, Standard Reference Material 1648, Urban Particulate Matter. National Institute of Standards and Technology, Gaithersburg, MD, USA, 28 April 1998

Odabbasi M, Muezzinoglu A, Bozlaker A. 2002. Ambient concentrations and dry deposition fluxes of trace elements in Izmir, Turkey. Atmos. Environ. **36**, 5841-5851

Okuda T, Kato J, Mori J, Tenmoku M, Suda Y, Tanaka S, He K, Ma Y, Yang F, Yu X, Duan F, Lei Y. 2002. Daily concentrations of trace metals in aerosols in Beijing, China, Determined by using inductively coupled plasma mass spectrometry equipped with laser ablation analysis, and source identification of aerosols. Science of the total environment **330**, 145-158.

Oros D.R. and B.R.T. Simoneit. 2000. Identification and emissions rates of molecular traces in coal smoke particulate matter. Fuel **79**, 515-536

Park S.S and Kim Y.J. 2004. $PM_{2.5}$ particles and size-segregated ionic species measured during fall season in three urban sites in Korea. Atmos Environ. **38**, 1459-1471

PCAQ, Polk County Air Quality. 2004. Particulate matter $PM_{2,5}$ http://www.airquality.co.polk.ia.us

Pitts B.J.F and Pitts J.N, JR. (1986). Chapter 12, particulate matter in the atmosphere. Primary and secondary particles. A Wiley-interscience publication ?

Querol X., Alastuey, A., Rodriguez, S., Plana, F., Ruiz, C.R., Cors, N., massague, G., and Puig, O. (2001). PM_{10} and $PM_{2.5}$ source apportionment in the Barcelona Metropolitan area, Catalonia, Spain. Atmos. Environ. **35**, 6407-6419

Roy L. Bennett and Leonard Stockburger. Environmental protection agency. November, 1994. Sampling carbonaceous aerosols: A review of methods and previous measurements. www.epa.gov

Salam A, Bauer H and Puxbaum H. 2000. Dual site study of elemental carbon and organic carbon in $PM_{2.5}$ and PM_{10} aerosols in the area of greater Vienna, Austria. www.dal.ca/~ab481 920/paper4.pdf

Salam A, Bauer H, Kassin K, Ullah S.M, Puxbaum H. 2003. Aerosol chemical characteristics of a mega-city in Southeast Asia (Dhaka-Bangladesh). Atmos. Environ **37**, 2517-2528

Salama I, Chi X., and Maenhaut W. 2004. Elemental and organic carbon in urban canyon and background environments in Budapest, Hungary. Atmos Environ. **38,** 27-36

Schulte E.E. 1995. Recommended soil organic matter tests, Chapter 8. http://ag.udel.edu/extension

Miller J.N and Miller J.C. 2000.Statistics and chemometrics for analytical chemistry.Chapter 5, Calibration methods in instrumental analysis: regression and correlation

SCMP, South China Monitoring Post. 2004. Taiyuan.
http://china.scmp.com/map/taiyuan_index.html

Seinfeld J.H. and Pandis S.N. 1998. Atmospheric chemistry and physics. John Wiley & Sons, INC. Canada

Seinfeld J.H. and Pankow J.F. 2003. Organic atmospheric particulate material. Annual review of physical chemistry. **54**, 121-140

Skoog D.A., Holler F.J. and Nieman T.A. 1998. Principle of instrumental analysis. Saunders college publishing

Streets D.G., Shalini Gupta, Stephanie T. Waldhoff, Michael Q. Wang, Tami C. Bond and Bo Yiyun. 2001. Black carbon emissions in China. Atmospheric Environment **35**, 4281-4296

Streets D. G., Kejun Jiang, Xiulian Hu, Jonathan E. Sinton, Xiao-Quen Zhang, Deying Xu, Mark Z. Jacobson, James E. Hansen. 2001 Recent reductions in China's greenhouse gas emissions. Science **294.**

Theodora. www.theodora.com

Taylor S.R. 1964. Abundance of chemical elements in the continental crust: a new table. Geochim. Cosmochim **28**. Acta

Tsitouridou-R.T. (2004). Carbonaceous species of TSP in urban and rural sites around coal-fired power stations in northwestern Greece. Talanta. **62,** 115-122

U.S. embassy Beijing. If Shanxi can do it (clean up), anybody can. A June 2001 report from U.S. embassy Beijing. http://www.usembassy-china.org.cn/sandt/Shanxi.htm.

UND, University of North Dakota. EERC, Energy &Environmental Center. 20th Jan, 2005. Terms and definitions. Coal combustion byproduts.

Wayne R.P. 2002. Chemistry of atmospheres. Third edition. Oxford

Wolff,G.T. and Klimisch,R.L. 1982. Particulate Carbon: Atmospheric Life Cycle. Eds. Plenum Press, New York

Wornat M.J., Ledesma E.B., and Sandrowitz A.K. 2001. Polycyclic aromatic hydrocarbons identified in soot extracts from domestic coal burning stoves of Henan province, China. Environ. Sci. Technol. **35**,1943-1952

The case for real CO reductions. Wunderground, Weather underground. 2004. Particulate matter pollution. http://www.wunderground.com

www. Millipore.com

Xie Ruikai. 2002. Characterization and apportionment of particulate matter (PM_{10}) in two Chinese cities. Department of chemistry, University of Oslo

Xie R.K., Seip H.M., Liu L and Zhang D.S. 2005. Individual particles (PM_{10}) characterization in Taiyuan city, China (Manuscript). The science of total environment, **343**, 261-272

Youguo He. International Energy Agency. 2003. China's coal demand outlook for 2020 and analysis of coal supply capacity. China coal industry development research and consulting Co. Ltd. www.iea.org/Textbase/work/2003/beijing/4 Youg.pdf

Yu J.Z., Tung J.W.T., Wu A.W.M., Lau A.K.H., Louie-K.P.K., and Fung J.C.H. 2004. Abundance and seasonal characteristics of elemental and organic carbon in Hong Kong PM_{10}. Atmos. Environ. **38**, 1511-1521

Appendix

Table A1. Amounts of ferrous sulphate used to prepare 0.05M solution during analytical steps in modified Walkley-Black method

Analytical steps	Weight (g)	Solution volume(L)
Determination of maximum oxidation temperature for $K_2Cr_2O_7$ solution	14.0564	1
Sucrose recovery	13.9100	1
Charcoal recovery	14.1546 & 13.8450	1
Validation	14.0093	1
LOD determination	14.0425& 13.9243	1
Sample 3	7.0413	0.5
Sample 6	7.0696	0.5
Sample 7	7.0552	0.5
Sample 8	7.0206	0.5
Sample 9	7.0216	0.5
Sample 10	7.0523	0.5
Sample 12	6.9291	0.5
Sample 13	7.0417	0.5

Table A2. Specifications of glass fibre filter

Description	Glass fibre disc without binder AP40 90 mm
Filter code	AP40
Filter diameter (mm)	90
Filter surface	Plain
Max operating temperature (°C)	550
Filter color	White
Filter material	Glass fibre without binder resin
Filter type	Depth filter
Wettability	Hydrophilic
Water flow rate (ml/min.cm^2)	6

Table A3. Specifications of fluoropore membrane filters (Teflon Filters)

Description	**Fluoropore disc PTFE hydrophobic 3.0 µm 90 mm white**
Bubble Point at 23 °C	0.07
Air Flow Rate, L/min cm^2	20
Brand Name	Fluoropore
Filter Code	FSLW
Gravimetric Extractables, %	0.5
Porosity %	85
Filter Diameter	90
Filter Surface	Plain
Max Operating Temperature, °C	130
Filter Color	White
Filter Material	PTFE
Filter Type	Screen Filter
Filter Pore Size, µm	3
Wettability	Hydrophobic
Water Flow Rate	286
Thickness, µm	175

Table A4. Abundance of chemical elements in the continental crust (Taylor, 1964)

Element	Crustal average
	%
Al	3,42
Fe	3,91
K	1,05
Mg	0,8
Na	0,43
Pb	0,66
Ti	0,4
Zn	0,48
	ppm
As	115
Co	18
Cu	609
Mn	786
Ni	82
Sb	45
Se	27
V	127

Table A5. Elemental concentration in reference material samples

	Crustal elemental content (%)	Concentration ppm							
		SRM1	SRM2	SRM3	SRM4	SRM5	SRM6	SRM7	SRM8
Al	3,42	13,421	11,515	16,482	8,534	14,087	12,099	10,170	7,073
Ca									
Fe	3,91	15,343	13,165	18,844	9,757	16,105	13,833	11,628	8,086
K	1,05	4,120	3,535	5,060	2,620	4,325	3,715	3,123	2,171
Mg	0,80	3,139	2,694	3,855	1,996	3,295	2,830	2,379	1,654
Na	0,43	1,668	1,431	2,048	1,060	1,751	1,504	1,264	0,879
Pb	0,66	2,570	2,205	3,157	1,634	2,698	2,317	1,948	1,355
Si	12,50	20,410	25,000	25,100	18,000	30,000	26,000	22,000	15,000
Ti	0,40	1,570	1,347	1,928	0,998	1,648	1,415	1,190	0,827
Zn	0,48	1,868	1,603	2,294	1,188	1,961	1,684	1,416	0,984
	ppm								
As	115,00	0,045	0,039	0,055	0,029	0,047	0,041	0,034	0,024
Bi									
Co	18,00	0,007	0,006	0,009	0,004	0,007	0,006	0,005	0,004
Cu	609,00	0,239	0,205	0,293	0,152	0,251	0,215	0,181	0,126
Mn	786,00	0,308	0,265	0,379	0,196	0,324	0,278	0,234	0,163
Ni	82,00	0,032	0,028	0,040	0,020	0,034	0,029	0,024	0,017
Sb	45,00	0,018	0,015	0,022	0,011	0,019	0,016	0,013	0,009
Se	27,00	0,011	0,009	0,013	0,007	0,011	0,010	0,008	0,006
Sn									
V	127,00	0,050	0,043	0,061	0,032	0,052	0,045	0,038	0,026

Table A6. Detected concentrations for reference material samples by ICP-AES and ICP-MS

		Detected Concentrations for reference material samples (ppm)							
	%	SRM1	SRM2	SRM3	SRM4	SRM5	SRM6	SRM7	SRM8
Al	3,42	13,16	11,73	16,28	8,536	14,681	12,252	10,159	6,969
Ca		24,507	21,567	29,434	15,794	26,669	22,499	18,949	13,054
Fe	3,91	16,165	14,314	19,762	10,318	17,439	14,964	12,534	8,617
K	1,05	3,817	3,361	4,831	2,336	4,276	3,447	2,817	1,747
Mg	0,80	3,417	3,036	4,137	2,209	3,669	3,153	2,641	1,862
Na	0,43	1,656	1,488	2,058	1,065	1,851	1,517	1,268	0,864
Pb	0,66	2,757	2,585	3,334	1,79	2,872	2,457	2,141	1,503
Si	12,50	14,497	14,987	1,98	12,23	16,788	15,554	14,335	11,204
Ti	0,40	1,596	1,222	1,878	0,998	1,572	1,451	1,229	0,875
Zn	0,48	1,857	1,719	2,321	1,253	2,068	1,824	1,509	1,069
	ppm	SRM1	SRM2	SRM3	SRM4	SRM5	SRM6	SRM7	SRM8
As	115,00	0,0415	0,0419	0,0502	0,0304	0,0501	0,04202	0,0373	0,0264
Bi		0,0034	0,0028	0,0039	0,002358	0,0032	0,00307	0,0024	0,0018
Co	18,00	0,01145	0,00724	0,01399	0,00489	0,00856	0,00732	0,00663	0,00442
Cu	609,00	0,2138	0,1959	0,263	0,146	0,2308	0,1997	0,1654	0,114
Cr	403,00	0,0677	0,0434	0,075	0,0506	0,057	0,126	0,108	0,0801
Mn	786,00	0,352	0,2704	0,35	0,202	0,3356	0,291	0,242	0,164
Ni	82,00	0,03134	0,0263	0,04	0,0193	0,03395	0,0294	0,0207	0,0125
Sb	45,00	0,0124	0,0131	0,0153	0,0102	0,0168	0,01579	0,0132	0,0086
Se	27,00	0,0116	0,0117	0,0153	0,00799	0,0079	0,0083	0,00999	0,0058
Sn		0,0206	0,016	0,0238	0,0117	0,0267	0,0153	0,0234	0,0172
V	127,00	0,0467	0,0407	0,059	0,0336	0,0498	0,0476	0,038	0,0252

Table A7. Solubilities of PAHs in water at 25 °C

Compound	Solubility (µg/L)
Naphthalene	31,700
1-Methylnaphthalene	28,500
2-Methylnaphthalene	25,400
Biphenyl	7,000
Acenaphthylene	3,930
Fluorene	1,980
Phenanthrene	1,290
Anthracene	73
Pyrene	135
Fluoranthene	260
Benzo(a)fluorine	45
Benzo(b)fluorine	2.0
Chrysene	2.0
Triphenylene	43
Benz(a)anthracene	14
Benze(a)pyrene	0.05
Benzo(e)pyrene	3.8
Coronene	0.1

Table A8. The distribution of some PAHs in gas and particle phase (ARB, 2005)

Gas-Phase PAHs	Particle-Phase PAHs
1-methylnaphthalene	1,2-benzofuorene
2-methylnapthalene	Anthracene
Anthracene	Benz[a]anthracene
Benz[a]anthracene	Benzo[a]pyrene
Chrysene	Benzo[b]fluoranthene
Fluoranthene	Benzo[k]fluoranthene
Fluorene	Chrysene
Naphthalene	Fluoranthene
Phenanthrene	Phenanthrene
Pyrene	Pyrene
	Triphenylene
	Coronene

Table A9. Estimated atmospheric lifetimes of some PAHs (Wayne, 2002)

PAHs	**Lifetime due to reaction with:**		
	OH	**NO_3**	**O_3**
Naphthalene	8 h	54 d	
1-methylnaphthalene	3.5 h	50 d	> 125 d
2-methylnapthalene	3.6 h	40 d	> 40 d
Biphenyl	2 d	> 11 y	
Phenanthrene	5.6 h		
Anthracene	1.3 h		
Fluoranthene	15.7 h	38 d	
Pyrene	~ 3.5 h	13 d	

Statistics Formulas

Standard Deviation

$$S = \sqrt{\frac{\sum_i (x_i - x^-)^2}{n-1}}$$

Where s is standard deviation, $\bar{x}$ is arithmetic mean, n-1 is degree of freedom

Geometric Mean

$$\mu_g = \sqrt[n]{A_1} A_2 ... A_n .$$

where μ_g is geometric mean, A_1, A_2 ,…..A_n are a set of numbers

Geometric Standard Deviation

$$\sigma_g = \exp\left(\sqrt{\frac{\sum_{i=1}^{n} (\ln A_i - \ln \mu_g)^2}{n}}\right)$$ where σ_g is geometric standard deviation

Program setting for glass fiber filter during analysis by carbon analyzer

```
                                glass.par
' quartz.par
' sample carbon analyzer Parameter file for Sunset Lab;
' analyzes for organic andelemental carbon .
' by Robert A. Cary.
'  1995 Feb 15: added calibrationO2 mode.
' mode <comma> time <comma> temperature
' @ regimen must end 'Offline' mode.
' .
' purge for 10 sec with blower off.
'
Helium, 10, 1
' start ramping the temperature
Helium, 60, 220
Helium, 60, 360
Helium, 60, 525
Helium, 90, 620
' let the oven cool before starting elemental
Helium, 75, 0
' elemental
Oxygen, 30, 550
Oxygen, 30, 650
Oxygen, 30, 720
Oxygen, 40, 790
Oxygen, 30, 820
Oxygen, 20, 860
Oxygen, 40, 890
CalibrationOx, 110, 0
' All done!
' this last mode persists until we start a new sample.
' The last entry *must* be "go offline and turn blower on".
Offline, 1, 0
' end.
```

Program setting for quartz filter during analysis by carbon analyzer

```
                                    Quartz.par
' quartz.par
' sample carbon analyzer Parameter file for Sunset Lab;
' analyzes for organic andelemental carbon .
' by Robert A. Cary.
'  1995 Feb 15: added calibrationO2 mode.
' mode <comma> time <comma> temperature
' @ regimen must end 'Offline' mode.
' .
' purge for 10 sec with blower off.
'
Helium, 10, 1
' start ramping the temperature
Helium, 60, 220
Helium, 60, 360
Helium, 60, 525
Helium, 90, 850
' let the oven cool before starting elemental
Helium, 66, 0
' elemental
Oxygen, 30, 550
Oxygen, 30, 650
Oxygen, 30, 720
Oxygen, 40, 790
Oxygen, 30, 820
Oxygen, 20, 860
Oxygen, 40, 890
CalibrationOx, 110, 0
' All done!
' this last mode persists until we start a new sample.
' The last entry *must* be "go offline and turn blower on".
Offline, 1, 0
' end.
```

Sample ID: Taiyuan no. 7
Analysis Date/Time 11.05.05 12:58:57

Organic C =	**141.31 +-7.27**	**ug/sq cm**
Carbonate C =	**0.00 +-**	**ug/sq cm**
Elemental C =	**128.71 +-6.64**	**ug/sq cm**
Total C =	**270.02 +-13.80**	**ug/sq cm**
EC/TC ratio =	**0.477**	

FID: FID:OK FID2:OK DL= 10 Punch Area, sq cm = 1
Calibration area Used = 101865.0 Calibration Constant =
FID2 Calibration area = 24469.0
Laser correction factor = 0.88
Split time Used = 455 seconds Split time Calculated = 455 seconds
Pk1= 1.44 Pk2= 10.63 Pk3= 24.84 Pk4= 38.38

FID GRAPHIC SCALE= 10

FID1 FID2 Laser Transmission Temperature Absorbance

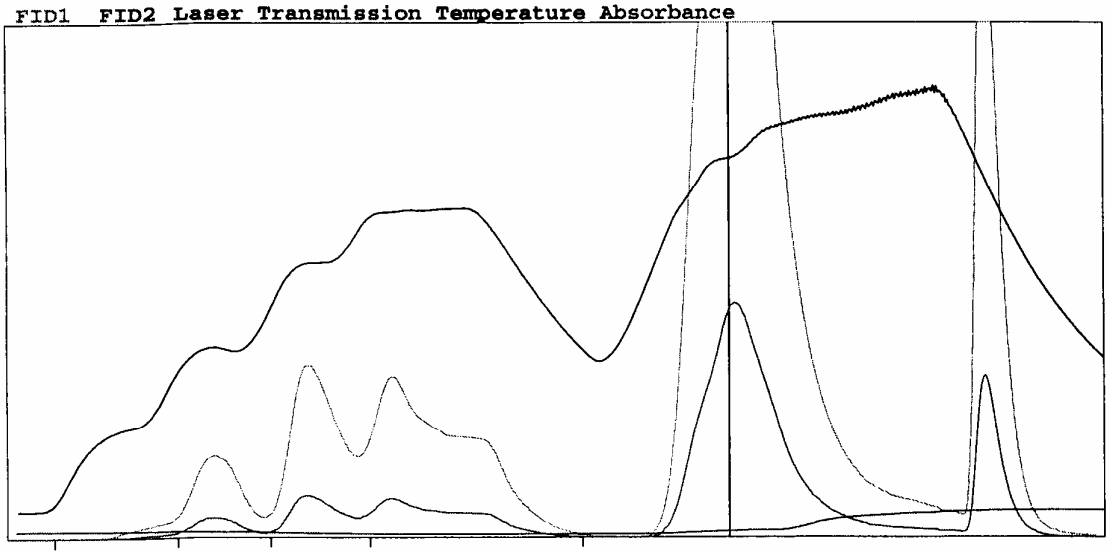

Inital absorbance = 1.414 Absorbance at StartPyrolize = 2.112
Absorbtion Coefficient of original elemental C = 1.1
Absorbance plotted from 0 to 6

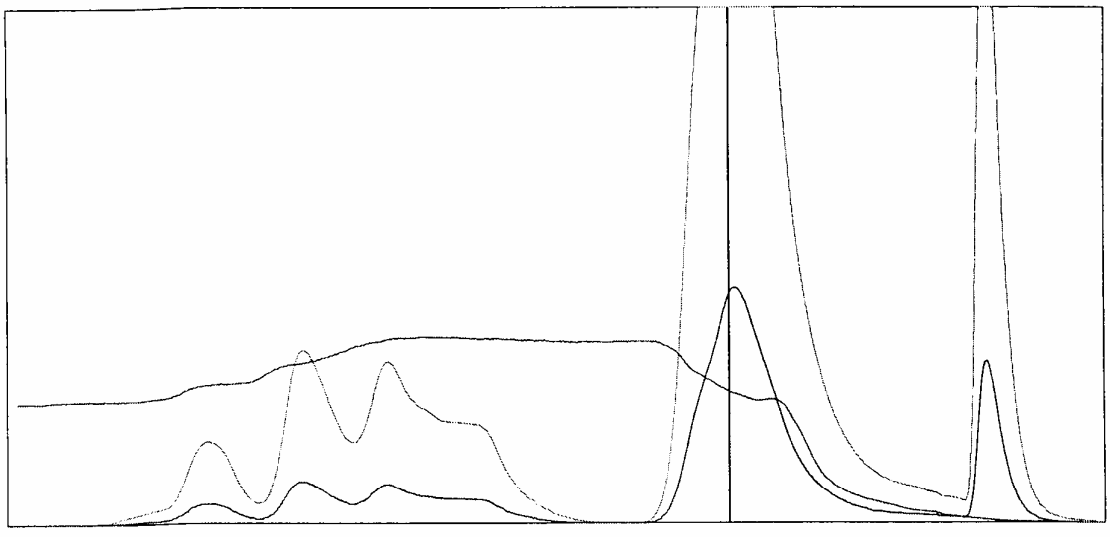

OC/EC Analysis Program (c) Sunset Laboratory, Inc. Analyst - Showa

Sample ID: Sample 9b
Analysis Date/Time 02.06.05 11:45:52

Organic C =	**73.06**	**+-3.85**	**ug/sq cm**
Carbonate C =	**0.00**	**+-**	**ug/sq cm**
Elemental C =	**70.33**	**+-3.72**	**ug/sq cm**
Total C =	**143.39**	**+-7.47**	**ug/sq cm**
EC/TC ratio =	**0.490**		

FID: FID:OK FID2:OK DL= 10 Punch Area, sq cm = 1
Calibration area Used = 236021.0 Calibration Constant = 43.7
FID2 Calibration area = 57223.0
Laser correction factor = 0.97
Split time Used = 438 seconds Split time Calculated = 438 seconds
Pk1= 6.46 Pk2= 8.94 Pk3= 13.24 Pk4= 7.55

FID GRAPHIC SCALE= 10

FID1 **FID2 Laser Transmission Temperature Absorbance**

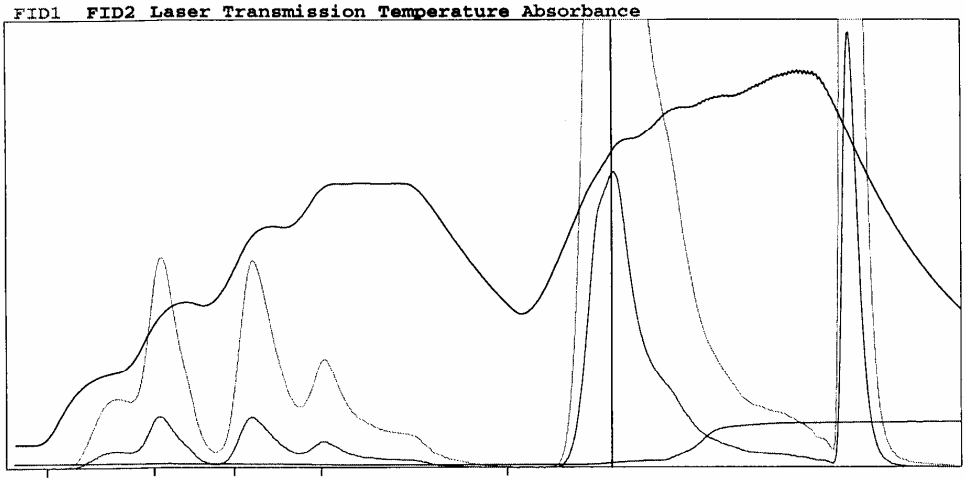

Inital absorbance = 2.374 Absorbance at StartPyrolize = 2.914
Absorbtion Coefficient of original elemental C = 3.4
Absorbance plotted from 0 to 6

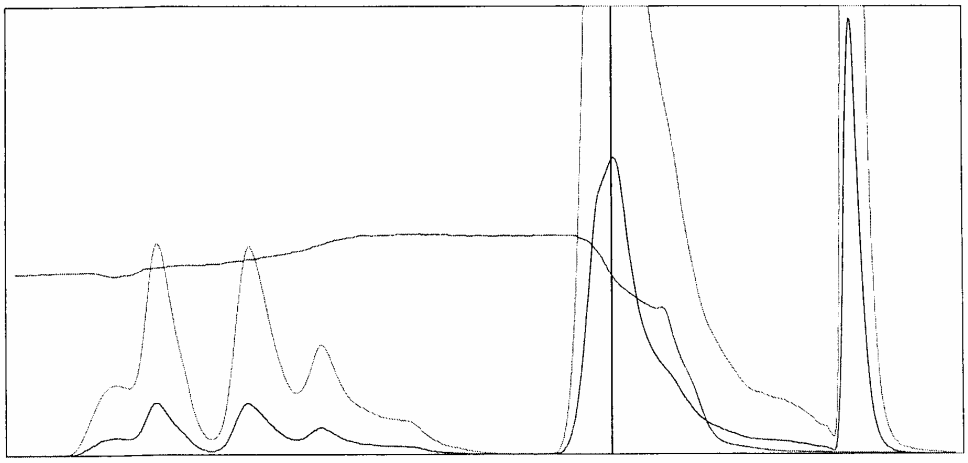

OC/EC Analysis Program (c) Sunset Laboratory, Inc. Analyst - ab